SEDIMENTATION AND EROSION PATTERNS WITHIN ANABRANCHING CHANNELS IN A LOWLAND RIVER RESTORATION PROJECT

By

Ivan Medel

A Thesis Presented to

The Faculty of Humboldt State University

In Partial Fulfillment of the Requirements for the Degree

Master of Science in Natural Resources: Forest, Watershed and Wildland Sciences

Committee Membership

Dr. Andrew Stubblefield, Committee Chair

Dr. Conor Shea, Committee Member

Dr. Margaret Lang, Committee Member

Dr. Alison O'Dowd, Graduate Coordinator

December 2017

ABSTRACT

SEDIMENTATION AND EROSION PATTERNS WITHIN ANABRANCHING CHANNELS IN A LOWLAND RIVER RESTORATION PROJECT

Ivan Medel

Phase 2A of the Salt River Ecosystem Restoration Project (SRERP) was implemented to increase transport efficiency of water and sediment through a low gradient river reach to alleviate flooding on adjacent properties. The SRERP utilizes a unique anabranching channel design that concentrates base flows within a single deep, narrow channel overflowing onto an alternating series of higher elevation active benches at flood stages. This paper investigated the performance of the project's hydraulic conveyance and general utility of anabranching channels as a restoration alternative by assessing the distribution and magnitude of deposition and erosion response patterns.

Aggradation was not observed within the main channel. High-resolution surveyed reaches experienced mean elevation decreases between 0.08m and 0.29m indicating effective discharge rates transported dominant grain sizes in suspension. Along some reaches, bed scour was sufficient to undercut banks, producing slumps which may affect long-term conveyance capacities. Lateral bank scour was limited to reaches exposed to daily tidal flows.

Variable deposition patterns were observed within secondary channels, depending on cumulative precipitation, dominant hydrology, and channel entrance orientation. Isolated tidal flows resulted in deposition, while long duration flood flows produced intertidal floodplain scour. Within fluvially-dominated benches, uniform longitudinal deposition of fine-grained sediments was associated with low channel entrance flow rates. Higher

entrance flow rates resulted in concentrated deposition of coarse-grained particles, up to 0.21m, and a longitudinal gradient of decreasing sediment sizes and magnitude. This project confirmed the suitability of anabranching channel systems for efficient hydraulic conveyance within fluvial reaches of lowland rivers and provides general recommendations for future designs.

TABLE OF CONTENTS

LIST OF TABLES

LIST OF FIGURES

INTRODUCTION

Riverine systems are among our most valuable natural resources and support high proportions of the global biodiversity; (Naiman et al. 1993) however, they have been subjected to intense degradation due to human influence and manipulation (Wohl 2005). Human impacts to natural hydrological and geomorphic cycles affect up to 98 percent of river systems within the contiguous United States (Benke 1990, Graf 2001). A National Water Quality Inventory conducted by the US Environmental Protection Agency in 2009 identified 45 percent of the river systems as 'impaired.' One major cause of impairment within stream systems is unnaturally high sediment loads resulting from high erosion rates in response to land use practices such as timber harvesting, road construction, grazing, and agriculture (Fitzpatrick et al. 1999, Ward and Trimble 2004, Allen 1997). Sediment loads exceeding a stream's sediment transport capacity leads to channel aggradation; negatively affecting biological, hydrological, and hydraulic functions (Berry et al. 2003, DeFries and Eschleman 2004).

Increased overland flow rates are the primary contributor to high erosion rates and sediment yields from land use modifications (Al-Hamdan et al. 2013, Brooks et al. 2013). At water surface elevations insufficient to spill onto floodplains, erosive potential increases with flow rate as shear stress (i.e. the external force acting to detach sediment grains) increases and has been identified as a function of flow rate, velocity, slope gradient, and channel cross-sectional geometry (Einstein and Banks 1950, Foster 1982). As erosion increases, water concentrates in fewer, but larger drainage paths leading to

increased bank erosion, widening and deepening of relatively high slope stream reaches, and creation of gullies in upland areas (Ward and Trimble 2004). The trajectory is self-perpetuating as water continues to concentrate, leading to larger shear stresses and erosion rates. Additionally, deeper channels and increased discharges are capable of conveying larger quantities of water and sediment (Price et al. 2013). Multiple studies and theoretical equations have demonstrated that the increased sediment yields are then deposited on lower reaches and floodplains as transport conveyance decreases in response to decreased slope and velocity (Hjulstrøm 1939, Engelung and Hansen 1967, Dedkov 2004).

High sedimentation rates often disrupt a channel's ability to efficiently convey water and sediment, effectively clogging the stream and resulting in flooding (Allen 1997). This response can be particularly dramatic at the base of watersheds on alluvial floodplains as slopes are generally very low in gradient, channel cross-sectional areas are large, and sediment loads are at their highest. These watersheds typically are associated with a history of land use modifications such as logging, mining, and dam removals that result in increased sediment loads that exceed a stream's carrying capacity or significant reductions in runoff volumes (Mount 1995, Ward and Stanford 1995, Graf 2006).

A combination of historic land use practices and unstable upslope geology within the Salt River Watershed, in coastal, central Humboldt County, have created conditions of increased downstream aggradation and prolonged flooding (GEC 2011). The Salt River Watershed's physiography is characterized by an upper watershed draining the

geologically unstable, high sediment yield Wildcat Range transitioning to a low gradient lowland river system within the lower watershed. The lower Salt River converges into intertidal flow regime creating a mixture of both fluvial and intertidal hydrologic processes.

Sediment yields may be dominated by unconsolidated sediments caused by mass movements within tributary basins (Benda and Berg 2007). However, increased runoff and bank erosion rates following post-European settlement land use modifications, particularly upper watershed resource extraction practices, have contributed to prolonged flooding within adjacent communities for periods longer than would be expected under non-impacted conditions. Kamman Hydrology and Engineering, Inc. (KHE 2011) estimated that 2.6 million cubic meters of sediment has been deposited within the lower Salt River in the 50-year period between 1967 and 2006. High spatial variability was observed in deposition depths with largest deposition depths increasing historic channel elevations by over three meters at the mouth of Francis Creek. The large influx of sediment constrained the river's ability to efficiently convey storm discharges, resulting in prolonged flooding for up to eight months of the year. One possible restoration technique to remedy these impairments is the installation of an anabranching channel system.

Anabranching rivers are similar to braided rivers as both have multiple channels, but anabranching channels are differentiated by a lower width-to-depth ratio, exposed vegetated islands at bankfull flows, and a stable main channel responsible for conveying

base flows (Nanson and Gibling 1978). Eaton et al. (2010) interpret anabranching channels as stable, multiple-thread channels which constitute an intermediate configuration between braided and single-thread channel networks. Jansen and Nanson (2010) found that hydraulic geometries of anabranching channels can increase the efficiency of bedload transport up to 30% compared to wide, single channels, as the flows are concentrated within a single deep and narrow main channel. The vegetated islands restrict channel widening to maintain low width-to-depth ratios, consequently promoting efficient hydraulic conductivity without a significant reduction in slope (Huang and Nanson 2007, Jansen and Nanson 2010). At periods of low flows, anabranching channel networks function similarly to single-thread river systems, however, the developed root structures of the vegetated islands allows for steeper channel banks, resulting in increased flow velocities and transport capacities. Latrubesse (2008) highlighted how fluvial anabranching channel networks are characteristic configurations within the lower drainages of many river systems with high sediment loads.

Historically, anabranching channels were not distinctly classified and were grouped generically with braided rivers, thus complicating the extraction of anabranching-specific research. Currently, there is still no universally accepted definition for anabranching channels (Makaske 2001). Consequently, the majority of pioneering research on anabranching channels in the 1980's and 1990's focused on their identification, description, and classification (Gregory 1985, Nanson and Knighton 1996, Huang and Nanson 2007). As a result, limited literature is available examining in-depth

characterizations of functional processes and channel evolution mechanisms, specifically within North America. A study of historic sedimentation rates within Australian anabranching rivers identified extremely low accretion rates (~ 0.41 m kyr^{-1}) demonstrating their capability for long-term stability and efficient bed load transport (Jansen and Nanson 2010). A study, conducted in North America along the upper Columbia River, found natural levee and in-channel vertical accretion rates were larger along higher gradient, upper anastomosing reaches than lower slope downstream reaches (Makaske et al. 2009). Additionally, the study found that approximately 87% of water and more than 90% of sediment were transported within the main channel. This encouraged slow evolution patterns of secondary channels.

A large-scale, multi-phase restoration project, the Salt River Ecosystem Restoration Project (SRERP), began in 2012. Phase 1, completed in 2013, restored a 180 ha (444 ac) fully tidal salt marsh at the terminus of the Salt River immediately adjacent to the Eel River Estuary. Phase 2A (Lower and Middle), completed from 2014 to 2015, recontoured 2.4 km of stream channels using an anabranching stream design to re-establish hydraulic functions to efficiently convey water and sediment and alleviate downstream flooding. Areas restored during these phases (i.e. Phases 2A Lower and Middle) compose the study area for this research project. Phase 2A (Upper), an upstream extension of phase 2, is currently undergoing construction and is expected to be completed by October 2019. Anabranching channels were identified as an appropriate design for the objectives of the fluvial reaches of the SRERP (i.e. Phase 2) because of their hydraulic and morphological

characteristics (Shea 2011). The project was designed to increase downstream transport capacity to reduce aggradation, yet still allows for floodplain interaction and natural sediment sequestration within secondary channels or 'benches.'

Many authors have advocated the use of objective post-project assessments of stream restoration projects to evaluate the effectiveness of projects in term of goals and to identify effective components of the design to inform future projects (Kondolf and Micheli 1995, Kondolf 1998, Palmer et al. 2007). The SRERP has developed a comprehensive monitoring strategy (HTHA 2011) evaluating a range of parameters, however, this study will provide a higher resolution assessment of the project's effectiveness to accomplish the primary objectives of increasing stream sediment and water transport capacity for flood management while maintaining long-term form and function.

Additionally, the project will evaluate the effectiveness of an anabranching channel design to inform its use in future stream restoration projects. While the existence of natural anabranching river networks are globally ubiquitous (Nanson and Knighton 1996) across a continuum of geologic, geomorphic, and climatic settings, many have been lost within North America due to channel re-alignments and upstream sediment and hydrology impacts (Brown 2002). Consequently, anabranching river configurations are seldom identified as restoration design alternatives within North America. This project, therefore, provides an opportunity to objectively assess the effectiveness of an uncommon restoration design practice.

Objectives

Primary research objectives are focused on the evaluation of hydraulic and geomorphic performance of the Salt River Ecosystem Restoration Project to assess the project's effectiveness in meeting restoration goals. Future stream restoration project planners will benefit from insights gleaned on the hydraulic processes and performance of an understudied, and seldom implemented anabranching channel design. Additionally, it is critical to the project's long-term success to provide information addressing the expected evolution of channel morphology and discharge capacities by incorporating anticipated changes in storm frequency and duration due to climate change.

Research Objectives

1. Characterize the distribution and rate of deposition and erosion within the main channel and active bench.
2. Quantify the volume and efficiency of water and sediment discharge within the main channel.

Sub-objectives

3. Identify locations not meeting performance standards and provide data to inform the implementation of adaptive management protocols.
4. Develop a model to determine the long-term trajectory of hydraulic conveyance capacities and evolution of channel morphologies.
5. Extrapolate the long-term ability of the project to accomplish project goals.
6. Provide recommendations to inform the implementation of similar future projects.

Site Description

The Salt River is located in western Humboldt County, California, adjacent to the city of Ferndale and is approximately 25 km south of Eureka (Figure 1). The river is approximately 20 km long with its headwaters originating in the Wildcat Mountains immediately to the south and its terminus within the Eel River estuary. The watershed encompasses approximately 12,300 ha (30,425 ac) and is drained by four main tributaries: Williams Creek, Francis Creek, Reas Creek, and Smith Creek. The lowermost 58% of the drainage area is located within the relatively flat Salt River Delta ranging from one to 25 m above mean sea level while the remaining 42% consists of the upslope tributaries within the high relief Wildcat Mountains.

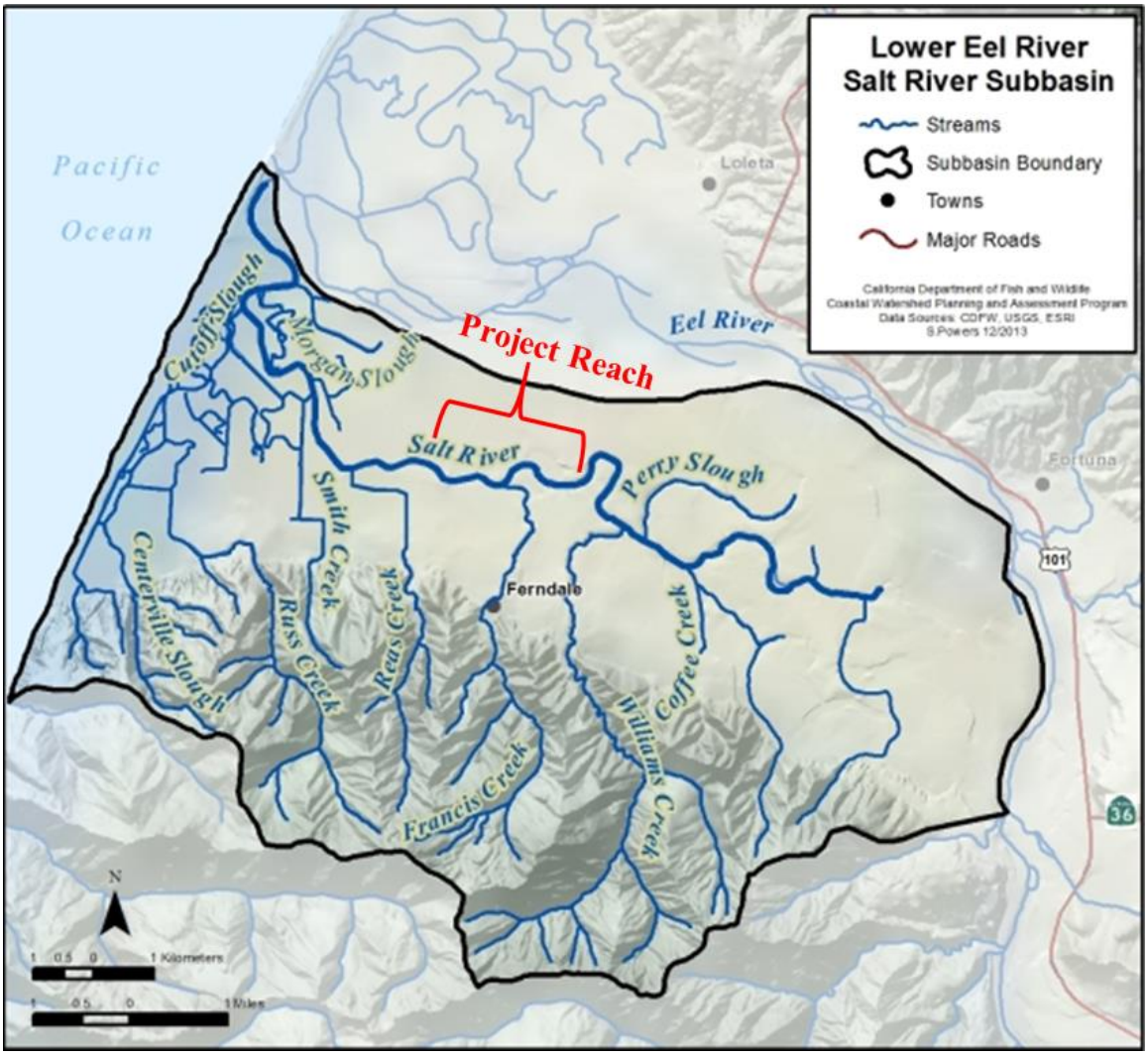

Figure 1. Map of the Salt River and tributaries. The project reach is highlighted in red. Source: CA Dept. of Fish and Wildlife.

Historically, the river likely functioned as an overflow drainage for the Eel River during large flood events (GEC 2011); however, watershed impacts following European settlement of the Eel River Watershed resulted in substantial aggradation of the Salt River's channel leading to hydrologic disconnection with the mainstem Eel River. Land use practices leading to the degradation of the Salt River are varied and complicated; however, several large impairments can be identified (C Shea, pers. comm. 2017). The

initial impairment was the construction of dikes and levees which drained/ disconnected the lower Salt River salt marsh eliminating navigability in the late 1890's. Following the floods of 1964, the Leonardo Levee was constructed in Fortuna to reduce flooding to valuable agricultural lands; however, this eliminated the historic overtopping of the Eel River into the Salt River system and associated episodic flushing (HCRCD 2014). Within the Salt River watershed, upslope impairments and land use practices including grazing, timber production, road construction, and agriculture, combined with the unstable geology and erodible soils of the Wildcat Mountains led to high sedimentation rates (Benda and Berg 2007, GEC 2011). Increased sediment delivery to the Salt River has resulted in up to three meter aggradations along some reaches below Francis Creek (KHE 2011). The build-up of sediments severely impacted the ability of the River to effectively transport water and sediment to the Eel River estuary and resulted in extensive and prolonged flooding of pasture lands within the flat Salt River delta. The scale of sediment accumulation is well demonstrated by the channel geometry at the Dillon Rd. Bridge where the channel was 60 m wide and 5 m deep prior to European settlement (circa 1850s). The channel was navigable by large ships who transported goods from Humboldt to San Francisco. However, accumulated sediment reduced the channel to six meters width and only one meter depth by the mid-1960s.

The Salt River is currently under construction on the final stage of a large-scale multi-phase project designed to restore some of the historic processes along a 12.39 km reach. The final phase of the project is currently under construction and expected to be

completed by October 2019. According to the Final Environmental Impact Report (GEC 2011) of the SRERP, the goals of the restoration pertaining to the riparian corridor phase include:

- Restoring the Salt River channel and adjacent riparian floodplain by increasing hydraulic conveyance and constructing habitat features that re-establish ecological processes beneficial to fish and other native species;
- Restoring former estuarine habitat and tidal connectivity within the lower Salt River;
- Improving water quality and drainage efficiency across the floodplain;
- Managing excess sediment loads by maximizing fluvial and tidal channel sediment transport capacity by designing and maintaining active and passive sediment management areas that minimize long-term impacts to land use (i.e. flooding)

METHODS AND PROCEDURES

Site Selection and Sampling Design

The research project was implemented along a 2.2 km reach encompassing the entire anabranching channel segment restored during the second phase of the SRERP. The reach extended from immediately upstream of the Reas Creek confluence on the downstream end to the extent of the completed project upstream (Figure 1).

To distinguish depositional environments resulting from varied hydrologic regimes, a nested sampling design was utilized, dividing the project reach into three discreet anabranch channel units (Figure 2). Each channel unit was subdivided into three transect sections (Figure 3). Each anabranching unit is dominated by a distinct hydrologic regime characterized by a fully intertidal environment within the furthest downstream channel unit (Unit 1), a mixed intertidal unit influenced by a mix of high tides and fluvial freshwater flows (Unit 2), and an upstream supratidal channel unit where the elevation is above tidal influence and experiences only freshwater flows (Unit 3).

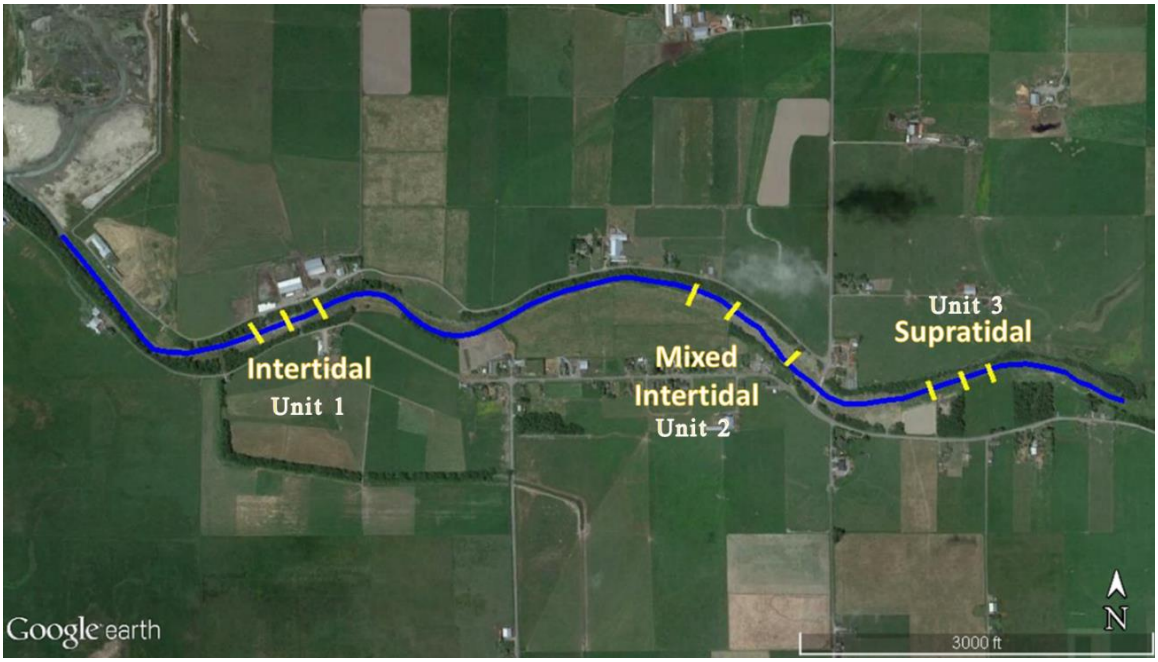

Figure 2. Map identifying the three anabranching channel units within the project reach.

Each anabranch channel unit was further subdivided into sections likely representative of different sediment transport and deposition characteristics within the floodplain areas. Upstream sections, or “expansion sections”, were hypothesized to experience increased deposition rates consisting of the coarsest material as cross-sectional area and roughness increase, effectively reducing the velocity of inflowing water from the main channel onto the floodplain and secondary channels. The “middle sections” were expected to exhibit uniform flow and be representative of typical hydraulic conditions within the active bench and floodplain. The downstream sections, or “backwater sections” were hypothesized to be in backwater conditions during storm events thus experiencing increased sedimentation rates of finer grained particles. Secondary channels (and the adjacent floodplains) alternate sides of the main channel within the project area and are separated by permanent vegetated islands which restrict channels from meandering and

confine base- and non-flood stage flows. Anabranch channel units are identified as a distinct secondary channel and adjacent floodplain with an inflow from the main channel and a return to the main channel (Figure 3). Dry season base flows are concentrated within the main channel resulting in near perennial flow conditions. However, flows within the secondary channels are ephemeral and limited only to flood stage conditions during precipitation events.

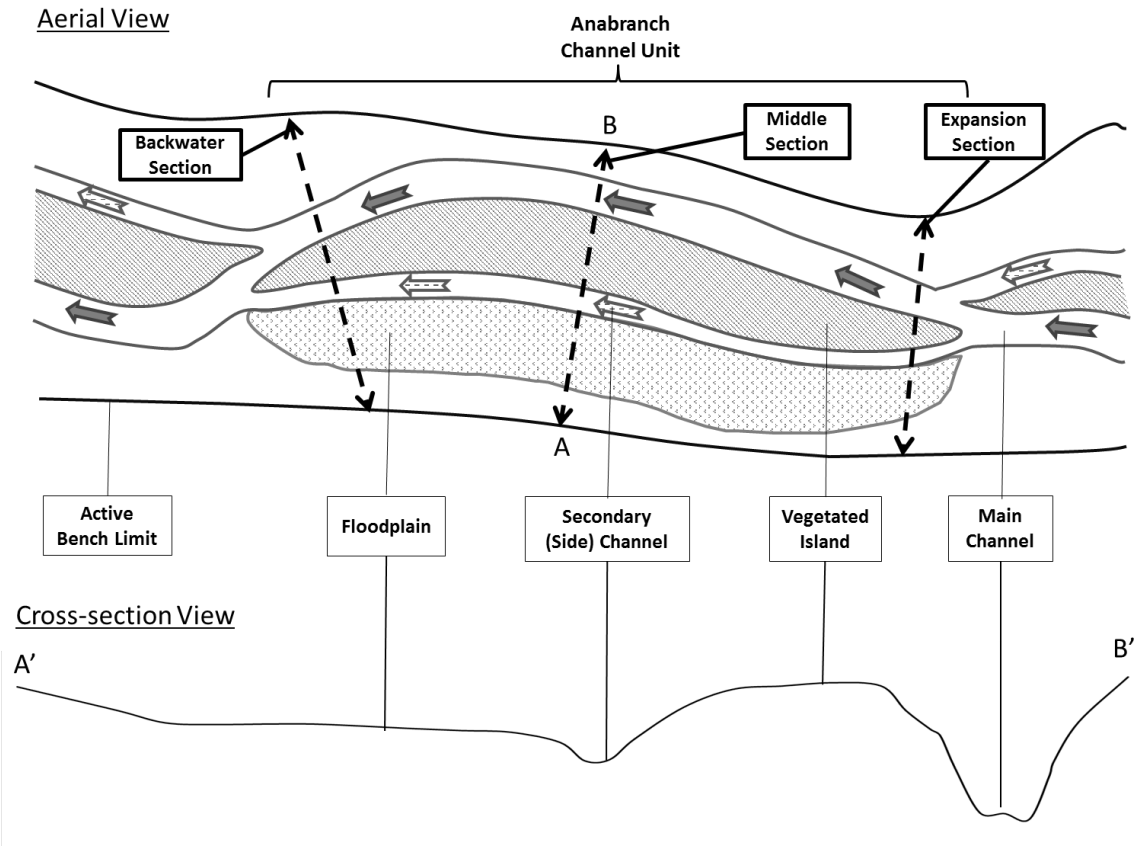

Figure 3. Aerial and cross-sectional schematics of a representative anabranch channel unit where dark arrows indicate the main channel and white arrows the secondary channels. Sampling transect sections are represented as dashed lines (solid yellow lines in Figure 2) and labelled in boxes at the top of the aerial view. Physical features are labelled below the aerial view.

Data Collection Methods

Data collection methods were designed to obtain information regarding specific hydraulic and hydrologic variables assessed independently for changes over time. The majority of collected data types were dissimilar between surveys, thereby preventing cross-survey statistical analyses. However, the data collection methods were designed to provide complementary information describing site patterns of erosion and deposition, to reinforce findings, and allow the development of a conceptual model describing the distribution of the site's dominant physical processes.

Elevation Surveys

Cross-section and Longitudinal Profile Surveys

Cross sections were implemented along two geometric planes based on orientation to channel flow. Longitudinal profiles extended parallel to the channel flow following the thalweg of the main channel to identify areas of deposition and scour along the length of the project reach and to calculate channel slope. Conversely, channel cross-section surveys were implemented perpendicular to channel flow spanning the width of the entire channel between the bankfull heights and incorporate both the main channel and active bench. While the cross-section and longitudinal profile surveys were conducted to capture different morphologies within the project area, the data collection methods were essentially the same.

Cross-section survey transect benchmarks were permanently established in December 2015 by hammering rebar into the ground at the beginning and end of each transect to

ensure repeat surveys were conducted in the same location. The coordinates of the start and ending marker of each transect were collected using a sub-meter Trimble Geo-XH GPS unit. Additionally, efforts were made to ensure all transect markers are placed above bankfull elevations to minimize the risk of disturbance from floodwaters. Surveys were conducted using an auto-level scope and stadia rod to measure distance and elevation. Real-time Kinematic (RTK) elevation profiling was conducted on 21 July 2016 using a Trimble RTK setup and network. The survey calculated the real-world start elevation of each permanent transect marker fitted to the North American Vertical Datum of 1988 (NAVD 88). United States Geological Survey (USGS) elevation benchmark SR-11 was used to calibrate RTK survey data to determine absolute elevation values.

After the height of instrument (i.e. auto-level scope) was determined by backsighting its height above the transect markers, elevation measurements were recorded at every major break in slope and on every major feature (e.g. floodplain, secondary channel, vegetated island, main channel) to capture topographic variability. Measurements were recorded at predefined meter markings to ensure repeatability. Data were recorded on waterproof Rite in the Rain ® paper with notes collected about each major feature (e.g. break in slope, tops of berms, scour pools).

Channel cross-section surveys were conducted within all nine anabranch channel unit sub-sections at a resolution of no less than one elevation reading for every two meter interval (higher resolution data were collected within areas with greater topographic complexity). Longitudinal profile surveys were collected along the entire length of the

2.2 km reach at a minimum resolution of one reading every five meters within anabranch channel units and two meters within five meter buffers of cross-section transect intersections. Between channel units, elevation data points were collected at a minimum resolution of 50 m.

Cross-section surveys were conducted three times over an 18-month period (Table 1). Winter 2015 surveys were conducted to establish a baseline immediately following the completion of the SRERP construction. Subsequent summer surveys were conducted following the wet seasons to compare topographic responses to baseline surveys. Cross-section data were imported to ArcMap to calculate channel area and quantify fill and scour at each cross-section for each survey season.

Table 1. Channel cross-section survey and establishment dates.

		Survey Dates		
Channel Unit	Established	Winter 2015	Summer 2016	Summer 2017
1	12/29/2015	12/29/2015	6/8/2016	5/15/2017
2	12/29/2015	12/29/2015	6/7/2016	5/16/2017
3	12/29/2015	12/29/2015	6/17/2016	5/16/2017

Longitudinal profile surveys required four work days to capture the complete 2.2 kilometer reach. At the conclusion of each survey day, a new temporary benchmark was created on a permanent feature (e.g. large rock, large wood structure) or permanent transect benchmark. Longitudinal profile surveys implemented in the summer of 2016 were conducted on 31 May, 6 June, 7 June, and 8 June. Summer 2017 surveys were conducted on 22, 24, 26 May, and 12 June 2017. The elevations of identical stationary surfaces (e.g. large woody structures, cross-section benchmarks, fence posts) were

collected during both surveys to allow a relative comparison and the calculation of vertical precision between survey years.

Total Station Surveys

High-resolution elevation surveys using a Nikon DTM 322 Total Station were conducted at floodplain inlets for all three anabranch channel units in the summer of 2016 and 2017. The surveys were intended to provide fine-scale information on the distribution of scour and erosion dynamics within the secondary channel entrances. NAVD88 elevations of the start benchmark of each expansion transect were used to calibrate the height of the total station. Depending on the topographic complexity of each survey unit, 100 to 300 independent elevation points were recorded to provide fine-scale detail of the inlet's elevation profile. Points were exported from the total station unit and imported into ArcMap 10.2 where Triangular Irregular Networks were created before being converted to high-resolution Digital Elevation Model rasters. The difference between the rasters (i.e. summer 2016 and summer 2017) was calculated on a pixel by pixel basis to produce a heatmap of the distribution of elevation changes within the secondary channel entrances.

Sedimentation Surveys

Tile Sedimentation

In-channel rates of sedimentation and erosion were calculated using an array of sediment tiles within the secondary channels and floodplain at each channel cross-section survey site. Sediment tiles consist of a 152 mm x 152 mm glazed ceramic tile placed level with

the substrate. Accumulated sediment depth (mm) was measured atop the plate following each wet season and was measured ad hoc following individual storm events throughout the season. The method was modified from Pasternack and Brush (1998). Three sediment tiles were installed within the thalweg of the secondary channels longitudinally at channel cross-section locations at five meter intervals (Figure 4). Additional tiles (dependent on longitudinal length and observed year 1 depositional variability) were installed within each secondary channel prior to the winter 2016 wet season to allow for the identification of higher resolution longitudinal changes in the quantity of deposited sediment. Additionally, sediment tile deposition depths within the downstream intertidal channel unit (i.e. Unit 1) were measured on 30 September 2016 at the end of the dry season to isolate the sedimentation and/or scour response from tidal dynamics in the absence of freshwater flows.

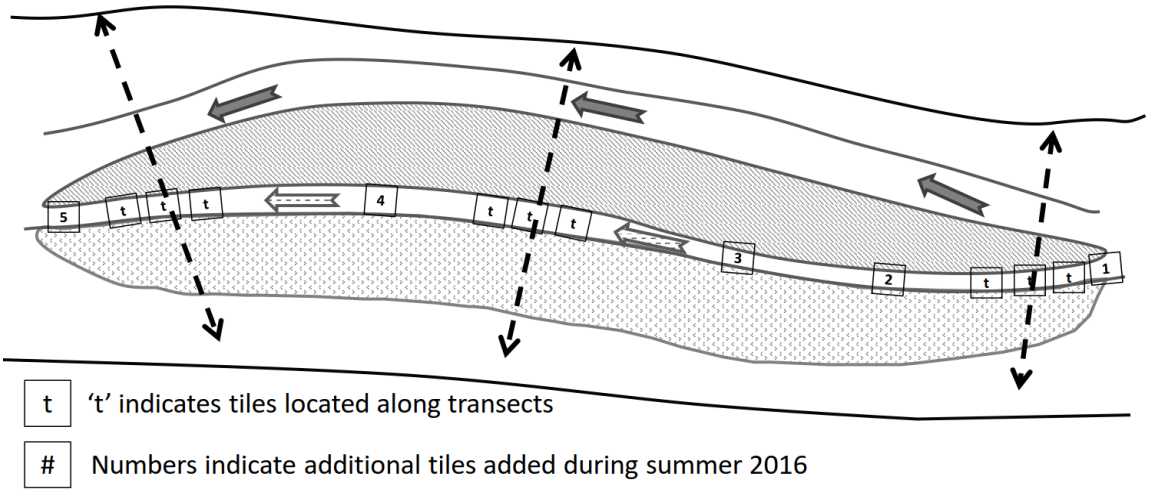

Figure 4. Representative schematic indicating placement of secondary channel deposition tiles. Dashed lines indicate the location of cross-section transects.

Deposited depths of sediment for all tiles was measured and collected in the summer of 2016 and 2017. While deposition depths were measured for each collected tile, it was determined that performing comparative quantitative analyses between channel units on the deposited sediment mass would better reduce the potential effects of spatially varying bulk densities. Sediment deposited upon each tile was weighed to the nearest gram following the drying process described in the 'sediment grain size distribution analysis' section.

Some unit 'expansion section' tile depths (Figure 3) were measured opportunistically between rain storms in the winter of 2016 – 2017 to collect higher resolution temporal data on the deposition response to various sized rain events. A focus was given to Unit 3 expansion tiles as they displayed the greatest deposition depths following the first survey year and were, therefore, believed to generate the most measurable response to rain events. However, accurate depths of deposited sediment could not be collected during most rain events due to the presence of standing water.

Grain Size Distribution Analysis

Grain size samples were collected to provide high-resolution information regarding the proportional distribution of deposited grain sizes. These data characterize stream competence and the relative efficiency of transport capacity for various sized grains. Sediment deposited atop each sedimentation tile was collected at the end of the 2015 - 2016 wet season concurrently with cross-section surveys to correlate the evolution of channel profiles with the depth of deposited sediment. Prior to grain size analysis,

sediment from each tile was air dried for at least one week, then oven dried for 24 hrs at 40.5˚C before being weighed to the nearest tenth of a gram.

Following weighing and drying, sediment samples for each transect section were composited, mixed, and processed for proportional grain sizes less than 2 mm following United Stated Department Agriculture Method 3a (USDA 2014). Grain sizes larger than 2 mm (i.e. sand) were processed using a stacked or nested sieve methodology (Cheetham et al. 2008). Approximately 120 g of dry sample was placed into a coarse mesh sieve stacked on a nest of progressively smaller mesh sieves ranging from 500 to 62 µm. The stacked sieves were mechanically agitated for a period of five minutes. Following the agitation, the largest mesh sieve was removed and the remaining sediment was hand sieved onto a clean pan. Passed sediment was transferred to the next smaller sized sieve. This process was repeated for each sieve and the contents remaining on each sieve are weighed and divided by the total mass to determine the distribution of each size class by mass. The final data set consisted of the proportion of grain sizes for each transect location categorized as clay, silt, and sand.

River Discharge Surveys

Continuous Water Surface Elevation Loggers

One flood stage logger was deployed within all three anabranch channel units recording continuous water surface elevation (WSE) data at 15 minute intervals. The loggers recorded the flood stage height and time continuously throughout the duration of storm events and dry weather base flows. The flood stage loggers allowed mean velocity and

water's height survey data to be matched with the corresponding flood hydrograph stage. Essentially, I was able to identify whether storm survey events occurred during either the rising limb, peak discharge, or falling limb of the hydrograph. Continuous data from flood stage loggers were also used to calculate the percent of time flows remained in the main channel, occurred within the secondary channel or rose above the vegetated islands and formed a single large channel across the extent of the project width.

Due to difficulties in identifying appropriate locations providing velocity refugia from large flows, the devices were not deployed uniformly in relation to channel units. Loggers placed to capture WSE data for Units 1 and 2 were deployed at the active bench entrances, while the logger at Unit 3 was situated at the channel exit (Figure 2). Loggers were installed from 18 March 2016 to 20 March 2017 with a one month gap from 12 September 2016 to 12 October 2017 but were deployed prior to the first rains of the 2016 – 2017 storm season.

Floodplain Entrance Flow Rates

Mean water velocities were collected at the upstream connections of the secondary and main channels of the two upstream anabranch channel units (i.e. Units 2 and 3) where water enters the floodplain during flood events. Water velocities were collected using a Swoffer flow meter during four storm events in the winter of 2016, where rainfall depth exceeded two centimeters over a 24-hour period. Channel unit entrances were surveyed within one hour of each other to reduce the potential for WSE changes due to temporal variability. Channel entrance flow rates were surveyed on 10 December 2016, 04 January

2017, 19 January 2017, and 02 February 2017 during events ranging from 2.14 cm to 5.26 cm precipitation depth.

To allow the identification of water surface elevation (WSE) at the time of each sampling event, rebar was placed at the upstream end of each floodplain entrance and the NAVD88 elevation was recorded during Total Station surveys. WSE data were verified by measuring the distance of the wetted edge from the upstream transect benchmark and comparing to the summer 2017 cross-section survey.

Precipitation Data

Daily precipitation summaries were downloaded from the National Oceanic and Atmospheric Administrations' National Centers for Environmental Information Climate Data Online for the National Weather Service's Cooperative Observer Network gaging station located at the Fortuna Airport (i.e. Station ID GHCND:US1CAHM0029) for the 2016 and 2017 WY. The Fortuna Airport is located approximately 13.39 km inland from the SRERP with no major topographic features separating the areas. The gage was deemed an accurate substitute for an onsite rain gaging station.

Other Main Channel Surveys

Failure Inventory

Following each wet season (i.e. summer 2016 and 2017), the entire project reach was walked to identify and characterize channel bank failures, significant sloughs, major in-channel scouring and other major modifications to as-built project topographies. While 'failure' was not formally defined to encompass a minimum size or depth, areas were

identified loosely as ‘definite and observable deviations from the original constructed channel topography outside of normal equilibrium processes.’ As an example, bank sloughs were only recorded if they extended the entire height of the channel bank and a delineable failure plane could be identified. However, light side channel scouring and moderate undercutting was ignored as slight channel bank adjustments are to be expected immediately following construction. Large, easily identifiable failures constituted the majority of the recordings and, consequently, exert the most significant influence on analysis results rendering the lack of a finite distinction between failure and adjustment inconsequential.

The outline of all channel bank failures was delineated and recorded using a sub-meter Trimble Geo-XH GPS. Descriptive data were recorded for each location, including observable groundwater seepage, whether the failure occurred next to large woody debris or exists at a main/ side channel confluence. The mean depth of each failure was measured to allow for estimates of sediment volume discharged into the channel and comparisons to be made across survey years. Additionally, georeferenced images were captured of each failure to allow for qualitative visual comparisons between survey years. These data were provided to project managers in accordance with adaptive management procedures and to inform designs of future restoration projects by identifying grading elements and structures with high susceptibility to failure.

Channel Bank Pin Surveys

Small steel pins (1 mm diameter) were hammered into side banks within the main channel along all transects to calculate in-channel scour or deposition depths. Three hundred millimeter long pins were hammered into the banks to a depth of 250 mm, allowing the remaining 50 mm to protrude from the bank, allowing rapid location of the pins in conjunction with the use of a handheld Garrett Pro-pointer AT metal detector. Pins were placed similarly to the floodplain tiles (Figure 4), with center pins placed along the transect lines and adjacent pins placed five steps both upstream and downstream of the transect to identify and minimize variability over small longitudinal spatial scales. In addition, pins were placed at two elevations at each location to capture the variability of in-channel scour at different water depths. A lower pin was placed at the base flow water surface and the upper pin was placed halfway between the lower pin and the upper bank vegetation thought to be equivalent to the mean flood stage elevation. A total of 108 pins were deployed (3 replicate pins per bank x 2 elevations x 2 banks x 9 transects). Pins were deployed late in the winter 2015 – 2016 storm season as the project methods were in development. Pins were deployed within anabranch Units 1 and 2 on 14 February 2016 and 29 March 2016 within Unit 3. Scour depths were recorded on 19 August 2016.

RESULTS AND ANALYSIS

Elevation Surveys

Discussed in greater depth in the 'precipitation data' section, it should be noted that both survey years incorporated into this project (i.e. WY 2016 and 2017) occurred during abnormally wet years. As such, erosion and scour results were recorded during highly active rainfall years and may be atypical compared to water years with more moderate precipitation depths.

Channel Cross-sections

Results are presented for all nine cross-section survey locations (Figure 2) collected during three survey seasons (i.e. winter 2015, summer 2016, summer 2017) as cross-sectional profiles (Figures 5 – 13), and summarized by main channel cross-sectional areas (Table 2) and lowest thalweg elevation (Table 3). All elevation values are presented in the North American Vertical Datum of 1988 (NAVD 88). Main channel cross-section areas were determined by measuring the top of the vegetated island as the highest channel elevation benchmark as the vegetated island crest represents the full capacity of the main channel. Table 2 indicates a reduction in cross-sectional area between survey years for select cross-sections; however, this is largely a combination of deposition along channel banks (which increases channel capacity) still accompanied by a decrease in channel bottom elevation caused by scouring (Tables 3 and 4). All cross-sections experienced varying magnitudes of scouring along channel bottoms except for Unit 1 between 2015 and 2016, indicating an absence of sediment aggradation within the main channel (Table

3). Between the first (i.e. winter 2015) and last (i.e. summer 2017) survey seasons, the minimum elevation of every cross-section profile decreased between 0.08 m and 0.5 m. Only the Unit 3 backwater and Unit 3 expansion cross-sections were characterized by decreases in cross-sectional area across all survey seasons; however, these decreases were minor and may be due to the growth of dense vegetation along the channel banks complicating the identification of channel slope breaks or minor differences in tape tension between surveys.

Increases in cross-sectional area are additionally influenced by overbank deposition as the peak elevation of the vegetated island increases, raising the total capacity of the main channel. This may result in cross-sections experiencing net deposition but still increasing in channel area. Channel Units 1 and 3 experienced more deposition than scour during the relatively drier 2015 – 2016 rain season (1.64 m^2 deposition vs 0.5 m^2 scour and 2.08 m^2 deposition vs 0.6 m^2 scour, respectively). However, all three units experienced net scour during the wetter 2016 WY. Unit 2 was the only area to experience cumulative scour between all survey seasons (1.02 m^2 vs 2.09 m^2 and 1.21 m^2 vs 2.56 m^2, respectively).

The largest single season changes in cross-sectional area occurred between the summer 2016 and summer 2017 surveys within the furthest downstream channel unit (i.e. Unit 1 backwater and Unit 1 expansion; Table 2). Both transect locations experienced minor cross-sectional area reductions between the first surveys caused by deposition along channel banks (Figures 5 and 7; Table 4). However, cross-section profiles were both

characterized by heavy scouring and minimal deposition between summer 2016 and summer 2017 resulting in channel bottom elevation reductions of approximately 0.3 m (Tables 3 and 4).

The Unit 2 expansion cross-section experienced the largest areal change from winter 2015 to summer 2017 (Table 2; Figure 10). The lowest point of the cross-section decreased in elevation by a half meter and cross-sectional area increased by a sizeable percentage between each survey season (i.e. 13.49% from 2015 – 2016 and another 10.47% from 2016 to 2017). This transect experienced deep downcutting (0.33 m) during the winter 2015 – 2016 storm season, causing a bank slumps on both sides of the channel during the winter 2016 – 2017 season. The slump can be seen in the 16 May 2017 profile (Figure 10).

Cross-sections profiles (Figures 5 - 13) show the secondary channel and floodplain segments are generally stable and show low volume sedimentation at a majority of the survey stations. Within the active bench of the intertidal unit (Unit 1) there was slight deposition concentrated mainly within the floodplains ranging from 0.08 m within the backwater section increasing to 0.14 m within the expansion section from winter 2015 to summer 2016. However, there was essentially no elevation increase at any of the Unit 1 cross-sections from summer 2016 to summer 2017, with the exception of the middle transect, where elevation increased by approximately 0.04 m within the floodplain. Unit 2 showed slight elevation increases within all floodplain areas ranging from approximately zero meters in the middle sections to 0.04 m in the expansion section. However, these

minor changes may be partially attributed to vegetative growth between winter of 2015 and summer 2017 which obstructed clear views of the bare ground.

Cross-section profiles of the Unit 3 backwater and middle sections indicate formation of natural levees within the secondary channels. The relatively high magnitude of deposition occurs where open from confined channels to unconfined floodplain areas. As water spills onto the floodplain it reduces in velocity and competency resulting in the deposition of coarser grained sand particles immediately adjacent to the secondary channels. The most significant sedimentation within the project area was located within the upstream reaches of Unit 3, particularly the expansion section, across multiple surveys (e.g. deposition tiles, longitudinal profile, visual observations). The leveeing is most easily identifiable on the Unit 3 expansion cross-section (Figure 13) showing a 0.39 m^2 cross-sectional area of sand deposited adjacent to the secondary channel.

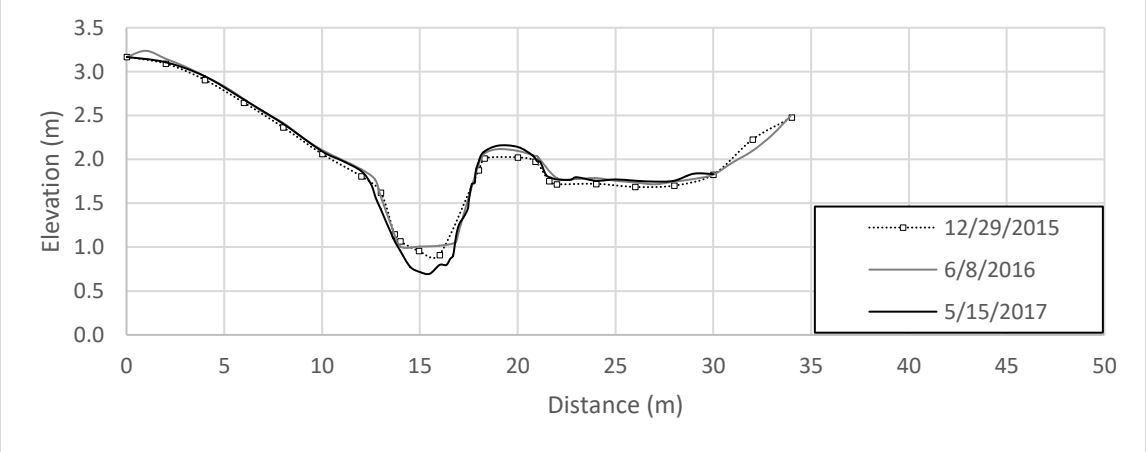

Figure 5. Cross-section profile of Unit 1 backwater transect.

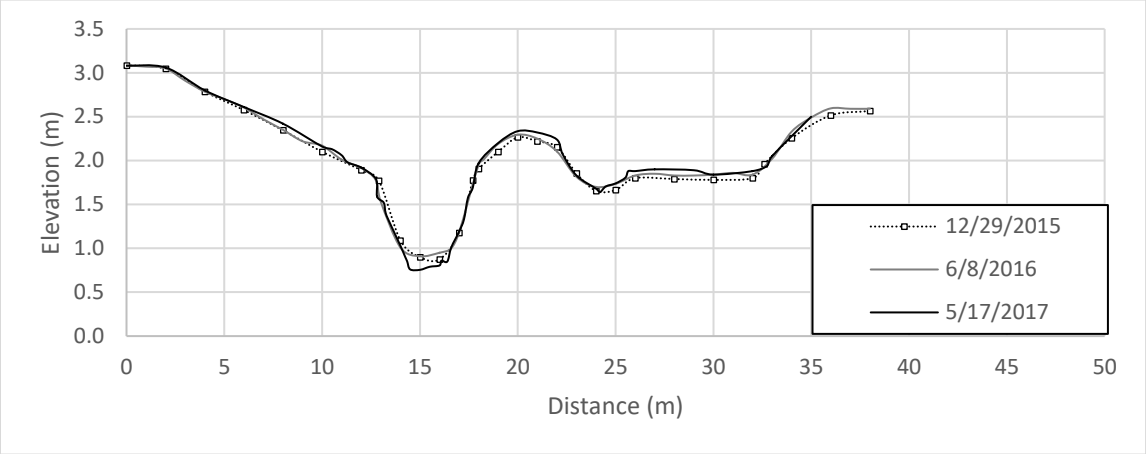

Figure 6. Cross-section profile of Unit 1 middle transect.

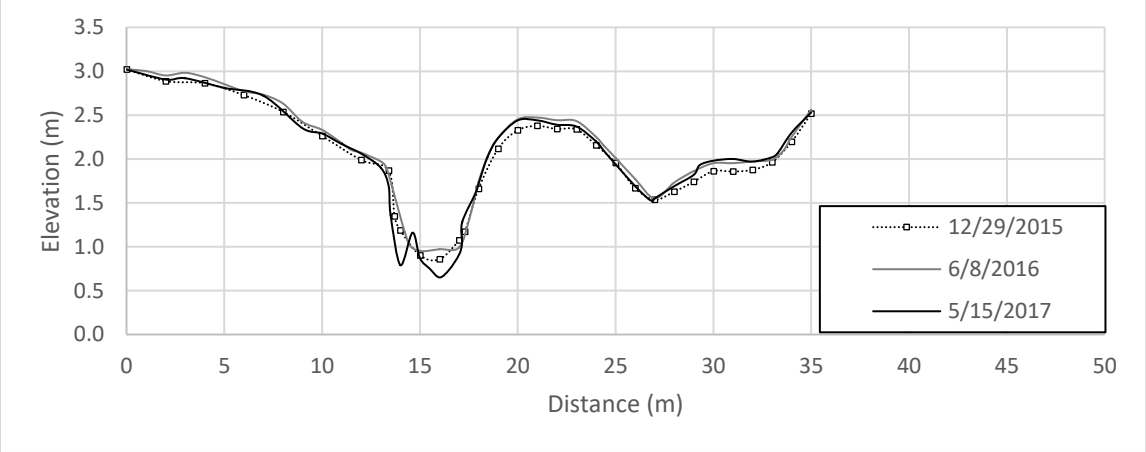

Figure 7. Cross-section profile of Unit 1 expansion transect.

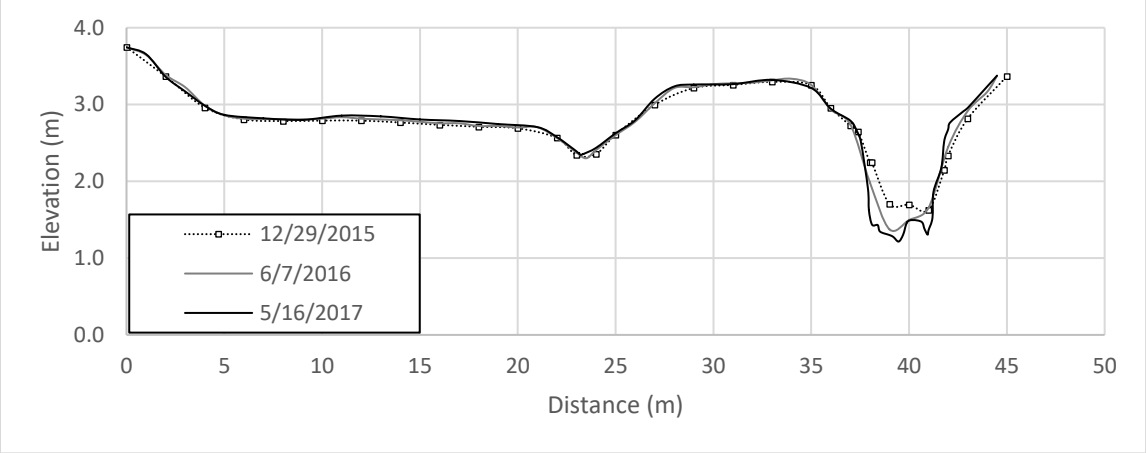

Figure 8. Cross-section profile of Unit 2 backwater transect.

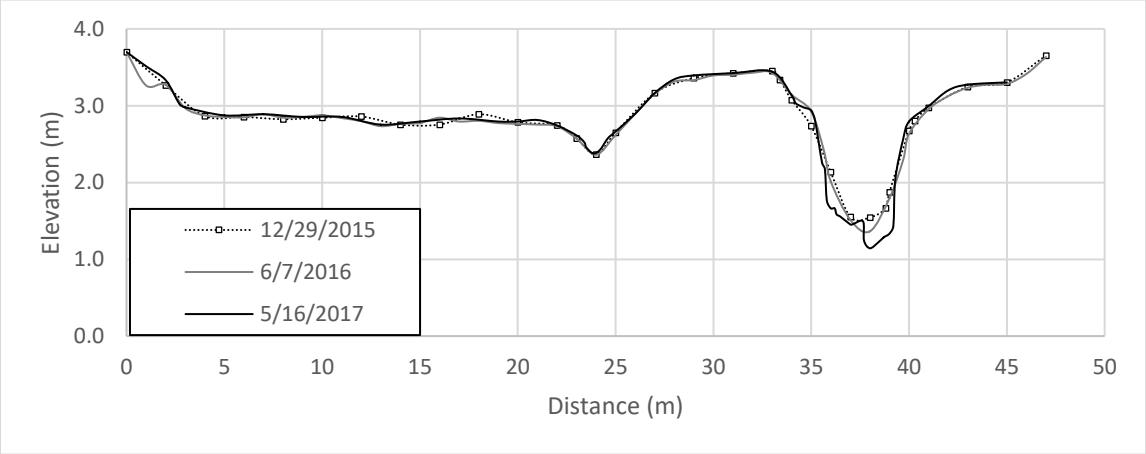

Figure 9. Cross-section profile of Unit 2 middle transect.

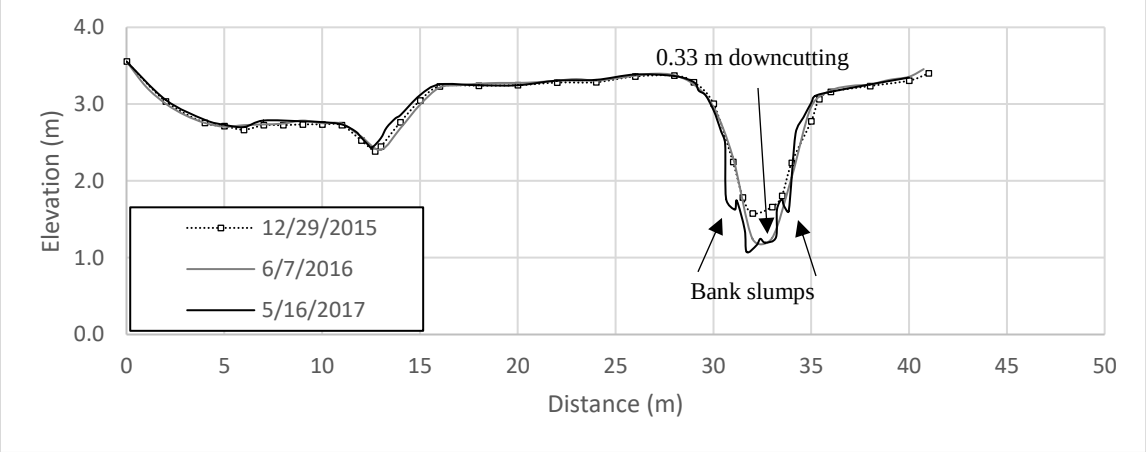

Figure 10. Cross-section profile of Unit 2 expansion transect.

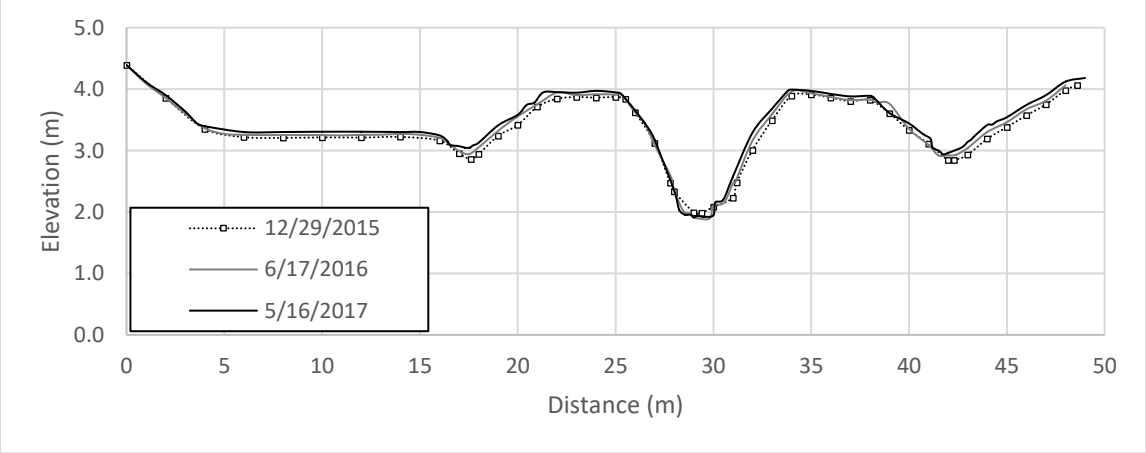

Figure 11. Cross-section profile of Unit 3 backwater transect.

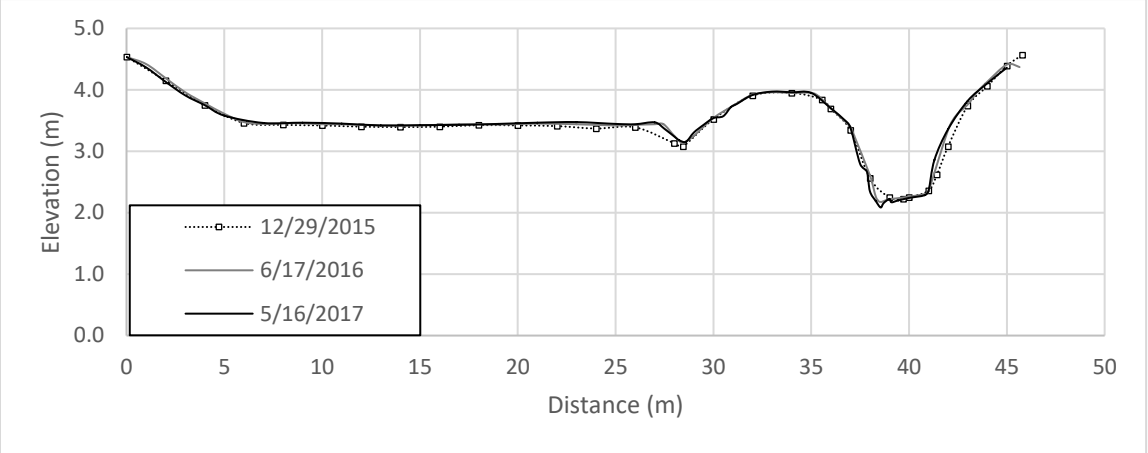

Figure 12. Cross-section profile of Unit 3 middle transect.

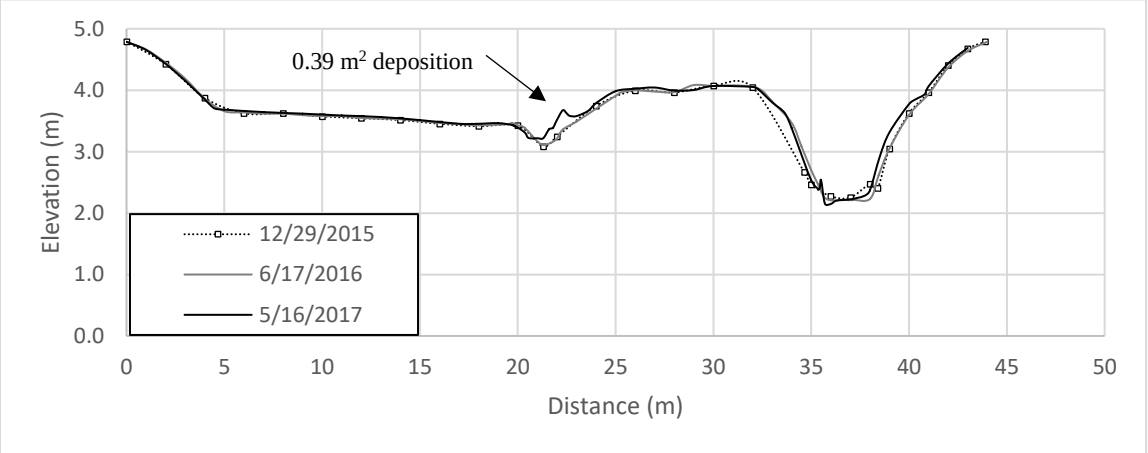

Figure 13. Cross-section profile of Unit 3 expansion transect.

Table 2. Cross-sectional areas within the main channel and percent change between surveys.

	Cross-sectional Area (m^2)			Percent Change	
Transect Location	Winter 2015	Summer 2016	Summer 2017	2015 - 2016	2016 - 2017
Unit 1 Backwater	4.51	4.45	5.30	-1.33	19.18
Unit 1 Middle	6.87	6.82	7.05	-0.78	3.34
Unit 1 Expansion	7.15	6.51	7.36	-8.87	13.05
Unit 2 Backwater	7.78	8.18	8.45	5.10	3.33
Unit 2 Middle	5.12	5.38	6.06	5.14	12.58
Unit 2 Expansion	4.64	5.27	5.82	13.49	10.47
Unit 3 Backwater	8.72	8.47	8.10	-2.91	-4.31
Unit 3 Middle	7.41	7.10	7.26	-4.09	2.24
Unit 3 Expansion	9.61	8.87	8.44	-7.73	-4.78

Table 3. Lowest elevation of main channel bed at each cross-section survey location.

	Lowest elevation NAVD 88 (m)			Difference (m)	
Transect	Winter 2015	Summer 2016	Summer 2017	2015 - 2016	2016 - 2017
Unit 1 Backwater	0.91	1.01	0.7	0.1	-0.31
Unit 1 Middle	0.87	0.91	0.76	0.04	-0.15
Unit 1 Expansion	0.86	0.95	0.65	0.09	-0.3
Unit 2 Backwater	1.63	1.38	1.22	-0.25	-0.16
Unit 2 Middle	1.54	1.36	1.14	-0.18	-0.22
Unit 2 Expansion	1.58	1.25	1.08	-0.33	-0.17
Unit 3 Backwater	1.99	1.89	1.91	-0.1	0.02
Unit 3 Middle	2.23	2.2	2.09	-0.03	-0.11
Unit 3 Expansion	2.25	2.21	2.15	-0.04	-0.06

Table 4. Deposition and scour for all channel cross-sections between survey seasons.

	2015 - 2016		2016 - 2017	
Transect	Deposition (m^2)	Scour (m^2)	Deposition (m^2)	Scour (m^2)
Unit 1 Backwater	0.46	0.23	0.05	0.89
Unit 1 Middle	0.29	0.23	0.08	0.47
Unit 1 Expansion	0.89	0.03	0.15	1.02
Unit 1 Total	***1.64***	***0.50***	***0.28***	***2.37***
Unit 2 Backwater	0.45	0.87	0.43	0.74
Unit 2 Middle	0.28	0.44	0.43	0.95
Unit 2 Expansion	0.29	0.79	0.35	0.87
Unit 2 Total	***1.02***	***2.09***	***1.21***	***2.56***
Unit 3 Backwater	0.49	0.19	0.47	0.09
Unit 3 Middle	0.53	0.14	0.15	0.30
Unit 3 Expansion	1.06	0.26	0.66	0.27
Unit 3 Total	***2.08***	***0.60***	***1.28***	***0.66***
Total	***7.41***	***5.79***	***4.26***	***10.54***

Longitudinal Profile

Main Channel

Due to the resolution of the longitudinal profile compared to the spatial scale of the main channel, the results are presented as a complete profile (Figure 14), the complete profile as a 50 period moving average trend line (Figure 15), and as individual segments (Figures 16 – 18) of 700 m lengths to provide clearer illustrations of the elevation trends. The reach ranging 1400 m – 1500 m was intentionally not included in the segmented figures as it was not adjacent to a channel unit, was subsequently surveyed at a 50 m resolution (i.e. only 3 data points) and its omission allows the display of equal scale (i.e. 700 m reach) figures for higher resolution areas. Additionally, elevation values were summarized as averages for each channel reach and the difference between the survey years was calculated (Table 5).

Due to the spatial and temporal scale of the main channel longitudinal profile survey (e.g. 2.2 km surveyed over 4 days), it was known prior to implementation that exact replication during the second survey season would be difficult. To calculate a measure of vertical precision between survey seasons, the elevations of identical stationary surfaces (e.g. large woody structures, cross-section benchmarks, fence posts) were collected during both surveys to allow a relative comparison. The standard deviation of surveyed stationary elevation was 0.015 m, applying a 95% confidence interval, the margin of error for surveyed points is calculated as ±0.03 m. Consequently, elevation values within 0.06 m between surveys years were within the margin of error and should be considered as ‘no

change.' Fortunately, all the average trends fell outside this margin for all assessed stream reaches.

In agreement with the channel cross-section surveys, longitudinal profile surveys show a dominant trend of scouring within the main channel demonstrated by elevation reductions from summer 2016 to summer 2017. However, as the survey was conducted within the thalweg (i.e. lowest point), this may be reflective of the scouring of a narrow thalweg within the middle portion of the channel while other portions of the channel bottom remain relatively stable. This trend is illustrated well by the Unit 2 middle and backwater cross-section profiles (Figures 8 and 9, respectively). When local elevation fluctuations are removed, the ubiquitous decrease in elevation is clearly visible in the 50 period moving average trend line (Figure 15) and the summary of average elevations (Table 5).

Beginning at the most upstream reach, the first 700 m of the main channel was the most stable of the entire project reach and only experienced 0.08 m mean lowering in elevation (Table 5). The majority of the larger elevation changes were due to the deepening of incipient pools between the summer 2016 and 2017 surveys (Figure 14). In particular, the pools at approximately 225 m and 480 m deepened by 0.56 m and 0.27 m, respectively while both elongating in length. Additionally, new pools formed at approximately the 275 m to 285 m distances immediately adjacent to the entrance to the Unit 2 active bench. Within the 701 m to 1400 m reach the most identifiable change is the development of a 50-meter-long pool from 755 m to 805 m along the profile (Figure 17). The pool is characterized by an average elevation reduction of 0.5 m with a maximum of 0.89 m

resulting in a total calculated scour area of 27.95 m^2. The pool is located within Unit 2 and occurs approximately 130 m downstream of a relatively sharp meander and the re-entrance of an unnamed secondary channel.

While the first 1500 m displayed relatively high spatial variability in scour depths, the furthest downstream 700 m, dominated by an intertidal hydrology regime, exhibited relatively uniform channel bed lowering, with the exception of a single point at 1800 m (Figure 18). Only three readings (1940 m – 1950 m) showed a drastic change in elevation due to the formation of a 10-meter-long pool. On average, the thalweg of the main channel within the Unit 1 decreased in elevation by 0.29 m with a small standard error of 0.013 (Table 5) indicating uniform lowering.

Mean channel bottom lowering increased from upstream to downstream. The highest upstream fluvial dominated channel unit (i.e. Unit 3) exhibited the smallest average elevation decrease (i.e. 0.08 m) and the largest increase was identified at the most downstream intertidal channel unit (i.e. Unit 1) with a decrease of 0.29 m (Table 5). However, the mixed intertidal main channel along Unit 2 exhibited the largest total topographic variability and largest increase in variability between survey years, represented by the standard deviation of elevation values (Table 5). The intertidal downstream unit (i.e. Unit 1) was characterized by the highest total topographic variability (i.e. largest fluctuations around the mean elevation) but showed the second highest increase in variability between survey years (Table 5).

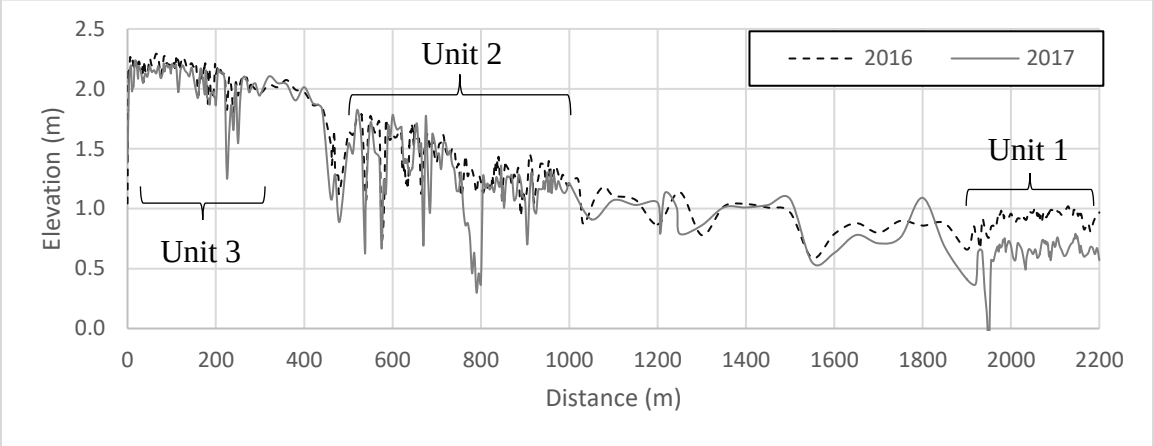

Figure 14. Longitudinal profile performed in summer 2016 and summer 2017 along the 2.2 km project reach.

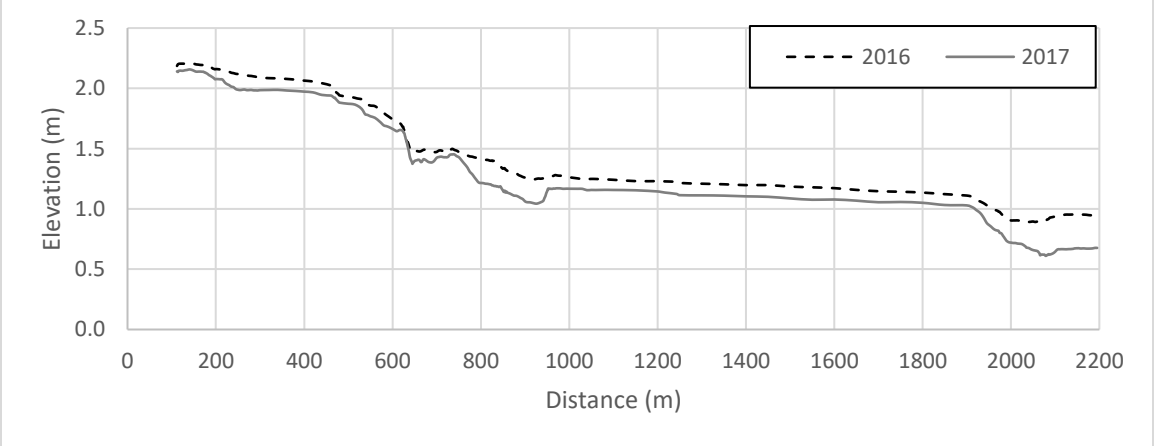

Figure 15. Fifty period moving average of longitudinal profile.

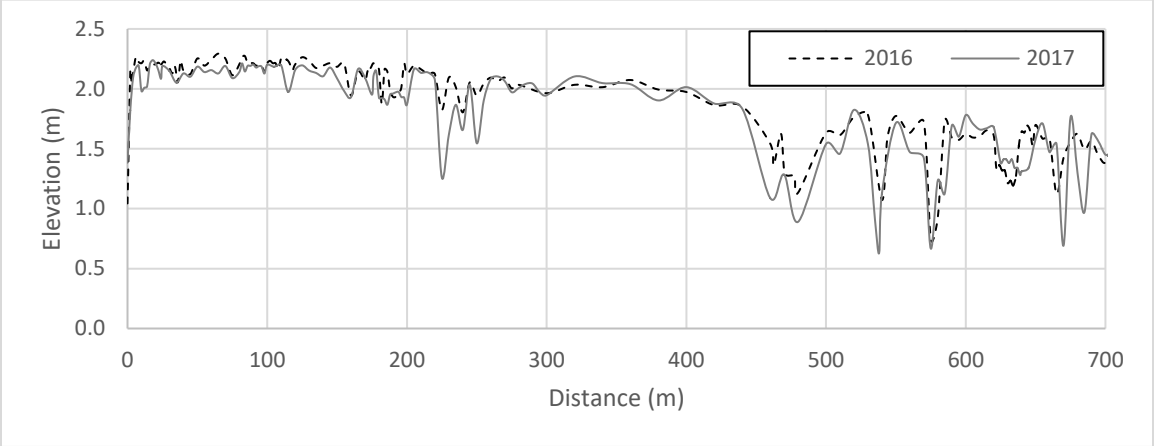

Figure 16. Segment of longitudinal profile covering the reach from 0 m (upstream) – 700 m (downstream).

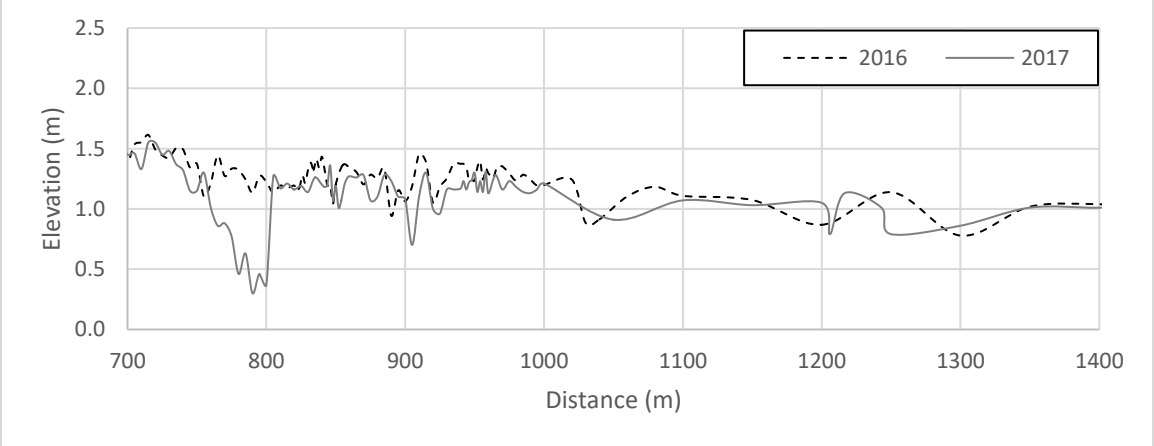

Figure 17. Segment of longitudinal profile covering the reach from 700 m (upstream) - 1400 m (downstream).

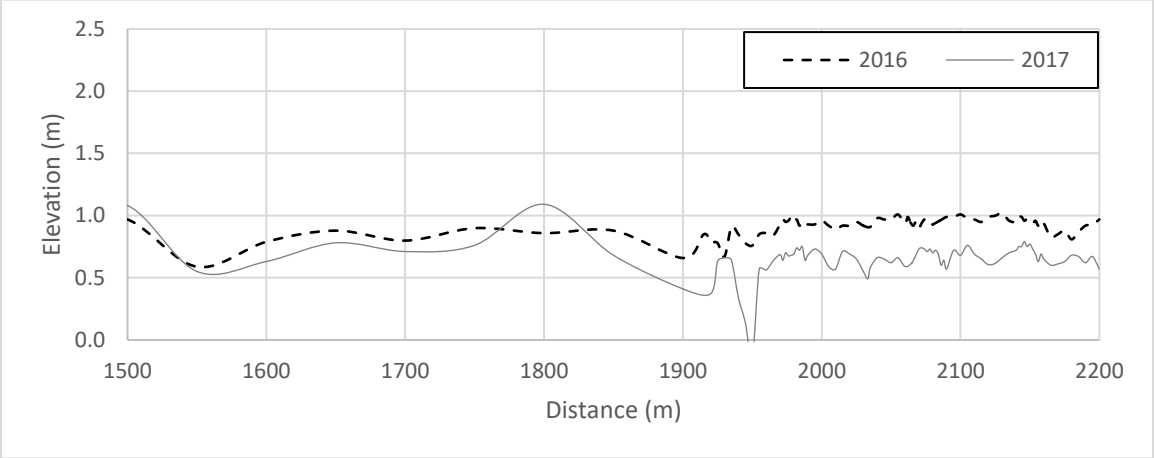

Figure 18. Segment of longitudinal profile covering the reach from 1500 m (upstream) – 2200 m (downstream).

Table 5. Average elevation and standard deviations within the main channel by channel unit from summer 2016 to summer 2017.

	Average elevation (m)			Standard Deviation	
	2016	2017	Change	2016	2017
Unit 1	0.93	0.64	-0.29	0.06	0.13
Unit 2	1.35	1.23	-0.12	0.18	0.29
Unit 3	2.13	2.05	-0.08	0.17	0.18

Secondary Channels

In general, the secondary channels within Units 2 and 3 were characterized by dominant depositional regimes while the Unit 1 side channel remained relatively stable and displayed scouring tendencies where changes were observed. Longitudinal profiles within the side channel of each channel unit were surveyed concurrently with the main channel (Figures 19, 21, and 22). Cumulative difference (i.e. the net change in area from year to year where scour is negative and deposition is positive) in cross-sectional areas were also calculated and presented with longitudinal active bench width to identify changes in the scour and deposition regimes across the range of channel geometries (Figures 23, 24, and

25). Changes in cross-sectional areas were also summarized by their scour and deposition characteristics for the entire secondary channel length (Table 6) and slopes for each year were calculated omitting the channel reach prior to and including the deposition peak (where applicable) (Table 7) so not to be skewed by a single point of high deposition. In effect, the relatively large elevation increase occurring at the channel entrances was removed because it would result in a larger slope than is present along the remainder of the channel.

Unit 1 exhibits an adverse slope increasing in elevation from the upstream to downstream (Figure 19) resulting in reverse water flows towards the upstream main channel flow direction during ebb tides (Figure 20). During flood tides, the floodplain and secondary channel fill from the upstream end and flow downstream until tidal heights are sufficient to overtop the downstream lip.

The upstream and downstream extents of the Unit 1 side channel remained relatively stable, with most elevation values changing ±20 mm between the two survey years. However, the middle portion (i.e. approximately 90 – 200 m on Figure 19) of the side channel exhibited demonstrable scouring with maximum scour depths in several survey points of up to 0.11 m. A steep increase in scour occurs as the channel expansion reaches its full width (Figure 23), suggesting the main mechanism driving the scour dynamics may be related to the interaction of incoming flows with the geometry of the floodplain. Across the entire profile, scour resulted in a total areal increase of 7.59 m^2 while deposition decreased the area of the profile by 1.59 m^2 (Table 6).

The Unit 2 side channel experienced the most uniform depositional dynamics between the summer of 2016 and 2017 and averaged a 0.13 m elevation increase across the entire profile (Figures 21 and 24) with a depositional area of 41.77 m^2 (Table 6). The distinct linear trend in Figure 24 demonstrates the strong uniformity of deposition within the Unit 2 secondary channel regardless of the channel width. Despite the relatively uniform deposition, the Unit 2 secondary channel slope increased between survey years from 0.0011 to 0.0013 (Table 7).

Unit 3 displayed variable deposition dynamics with large elevation increases at the upstream expansion sections, relatively stable elevation within the middle sections, and relatively moderate scouring within downstream backwater areas (Figures 21 and 24). A well-defined deposition peak exists at 70 m from the floodplain entrance exhibiting the largest elevation increase (i.e. 0.28 m) of all side channels (Table 6). The peak is strongly correlated with a rapid expansion of the channel width resulting in lower water depths and a decline in boundary shear stress and water velocities. At this point, the channel reaches a critical width where water velocities decline below a threshold capable of carrying the dominant grain sizes in suspension. Despite the large depositional environment at the upstream end of the channel unit the reach only exhibited a total change in area due to deposition of 11.82 m^2 compared to a 4.26 m^2 change due to scour (Table 6). The downstream area of the Unit 3 secondary channel (i.e. after the deposition peak at 70 m) also displayed the largest slope, increasing from the summer of 2016 to the summer of 2017 from 0.0016 to 0.002, respectively (Table 7).

Units 2 and 3 also display moderate deposition immediately at the channel entrance with elevations increasing 0.18 m and 0.16 m, respectively, followed by depressions where the side channels remain narrow. Similarly to the deposition peak described above for Unit 3, the rapid decrease in channel depth as water spills onto the floodplain results in a loss of carrying capacity and immediate deposition on the lip of the floodplain entrance. Following the immediate deposition, both channel unit entrances are characterized by variable length depressions of 36 m and 26 m within Units 2 and 3, respectively (Figures 20 and 21). Deposition occurs downstream of the depressions creating natural levees with maximum depths of 0.26 m within Unit 2 and 0.29 m within Unit 3. As a result, flood flows within the main channel may be sufficient to spill into the secondary channels but are blocked from flowing onto the floodplains. The depressions also create standing water conditions between rain events at the secondary channel unit entrances.

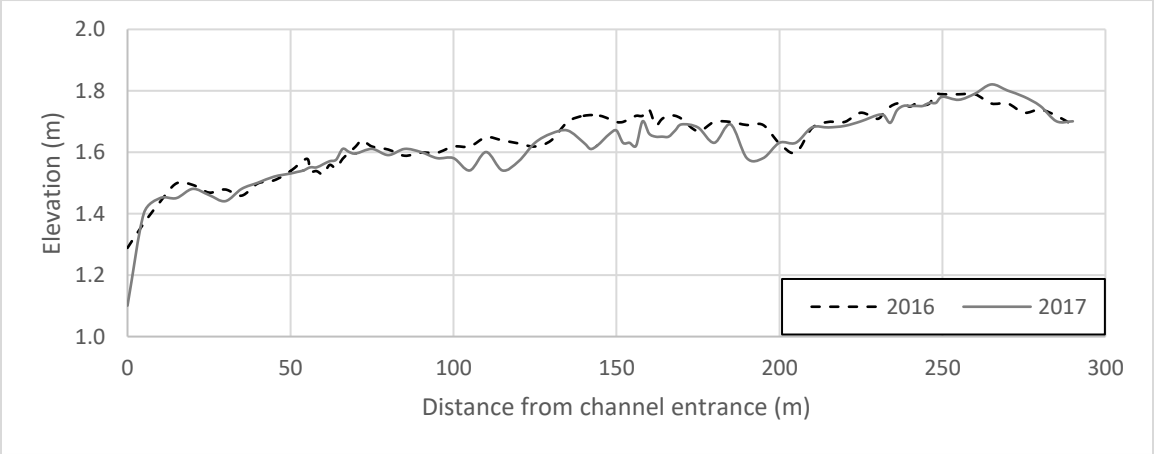

Figure 19. Longitudinal profile of Unit 1 secondary channel.

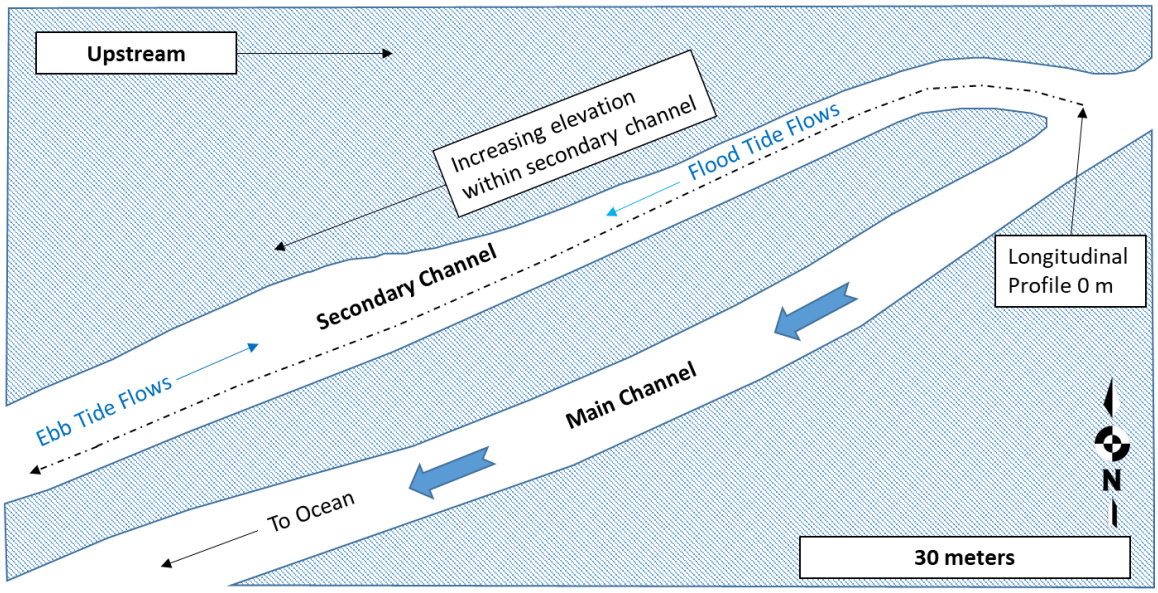

Figure 20. Scale schematic of Unit 1 secondary channel entrance illustrating the direction of tidal flows in relation to main channel flows.

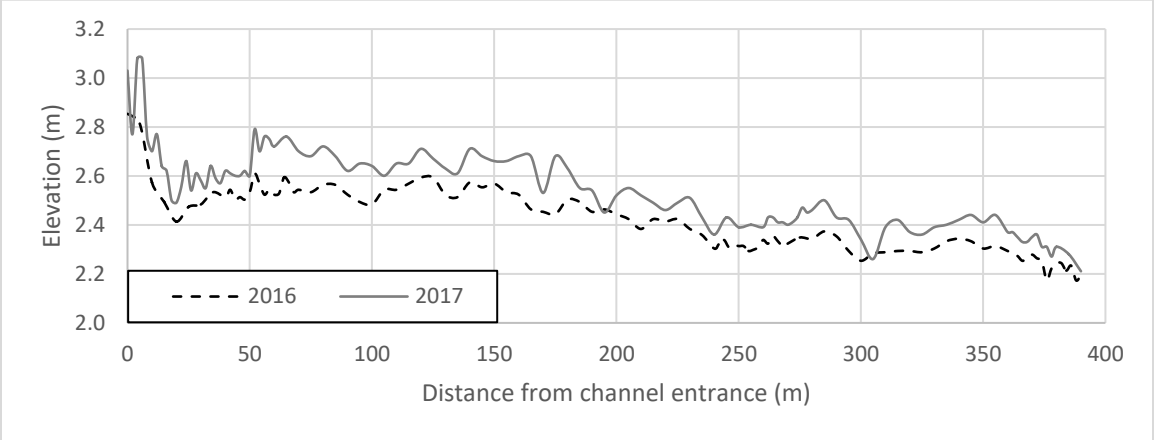

Figure 21. Longitudinal profile of Unit 2 secondary channel.

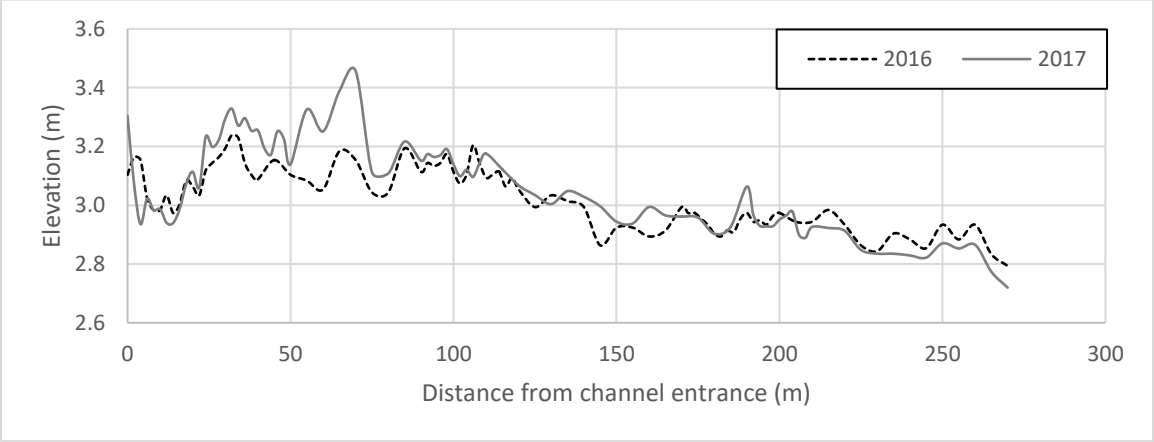

Figure 22. Longitudinal profile of Unit 3 secondary channel.

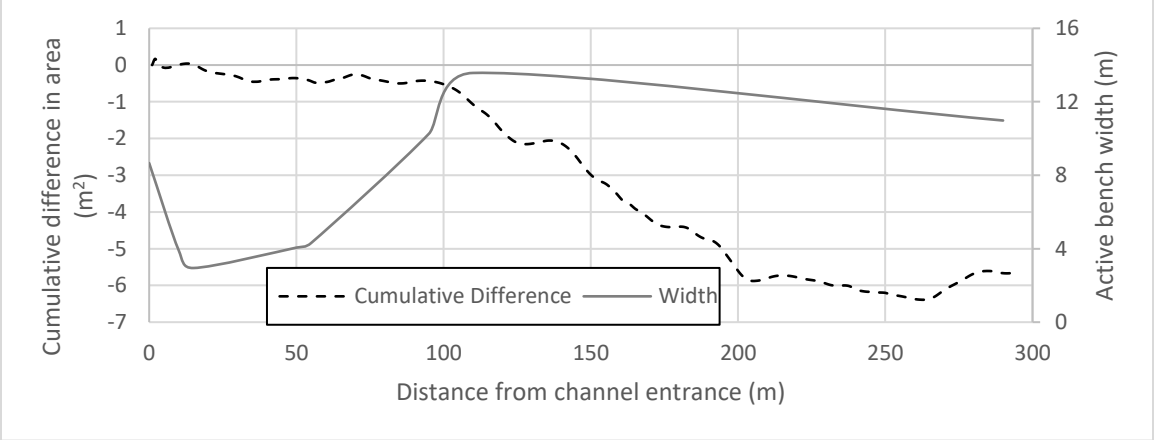

Figure 23. Cumulative difference (i.e. increases indicate deposition and decreases indicate scour) in cross-sectional area and active bench width within the Unit 1 secondary channel. Note the width is displayed on a secondary y-axis.

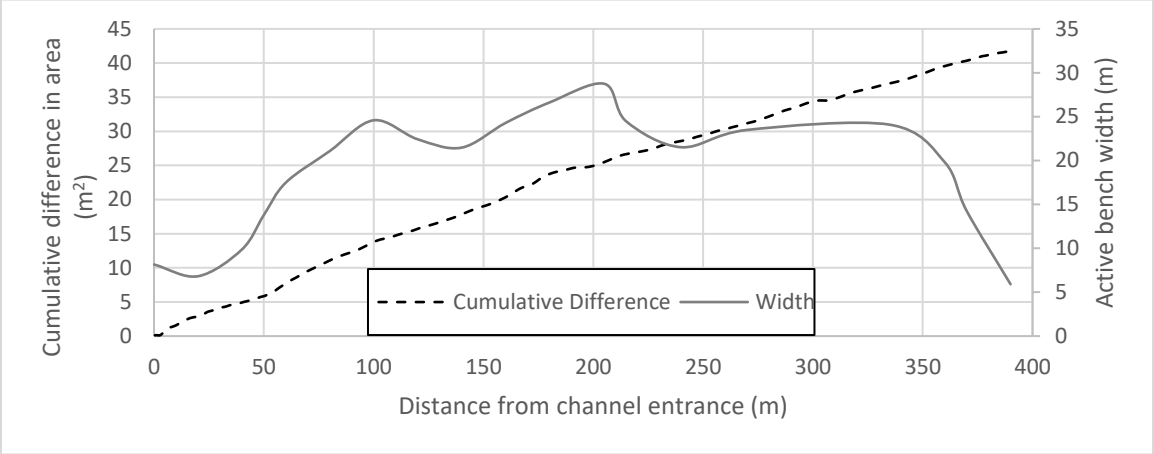

Figure 24. Cumulative difference (i.e. increases indicate deposition and decreases indicate scour) in cross-sectional area and active bench width within the Unit 2 secondary channel. Note the width is displayed on a secondary y-axis.

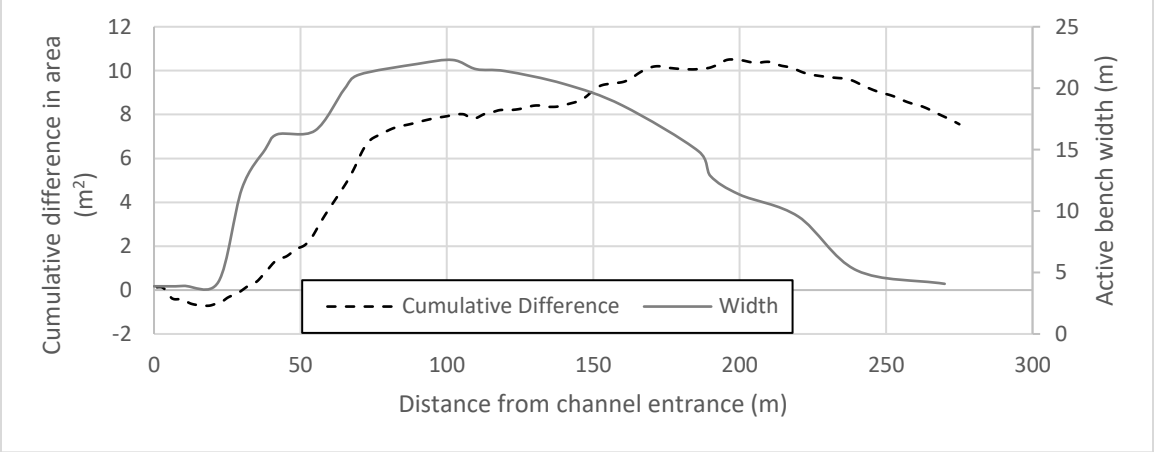

Figure 25. Cumulative difference (i.e. increases indicate deposition and decreases indicate scour) in cross-sectional area and active bench width within the Unit 3 secondary channel. Note the width is displayed on a secondary y-axis.

Table 6. Differences in cross-sectional area by channel unit.

	Observed Difference in cross-sectional area (m^2)		
	Unit 1	Unit 2	Unit 3
Deposition	1.59	41.77	11.82
Scour	-7.59	-0.05	-4.26

Table 7. Secondary channel slopes after deposition peak by unit and year.

	Unit 1	Unit 2	Unit 3
2016	0.001	0.0011	0.0016
2017	0.001	0.0013	0.002

Sedimentation Surveys

Tile Sedimentation

Mean deposition was significantly higher in summer 2017 compared to summer 2016 and the largest mean deposition for both survey years was recorded within the Unit 3 secondary channel of 2.75 ± 2.12 g/ cm^2 in WY 2016 and 6.35 ± 1.37 g/ cm^2 in WY 2017 (Figure 26). The lowest mean deposition within depositional areas was recorded within the Unit 2 secondary channel following the 2016 WY with deposition equaling 0.83 ± 0.28 g. Mean deposition in grams within each surveyed secondary channel unit was calculated following the 2016 WY and 2017 WY (Figure 26). Tile sedimentation surveys are only designed to monitor depositional environments and because the majority of Unit 1 was characterized by a mixed scour regime (Figure 19) in the summer 2017 surveys, most of the tiles were unable to capture any sediment and therefore they have been omitted in Figure 26. The only tile to capture sedimentation was located 5 m from the channel entrance and 3.65 g / cm^2 of sedimentation was recorded.

Welch's t-tests were performed on the mean deposition by survey year for channel Units 2 and 3 and indicated significantly higher deposition occurred following the 2017 WY year than 2016 with p-values of 0.0065 and 0.008, respectively. Mean deposition was also substantially higher within Unit 3 compared to Unit 2 but is highly skewed by a few

large values up to three standard deviations above the mean. These anomalous tile readings were located near the deposition maximum shown on the Unit 3 longitudinal profile at approximately 40 m distance from the entrance (Figure 22). The large deposition recorded atop these tiles explains why these results contradict the cumulative areal deposition results shown in Table 6 indicating greater total deposition occurred within the Unit 2 secondary channel.

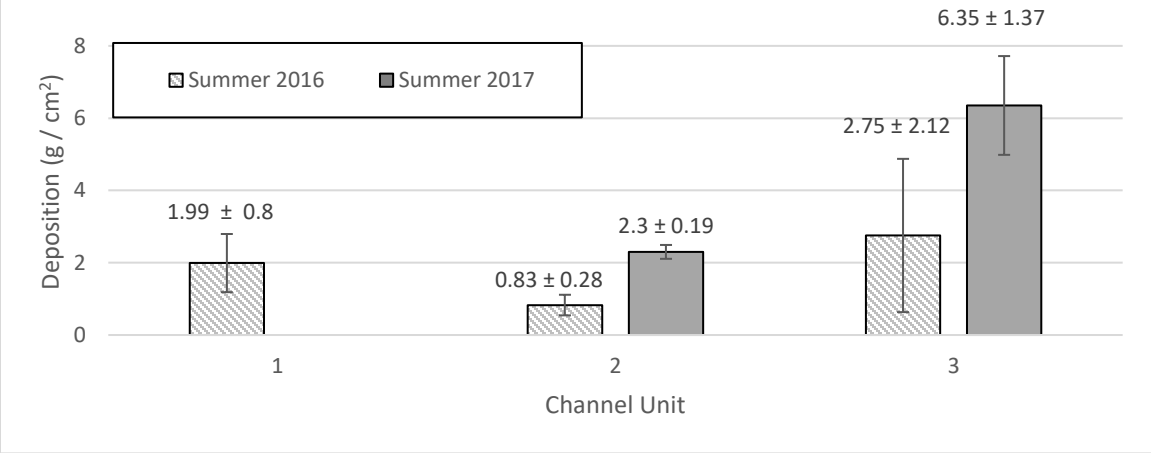

Figure 26. Mean deposition given in mass per unit area by channel unit and survey year; bars represent standard error.

To isolate tidal effects in the absence of fluvial inputs, the depths of deposition atop tiles within the tidally dominated Unit 1 secondary channel were recorded at the beginning and end of summer 2016. Deposition was recorded at each tile array with the lowest deposition depth occurring within the middle section (8.33 ± 1.06 mm) and largest deposition furthest from the entrance (16.56 ± 13.51 mm) (Figure 27). Combined with the dry season longitudinal profile, results indicate that tidal dynamics contribute to slow depositing of sediments onto the secondary channel which can remain in storage during moderate rainfall years (i.e. 2015 – 2016) or be re-suspended and scoured out of the

system during larger cumulative rainfall years (i.e. 2016 – 2017). Furthermore, tidal deposition within the Unit 1 secondary channel seems to be concentrated longitudinally at the channel entrance where water depths are immediately reduced and at the higher tide line elevations with less deposition occurring in the mid-tide elevations.

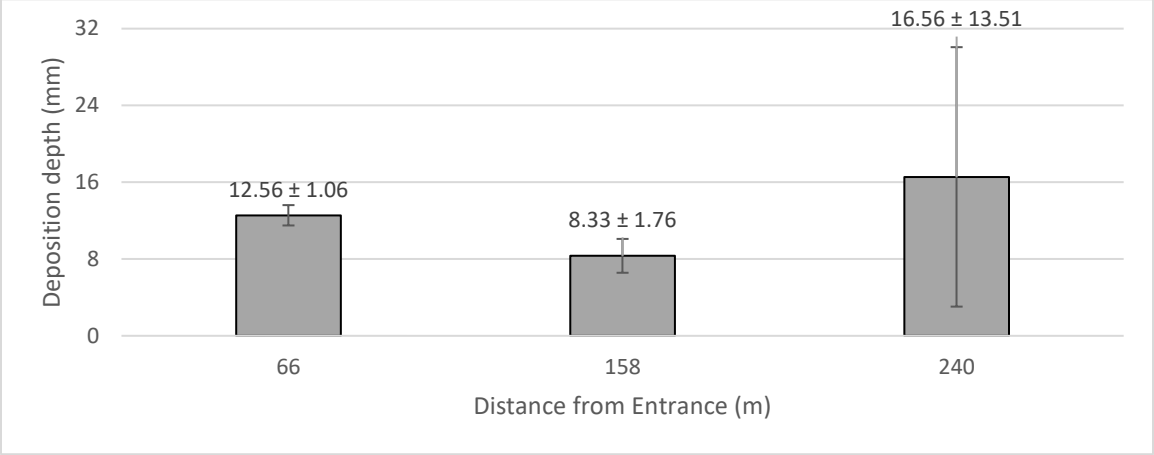

Figure 27. Tidal deposition recorded within the Unit 1 secondary channel during the summer 2016 dry season.

Additionally, the longitudinal distribution of deposition was calculated for the Unit 2 and 3 secondary channels (Figures 28 and 29). Tile deposition data support the findings of the longitudinal profile surveys (Figures 21 and 22) showing relatively uniform deposition occurring within the Unit 2 secondary channel (Figure 28) and highly variable deposition within Unit 3 (Figure 29). Large standard errors were calculated at the Unit 3 expansion cross-section (Figure 29, 24 m distance) where the mass of deposited sediment ranged from 1.69 g/ cm^2 – 19.04 g/ cm^2 in the summer of 2016 and from 3.74 – 26.44 g/ cm^2 in summer 2017. The large discrepancies occur because the tiles deployed at this location span the initial channel widening section where large volumes of sediment fall out of suspension as channel area increases and flow velocity decreases.

For reasons described in the ‘Methods’ section, depth was recorded opportunistically throughout the wet season concurrently with the entrance flow rate surveys at tiles near the Unit 3 secondary channel entrance (i.e. 20 m, 24 m, 28 m, and 40 m). When overlain with cumulative precipitation (Figure 30) for the entire season, it’s apparent that deposition in areas before the floodplain channel expansion occurs (20m and 24 m) only during the first flood events of the season. Conversely, tiles surveyed in areas after the floodplain expansion (28 m and 40 m) experience a linear increase in deposited sediment proportional to the season’s cumulative precipitation. The absence of additional deposition atop upstream tiles likely indicates channel depth within the narrow portion of the secondary channel has reached an equilibrium between peak flow and settling velocities.

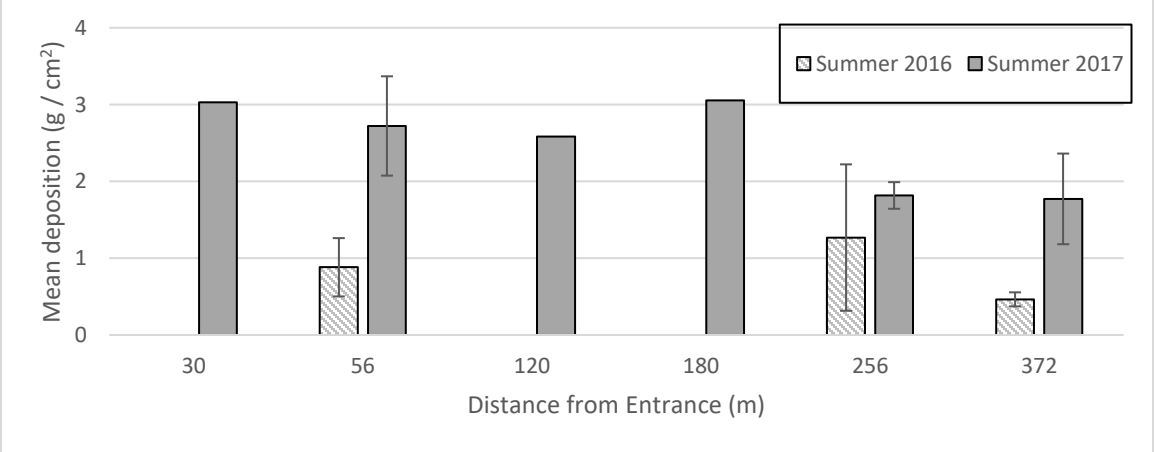

Figure 28. Mean deposition given in mass per unit area from the Unit 2 secondary channel entrance. Note: SE bars are shown for areas with multiple tiles located at cross-section transect locations.

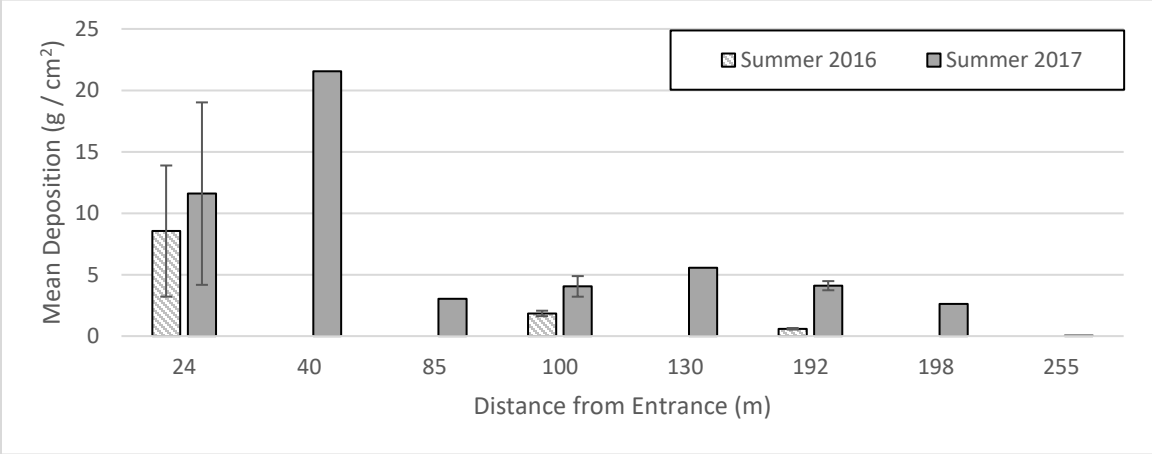

Figure 29. Mean deposition given in mass per unit area from the Unit 3 secondary channel entrance. Note: SE bars are shown for areas with multiple tiles located at cross-section transect locations.

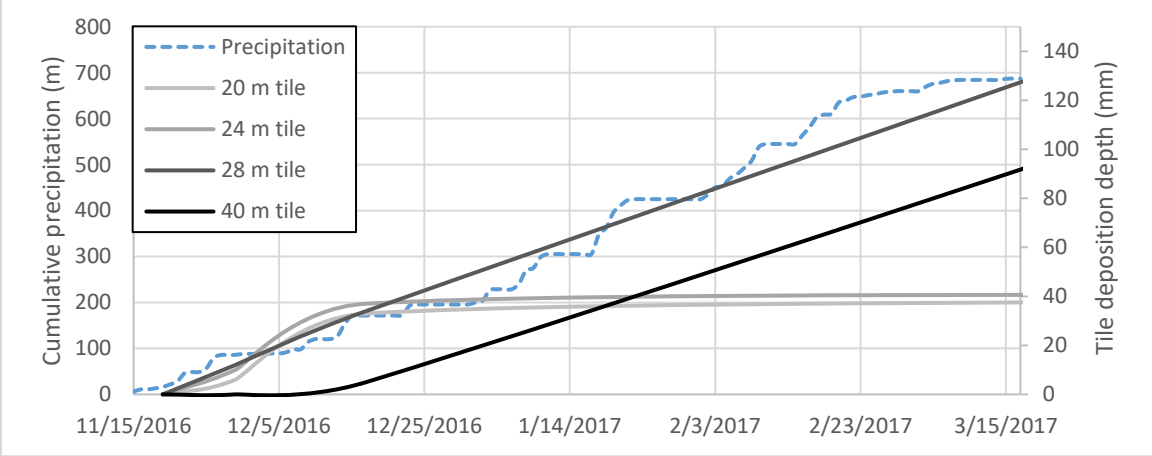

Figure 30. Deposition and precipitation accumulation over time during WY 2017 at four tiles closest to the Unit 3 entrance. Note tile accumulation lines increase in darkness as distance increases from the channel entrance and are presented on a secondary y-axis.

Grain Size Distributions

Soil grain size distribution analyses were conducted on sediment deposited atop secondary channel tiles collected during the summer 2016 surveys. Data are presented as a 100% stacked bar chart to illustrate the proportion of sand, silt, and clay for sediments at each cross-section location (Figure 31) and listed in Table 8. Grain size proportion data

have also been overlain on the USDA soil triangle to allow visualization of channel unit and section grouping by soil category (Figure 32). The percent sand content was also plotted by channel unit section to identify the gradient of the distribution of sand from upstream to downstream.

The coarsest proportions of grain sizes was identified at the Unit 3 expansion section with a total sand percentage of 86.3%. The largest proportion of fine grain sizes was recorded at the Unit 2 backwater section where silt and clay comprised a combined 95.1% of the sample (i.e. 37.9% clay and 57.2% silt). Unit 1 displayed the least variable grain size proportions. Figure 32 shows all the samples were clustered within the sandy loam classification.

The longitudinal gradient for sand proportion of deposited sediments was calculated for each secondary channel unit (Figure 33). Units 1 and 2 exhibited low sand proportions at secondary channel entrances and exits with the highest sand proportions identified within the middle of the units. A strong linear gradient of sand proportions was identified within the Unit 3 secondary channel, with coarse-grained particles deposited at the channel entrance decreasing to the deposition of primarily fine-grained sediments at the downstream end. Within Unit 3, sand proportions were highest at the upstream expansion section with 86.3% of deposited sediments consisting of sand-sized particles decreasing to 48% within the middle reach and only 15.3% at the downstream backwater transect tiles.

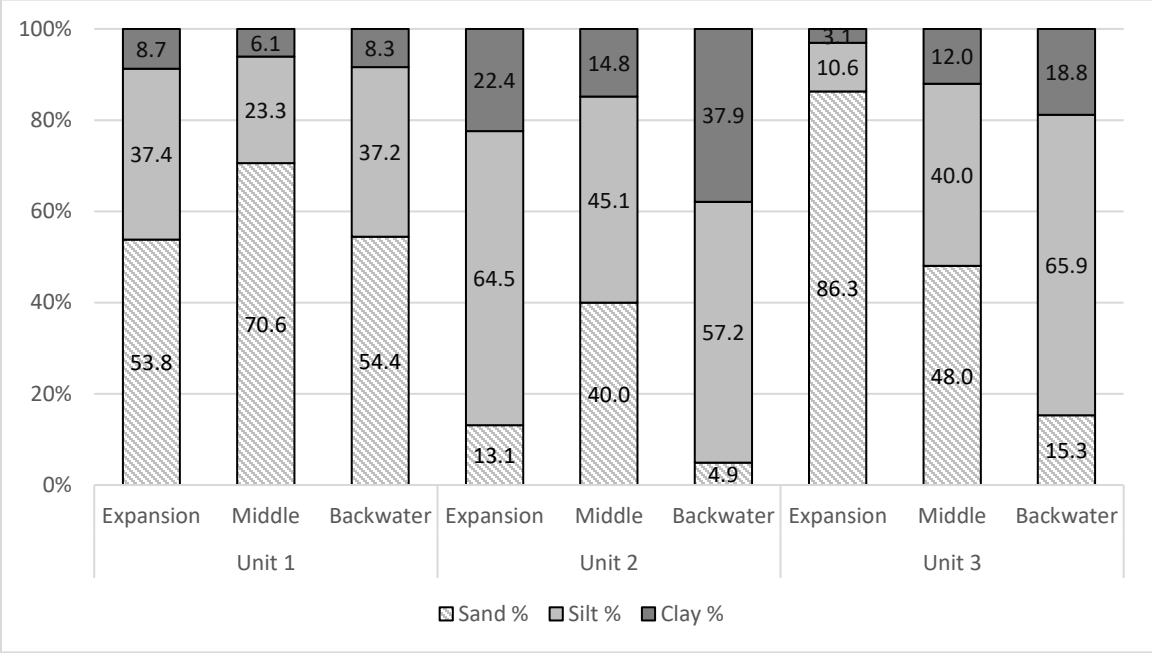

Figure 31. Grain size distribution of deposited sediment by transect collected during summer 2016. Expansion sections constitute upstream inflow areas of the secondary channels, backwater sections are the downstream areas where flows re-enter the main channel, and middle sections are located between the two.

Table 8. Distribution of grain sizes for each cross-section transect.

Cross-section ID	Sand %	Silt %	Clay %	Texture
1 Expansion	53.8	37.4	8.7	Sandy Loam
1 Middle	70.6	23.3	6.1	Sandy Loam
1 Backwater	54.4	37.2	8.3	Sandy Loam
2 Expansion	13.1	64.5	22.4	Silt Loam
2 Middle	40.0	45.1	14.8	Loam
2 Backwater	4.9	57.2	37.9	Silty Clay Loam
3 Expansion	86.3	10.6	3.1	Loamy Sand
3 Middle	48.0	40.0	12.0	Loam
3 Backwater	15.3	65.9	18.8	Silt Loam

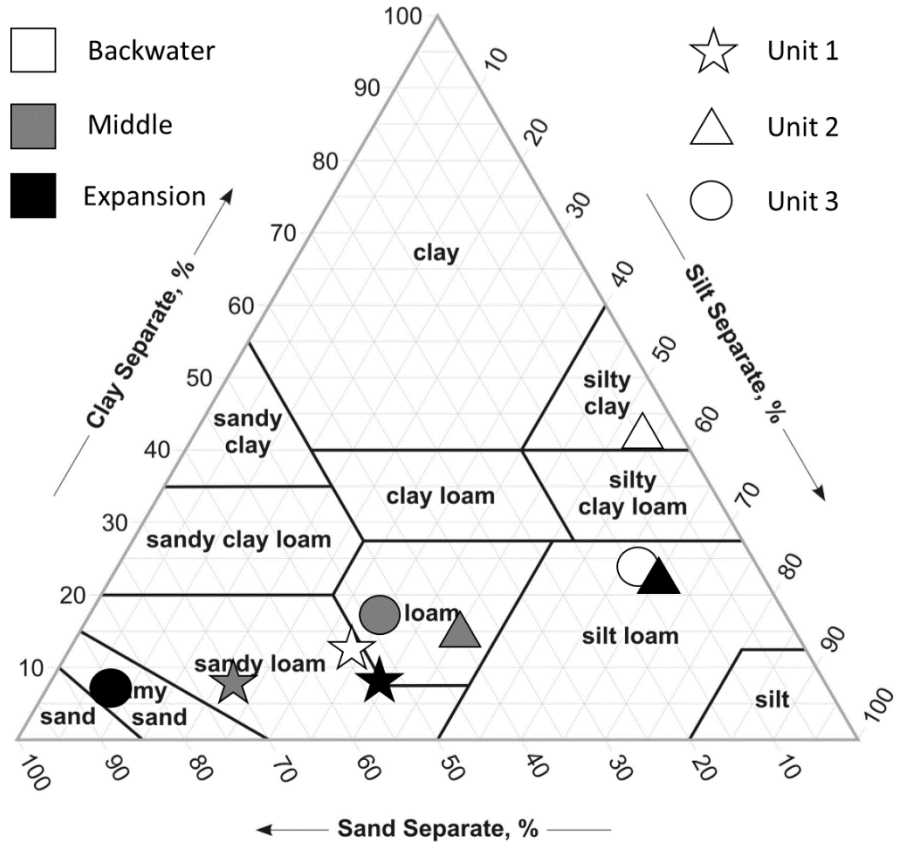

Figure 32. Grain sizes by channel unit and cross-section overlain on the USDA soil classification triangle.

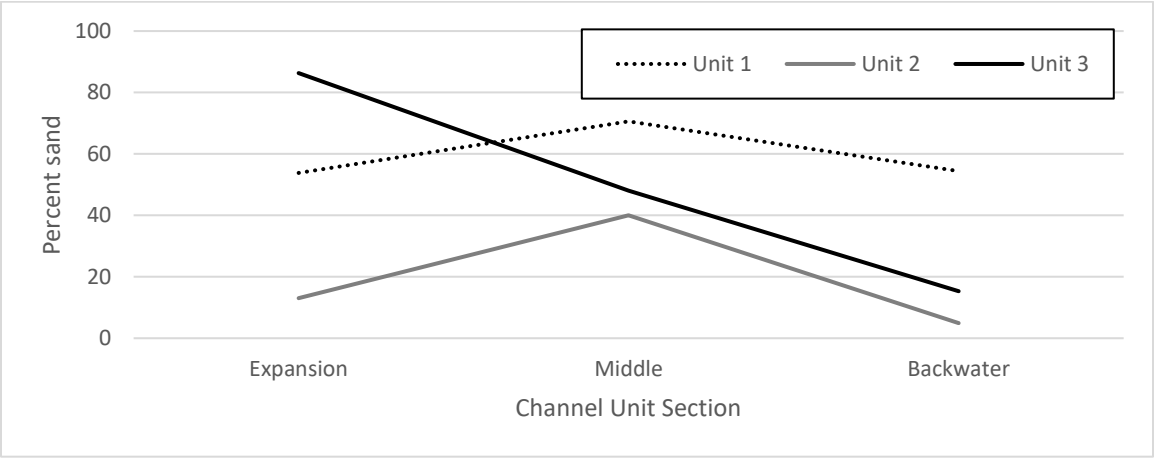

Figure 33. Percent sand of soil grain size sample by channel unit and section.

Total Station Surveys

Total station surveys are presented as elevation maps showing the relative elevation difference between summer 2016 and summer 2017 for the secondary channel entrances of Units 2 and 3 (Figures 34 and 35). Unit 1 survey results are not presented due to a calibration error creating dissimilar surfaces between the annual surveys and did not permit comparisons. Additionally, it should be noted, the area of the Unit 2 survey is roughly half the size of the Unit 3 survey (i.e. 80 m^2 vs. 180 m^2) due to the relative uniformity of deposition identified by the longitudinal profile surveys within the Unit 2 entrance and the presence of dense vegetation. Vegetation required the collection of a higher density of elevation data points to increase confidence in the final created surfaces as breaks in surface slope and general topographic features were unidentifiable in the field. Following the longitudinal profile survey of summer 2017 when it was determined longitudinal deposition occurred uniformly through the secondary channel, a decision was made to concentrate sampling efforts closer to the entrance to create a more accurate surface within the dense vegetation than poorly survey the entire survey area.

Results of the total station surveys generally support the findings of the longitudinal profile slices (Figures 21 and 22) showing relatively uniform deposition within the Unit 2 secondary channel entrance and variable erosion and scour dynamics within Unit 3. Figure 34 shows positive elevation increases of similar magnitude from summer 2016 to summer 2017 within almost the entire Unit 2 secondary channel entrance supporting the findings of the longitudinal profile (Figure 21). Larger relative deposition occurs along a

band roughly in-line with the observed thalweg (see ‘Channel Entrance Flow Rate’ results for additional information) on the northern half of the channel entrance.

Elevation differences were variable within the Unit 3 secondary channel entrance (Figure 35) with deposition occurring immediately at the entrance, followed by a relatively well-defined scour path. This pattern of variability is supported by the findings on the Unit 3 longitudinal profile survey (Figure 22). Additionally, the scour path roughly follows the observed entrance flow thalweg described in greater detail in the channel entrance flow rate results section. This suggests that, while sediment is falling out of suspension immediately at the channel entrance due to decreased depths, flow rates are sufficiently swift to entrain sediments along the thalweg to create the scour pool and leveeing observed on the longitudinal profile (Figure 22). Deposition at the downstream end of the survey is caused by the expansion of the channel width, allowing flows to spread out across the floodplain, effectively reducing depth and velocity below the settling velocity of coarser grained particles.

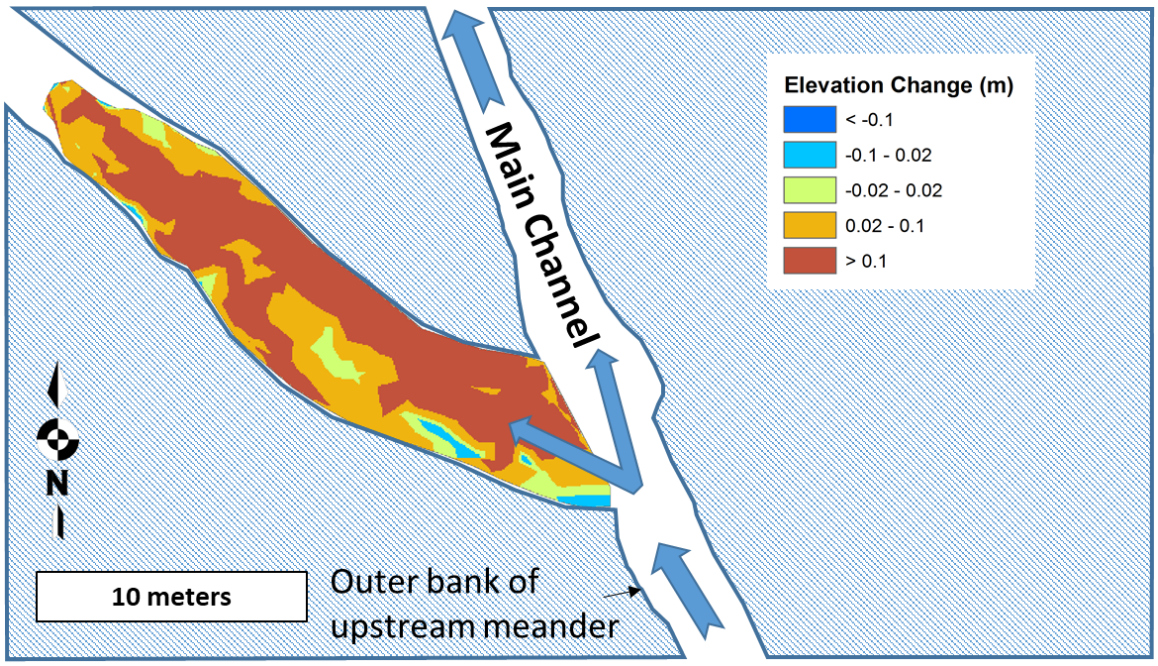

Figure 34. Elevation differences between summer 2016 and summer 2017 within the Unit 2 secondary channel entrance.

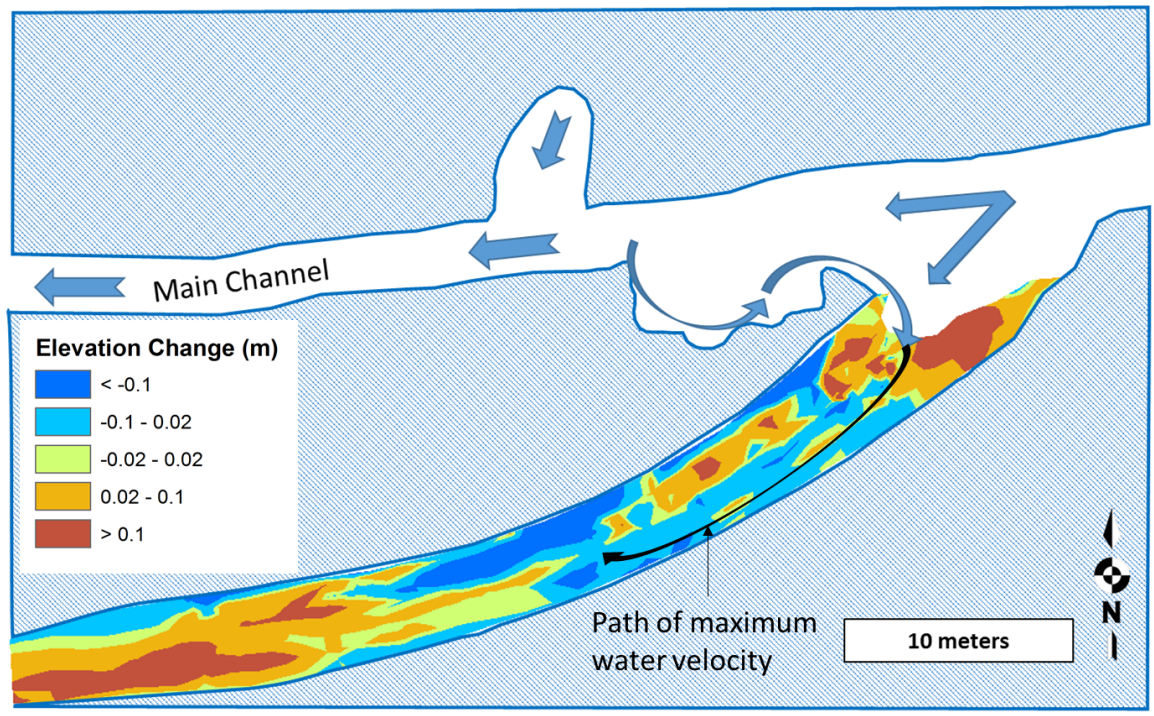

Figure 35. Elevation differences between summer 2016 and summer 2017 within the Unit 3 secondary channel entrance.

River Discharge surveys

Continuous Water Surface Elevation

Data are presented from March 2016 to March 2017 showing the continuous water surface elevation (WSE) of flows within the main channel at each channel unit by water year (WY) (Figures 36 – 40). Stage height monitoring equipment deployed to monitor water heights at Unit 1 malfunctioned due to exposure to daily tidal waters. As a result, data are not presented for the 2016 – 2017 WY. Gaps in the graphs indicate that WSEs were below the elevation of the stage height logger. Additionally, due to the larger temporal range, figures are separated by WY at each logging station. Additionally, WSE data for WY 2016 – 2017 were used in conjunction with secondary channel longitudinal profile channel entrance elevations to calculate percent time within the following flow regimes: a) base flows confined to only the main channel (Figure 41); b) flows entering the secondary channels and floodplains (Figure 42); and c) flows overtopping the permanently vegetated island separating the main and secondary channels forming a single large channel across the full extent of the project reach (Figure 43) (Table 9).

Because loggers were deployed late in the 2015 – 2016 WY, only a single storm event was captured occurring on 22 March 2016 and any other WSE fluctuations are a direct result of tidal influence. Figure 36 demonstrates Unit 1 is strongly dominated by an intertidal hydrology present throughout the year. The Unit 2 WSE data show the logger was inundated only during the most extreme spring high tides (Figure 37); however, as the logger is deployed at the furthest upstream extent of the unit, larger fractions of the

reach are subjected to tidal influence at lower high tides. The Unit 3 logger only experienced a few centimeters of tidal inundation during 10 high tide events from 18 March 2016 to 20 September 2016 (Figure 38). As the logger is located downstream of the secondary channel exit, the tide does not extend high enough to influence the channel unit creating conditions dominated by classic fluvial processes.

The WSE profiles are nearly identical for Units 2 and 3 for the 2016 – 2017 WY (Figures 39 and 40), but WSE data indicate water flowed onto the floodplain more frequently at Unit 3. Table 9 shows water flows under the secondary channel flow regime for 14.55% of the survey time span, as opposed to just 11.79% for the Unit 2 floodplain (Table 9). The difference over the course of the entire survey period equates to water flowing into the Unit 3 secondary channel an additional 4.5 days. As the percent time channel Units 2 and 3 experienced overtopping of the permanently vegetated island (i.e. 3.85% and 3.15%, respectively, Table 9) is nearly identical for the survey time period, this finding can be attributed to a larger relative elevation difference between the main channel bottom and the secondary channel entrance at Unit 2 compared to Unit 3. This fact was difficult to confirm based on the longitudinal profiles because large scour pools are present directly in front of both secondary channel entrances, complicating the identification of a representative main channel bottom elevation. However, this concept is confirmed based on water flow velocities measured at the same time described in the section below.

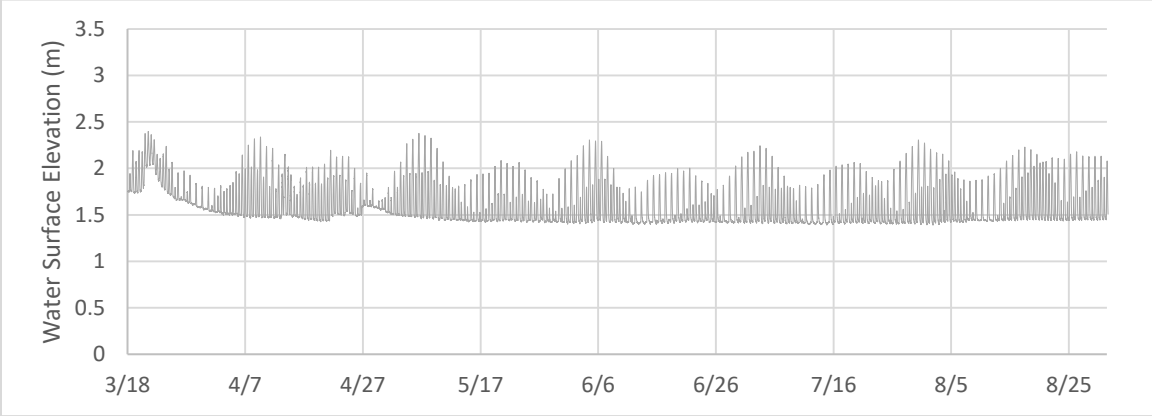

Figure 36. Water surface elevation from 18 March 2016 to 12 September 2016 at the Unit 1 secondary channel entrance.

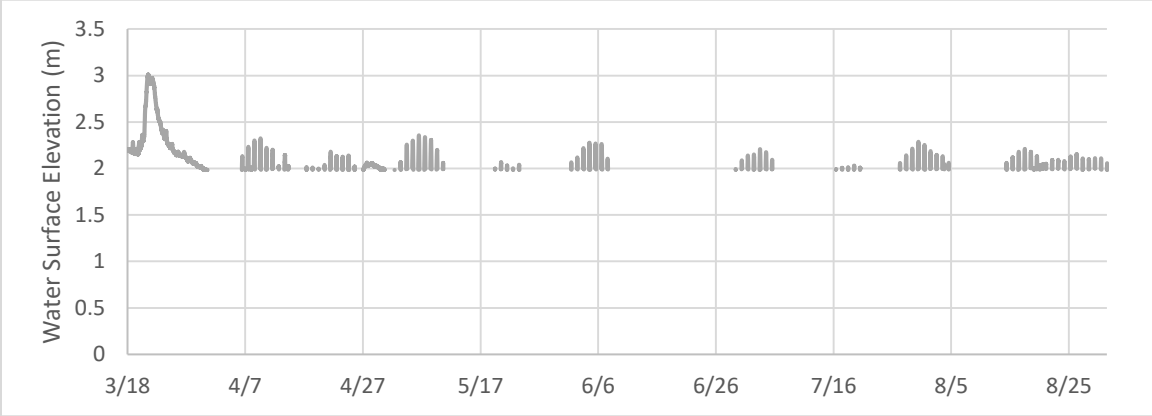

Figure 37. Water surface elevation from 18 March 2016 to 12 September 2016 at the Unit 2 secondary channel entrance.

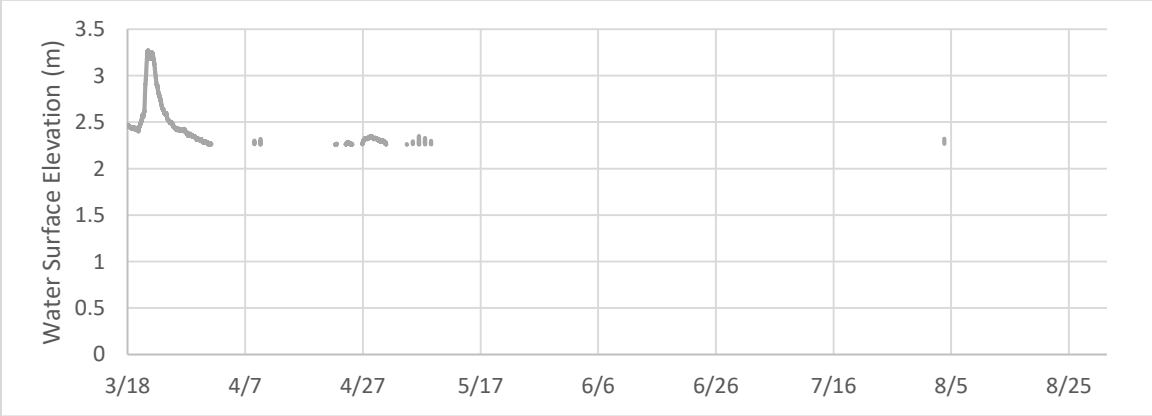

Figure 38. Water surface elevation from 18 March 2016 to 12 September 2016 at the Unit 3 secondary channel exit.

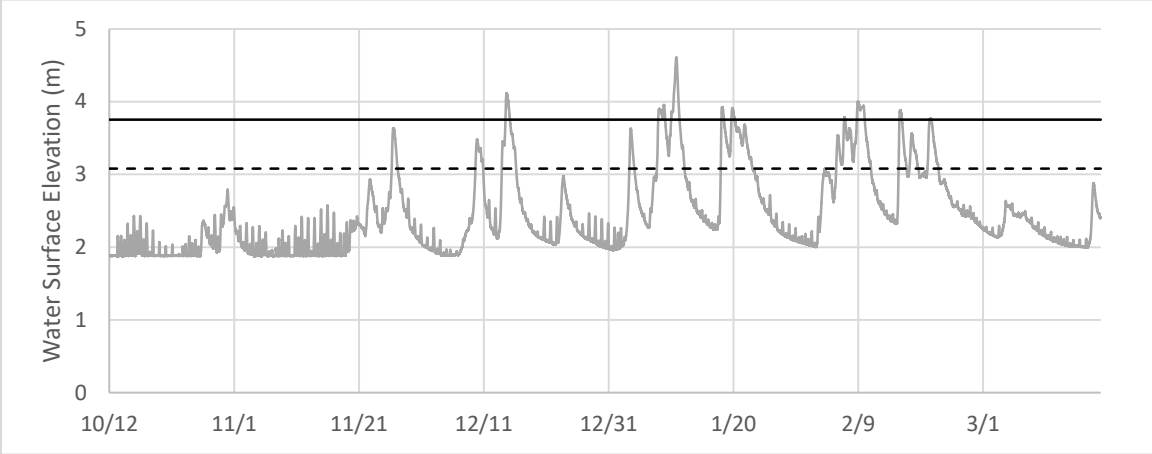

Figure 39. Water surface elevation from 12 Oct 2016 to 20 March 2017 at the Unit 2 secondary channel entrance. Elevation thresholds for flow regimes are indicated by horizontal lines (black dotted line = secondary channel entrance and black = flows over vegetated island).

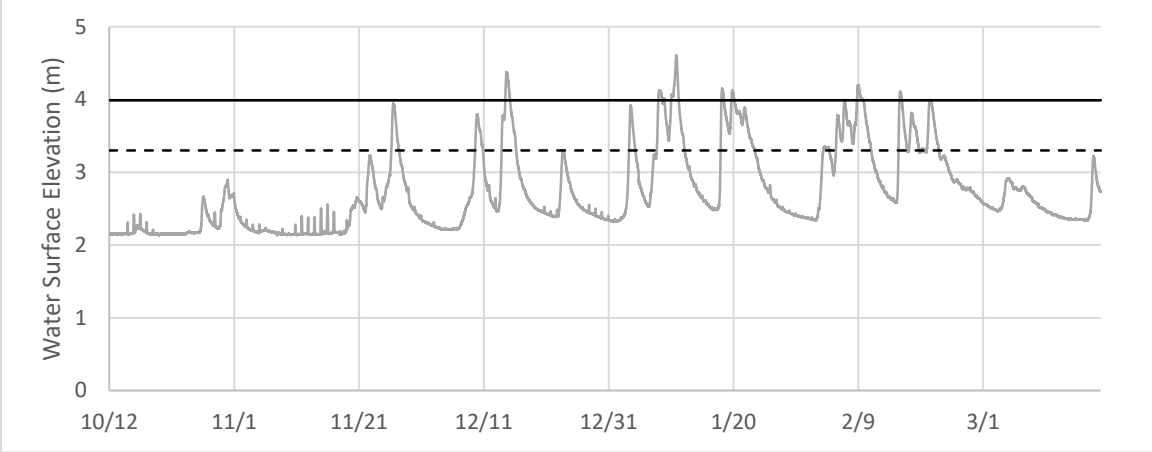

Figure 40. Water surface elevation from 12 Oct 2016 to 20 March 2017 at the Unit 3 secondary channel exit. Elevation thresholds for flow regimes are indicated by horizontal lines (black dotted line = secondary channel entrance and black = flows over vegetated island).

Figure 41. View of the base flow regime from the Dillon Rd. Bridge.

Figure 42. View of the channel flow regime taken from the Dillon Rd. Bridge.

Figure 43. View of the channel overtopping flow regime taken from the Dillon Rd. Bridge.

Table 9. Percent time channel Units 2 and 3 flowed within each flow regime.

	Proportion of time		Duration (days)	
	UNIT 2	UNIT 3	UNIT 2	UNIT 3
Base Flow	84.36%	82.33%	140.4	137.0
Channel Flow	11.79%	14.55%	19.6	24.2
Over Top	3.85%	3.12%	6.4	5.2

Floodplain Entrance Flow Rates

Flow rates were measured during four storm events during the 2016 – 2017 WY for the Unit 2 and 3 secondary channel entrances and plotted as a function of water surface elevation (Figures 44 and 45). Simple power functions were calculated quantifying the relationship between WSE and discharge rates, as originally described by Leopold and Maddock (1953). The original intent was to utilize these relationships to produce a ratings curve capable of estimating total water volumes entering the secondary channels based on the WSE logger data for the entire WY; however, it was not anticipated that flood heights would exceed the permanent vegetated islands on a regular basis. The power-law relationships are only applicable for flows confined to the secondary channels (see above section), and do not extend to the approximately three to four percent of the WY where flows occurred at heights large enough to overtop the vegetated islands to form a single large channel (Table 9). As a result, it would be possible to calculate minimum total flow volumes for the periods where flows were confined to the secondary channel, but would not yield any useful information for the functioning of the system. However, the surveyed flows did follow a tight power law trend (Unit 2 $R^2 = 0.9428$ and Unit 3 $R^2 = 0.9949$, Figures 44 and 45) during the secondary channel flow regime and are

presented as an initial step in the characterization of water flows for practitioners and project managers assessing the Salt River Ecosystem Restoration Project.

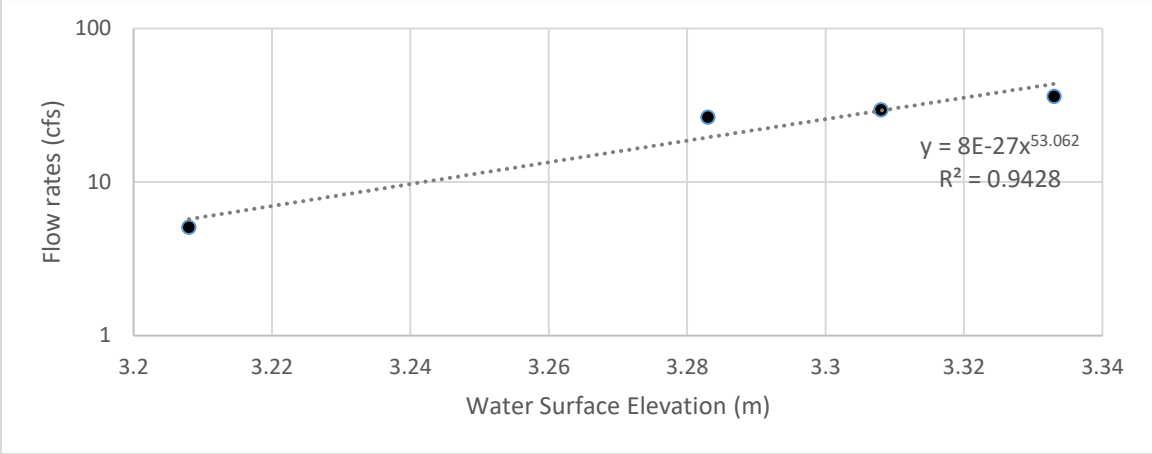

Figure 44. Power law curve identifying the relationship between WSE and flow rate at Unit 2 floodplain entrance.

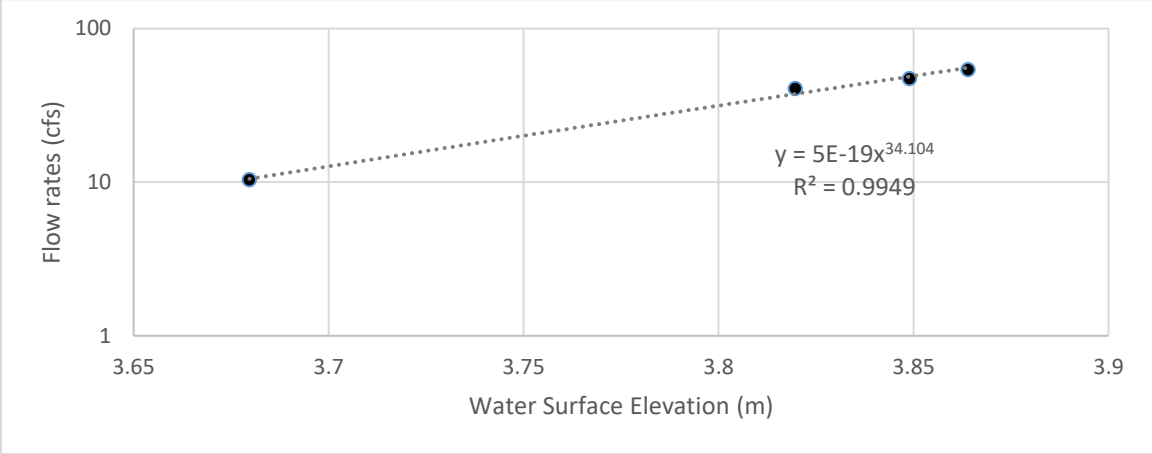

Figure 45. Power law curve identifying the relationship between WSE and flow rate at Unit 3 floodplain entrance.

While the total water volumes entering the secondary channels were not determined, the water velocity surveys did provide useful information regarding the relative differences between the secondary channel unit entrances. On average, flow rates were approximately 1.6 times larger (Figure 46) and had 2.54 times higher mean velocity

within the Unit 3 entrance than the Unit 2 entrance. These differences have implications for the distribution of dominant grain sizes and deposition characteristics within the channel units. The higher flow rates and velocities are responsible for the larger grain sizes observed within the Unit 3 secondary channel, as the higher shear velocities are capable of carrying larger particles in suspension. This also accounts for the large deposition observed at the expansion point as velocities decrease as width increases, and the sands fall quickly out of suspension. Conversely, the uniform deposition within the Unit 2 secondary channel may be caused by lower entrance velocities only capable of transporting smaller grain size particles which settle uniformly throughout the channel reach.

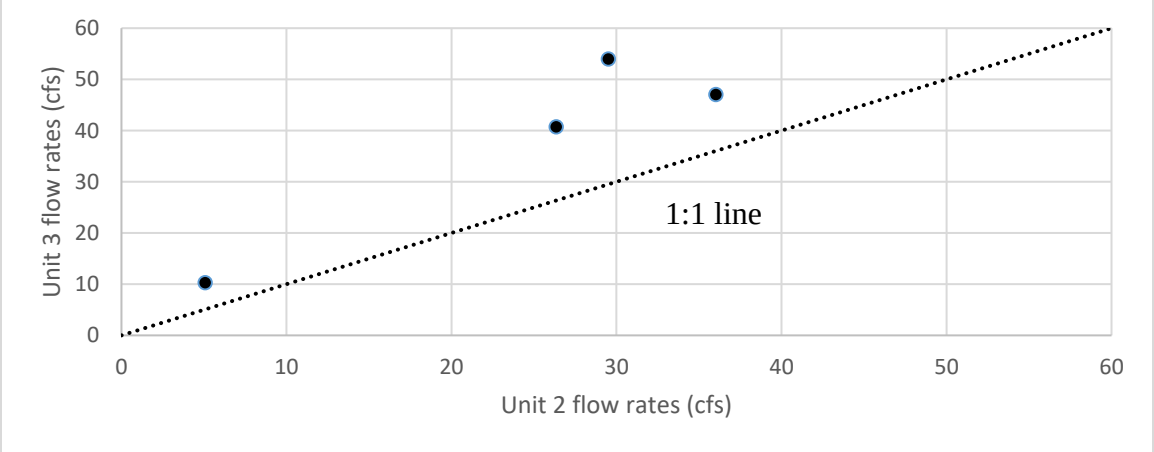

Figure 46. Flow rates for each survey at Unit 2 and 3 channel entrances.

Several differences were observed between the channel unit entrances contributing to the disparity in the quantity and velocity of water entering the secondary channels. Attempting to quantify the magnitude of the effects of the differences is beyond the scope of this project. However, a lack of quality information exists within the literature

regarding secondary channel confluences due to the uncommon implementation of anabranching channel restoration designs and the differences are worth noting to qualitatively inform future project designs. For visualization purposes, scale diagrams were created illustrating the setting of the secondary channel entrances for Units 2 and 3 (Figures 47 and 48). The differences between secondary channel entrances are summarized as follows:

- Unit 3 entrance has a more acute offshoot angle (~40°) from the main channel compared to Unit 2 (~50°);
- Unit 3 secondary channel is more narrow and uniform in width (~ 5.5 m) with a larger height: width ratio concentrating entrance flows compared to the Unit 2 entrance which flares to an approximate 11 m maximum width;
- Unit 2 channel entrance reach is very densely vegetated relative to Unit 3;
- Unit 2 channel entrance is higher relative to the main channel bottom (confirmed by percent time within the secondary channel flow regime described in above section) which results in lower secondary channel flow depths for equal main channel flows;
- A large eddy has formed just downstream of the Unit 3 entrance as the channel has widened due to a large bank slump. The rotation of channel flow is likely initiated by a large inflow pipe draining the adjacent grass fields and partially obstructs main channel flow. Anecdotal observations identify relatively high velocity flows shooting into the channel entrance from the eddy;

- Unit 2 is situated just downstream of the outer bank of an upstream meander and thalweg flows have likely shifted to the bank opposite the channel entrance. As a result, water entering the secondary channel is simply spilling onto the active bench due to the main channel WSE exceeding channel elevations but is not shooting into the channel due to water's own momentum and direction of travel as occurs at the Unit 3 entrance.

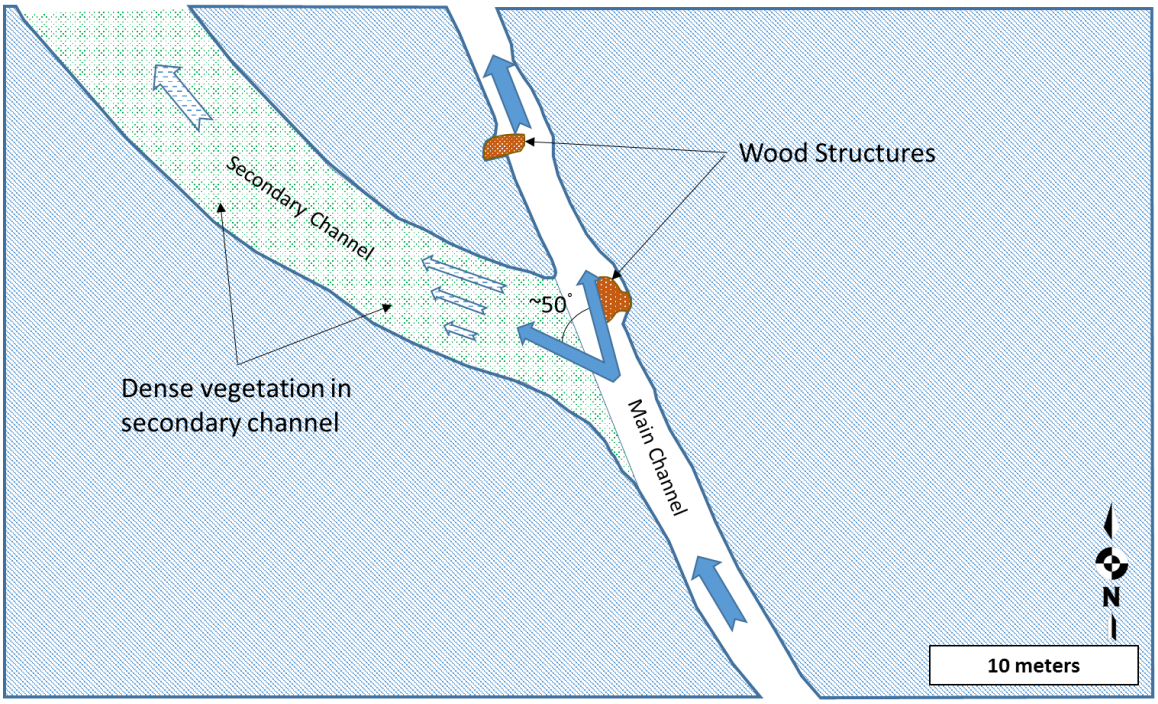

Figure 47. Scale illustration of inflow dynamics for the Unit 2 secondary channel entrance.

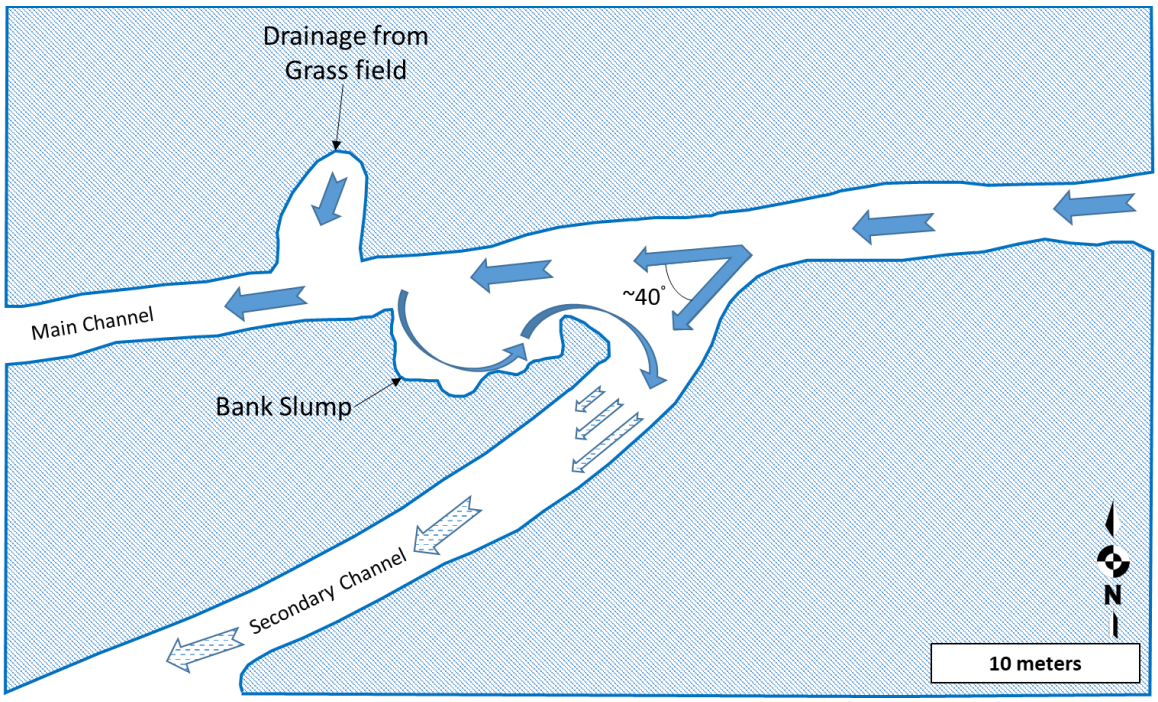

Figure 48. Scale illustration of inflow dynamics for the Unit 3 secondary channel entrance.

Precipitation Data

Precipitation data were downloaded for the National Weather Service's Cooperative Observer Network gaging station located at the Fortuna Airport and plotted as daily totals for the 2015 – 2016 WY (Figure 49) and 2016 – 2017 WY (Figure 50). The majority of rain events for both years occurred uniformly between November and April. To better understand the distribution of rainfall through the wet season (i.e. October through May), cumulative precipitation depths were plotted both water years (Figure 51). Precipitation totals were approximately 37% larger during the 2017 WY (1505.7 mm total) compared to the 2016 WY with a cumulative rainfall depth of 1093.2 mm (Figure 51; Table 10). In addition to greater total rainfall, the 2017 WY experienced almost twice as many rain events exceeding a 20 mm rainfall depth (i.e. 31 vs 17) (Figure 52; Table 10). The largest rain event of the 2016 – 2017 wet season also yielded a larger precipitation depth of 52.8 mm compared to the largest event in 2015 – 2016 of 45 mm. Precipitation totals for the 2016 – 2017 wet season were abnormally high but may become more standard as global temperatures continue to warm and increase atmospheric water vapor.

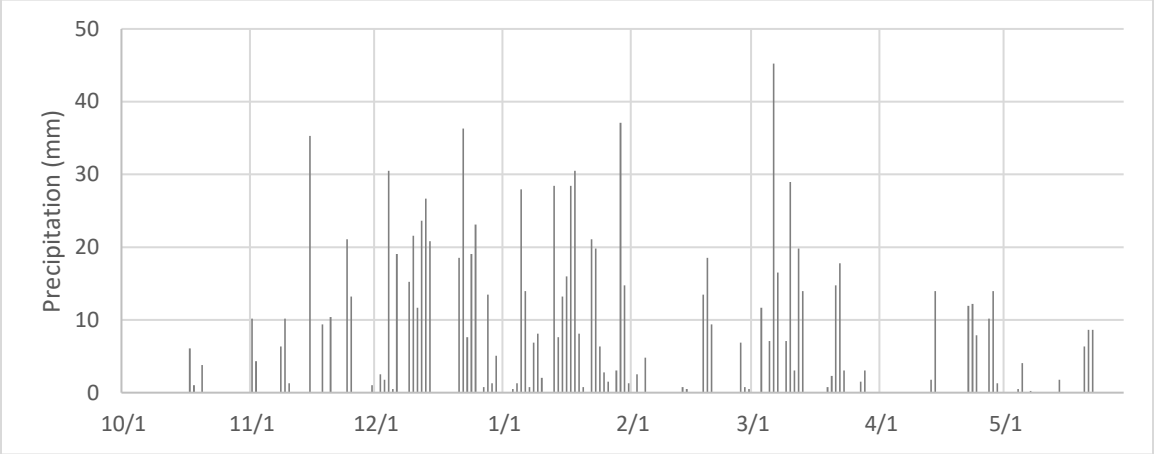

Figure 49. Daily precipitation records for the 2015 – 2016 WY.

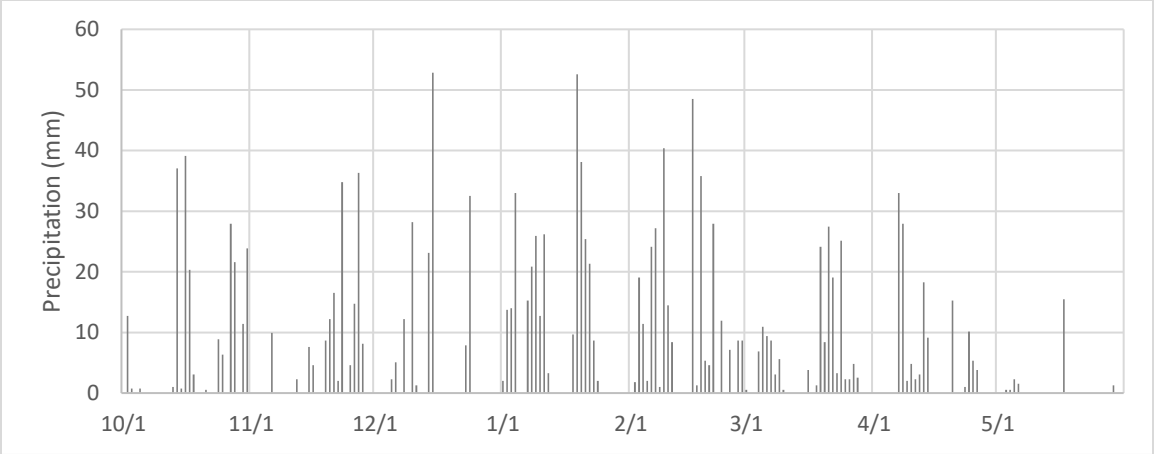

Figure 50. Daily precipitation records for the 2016 – 2017 WY.

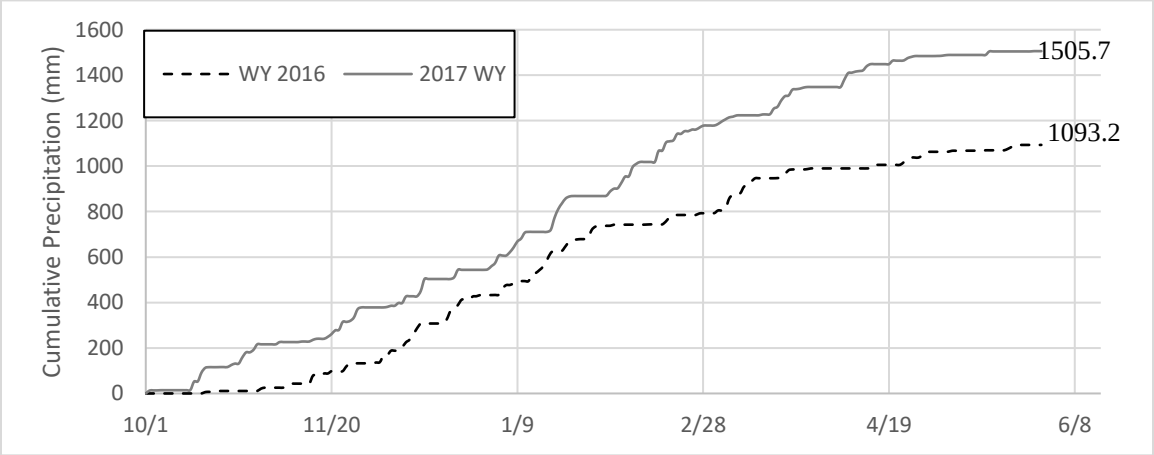

Figure 51. Cumulative precipitation for the 2015 - 2016 and 2016 - 2017 WY.

Table 10. Summary of precipitation events and total depths for the 2016 and 2017 WY.

Water Year	Total Rain Events	Rain Events > 20mm	Largest rain event (mm)	Total Precip. (mm)
2015 - 2016	101	17	45	1093.2
2016 - 2017	114	31	52.8	1505.7

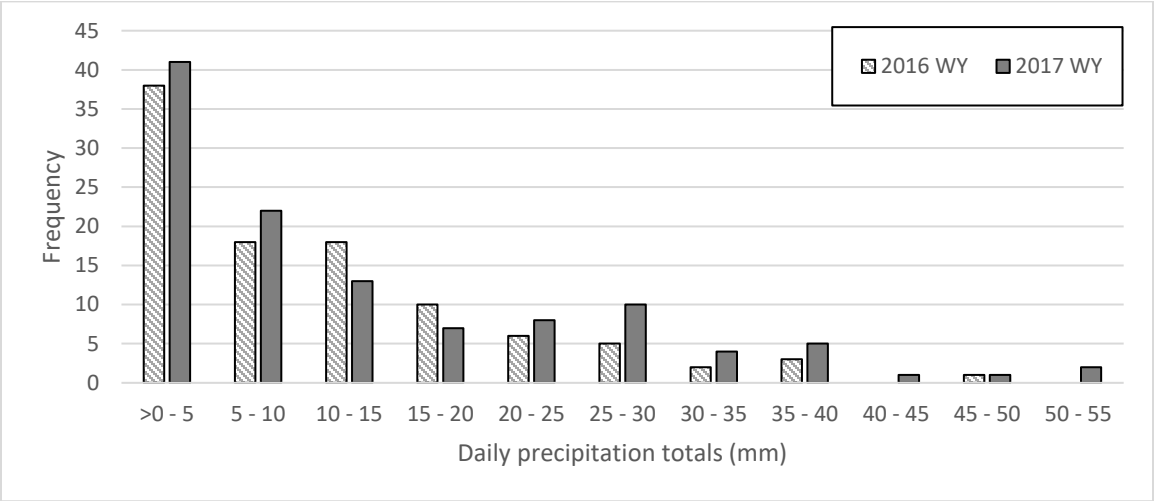

Figure 52. Histogram of rain events for WY 2016 and 2017.

Daily precipitation totals were plotted against average daily WSE data at the Unit 2 logger for the 2017 WY (Figure 53) to qualitatively assess flood stage levels within the main channel in response to precipitation. Due to the similarity of the WSE data for both Unit 2 and 3 sampling stations, Unit 3 data were omitted. In October, four sizable storm events occurred but only yielded minor spikes in WSE within the main channel. This response is typical of watershed hydrographs at the end of the dry season as the majority of first rains are absorbed into dry soils yielding little overland runoff (Ward and Trimble 2004). However, later during the wet season, water surface elevations respond as larger spikes to similar sized rain events as the watershed has become saturated and rainfall is unable to infiltrate producing large volumes of saturated overland flow.

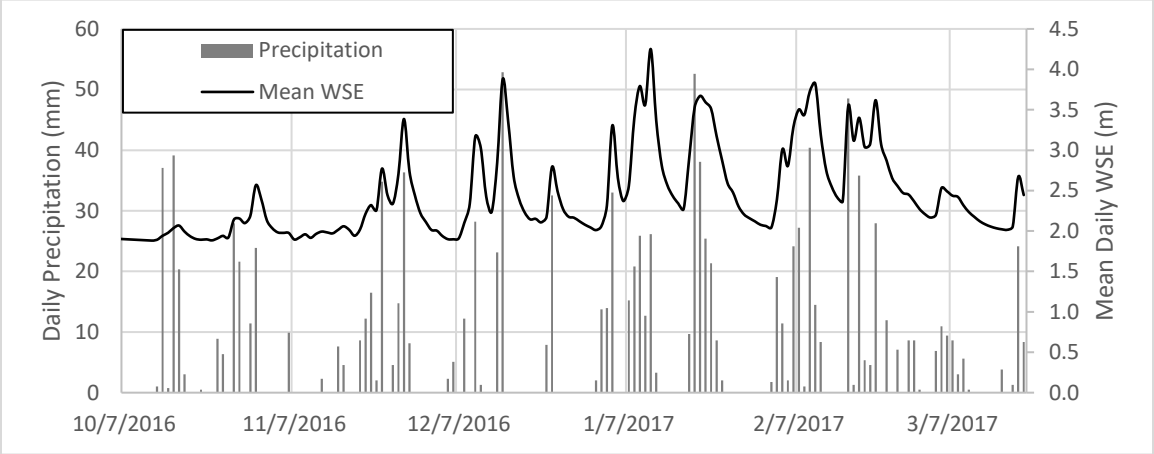

Figure 53. Daily precipitation and average daily water surface elevation at Unit 2 for WY 2017.

Precipitation data from the Fortuna Airport has only been recorded since 2010, to compare precipitation depths for the project time range to the larger temporal trends, the Eureka Forecast Office at Woodley Island (station ID GHCND:USW00024213) was used as a proxy. The Woodley Island station is located approximately 24.5 km from the Fortuna Airport and has recorded precipitation data since December of 1941 (i.e. 76 water years). To assess the comparability of data at the two stations, the correlation coefficient was calculated for cumulative precipitation at various temporal intervals (Figure 54). Only daily precipitation summaries were available from both stations, so hourly comparisons were not made, but the data show a moderate positive correlation on a daily scale (i.e. 0.54) and increasing at larger temporal scales. The two day cumulative precipitation records display a stronger correlation coefficient of 0.78 increasing to 0.93 when seven records are combined. The analysis achieves an asymptotic correlation coefficient of 0.95 when the data for the entire water year is summed. Based on this

analysis, data can be considered comparable at cumulative temporal scales of two days or more.

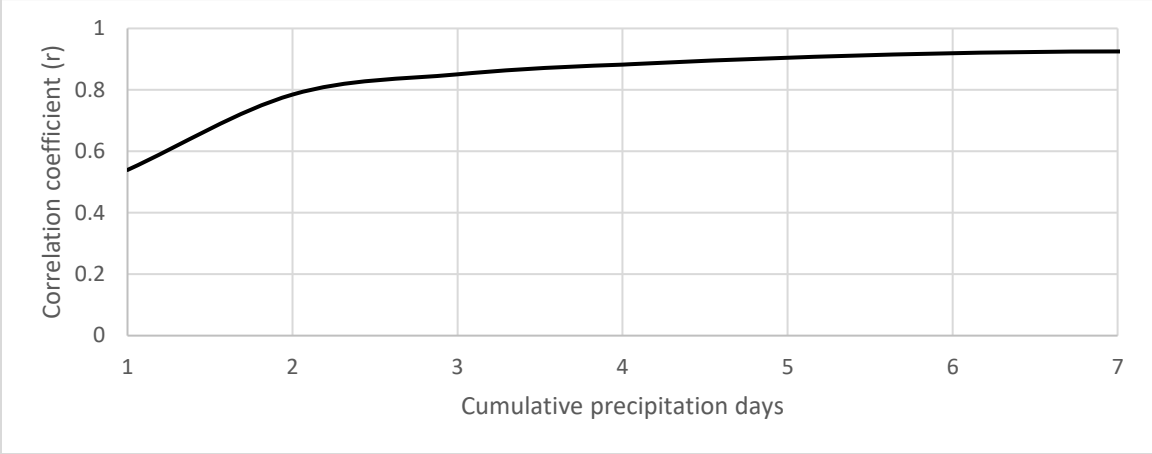

Figure 54. Correlation coefficient between Woodley Island and Fortuna Airport weather stations for different days of cumulative precipitation. To maintain an illustrative scale the correlation coefficient for the entire water year was not included (r = 0.95).

NOAA (NOAA 2017) has developed intensity duration frequency (IDF) curves identifying precipitation depth thresholds for probabilistic recurrence intervals at the Woodley Office station. The IDF curves allow the identification of average annual frequency of precipitation depths for different time periods (e.g. annual return intervals are calculated for 24-hour, 2-day, and 7-day precipitation events). A comparison of the WY 2016 and 2017 to the IDF curves show that cumulative precipitation at two to 60-day temporal scales occur frequently compared to the entire period of record (Table 11). The majority of precipitation depths are expected to occur every one to two years, with the exception of the 45 day records occurring, on average, every five to ten years. The largest recurrence interval was identified as the 2016 WY 60-day interval which is expected to occur every 10 – 25 years. This is unexpected as the 2017 WY exhibited larger

cumulative rainfall totals (Table 10). Data show the precipitation depths for two to 60 day scales occur on a relatively frequent basis and there were no abnormally high rainfall intensities.

Table 11. Annual recurrence intervals for the 2016 and 2017 WY for multiple days' cumulative precipitation at the Woodley Island Weather Forecast Station based on IDF curves developed by NOAA 2017.

	Annual Recurrence Interval for Multi-Day Cumulative Precipitation								
WY	2 day	3 day	4 day	7 day	10 day	20 day	30 day	45 day	60 day
2016	<1	1 - 2	1 - 2	1 - 2	2 - 5	2 - 5	2 - 5	5 - 10	10 - 25
2017	1 - 2	1 - 2	1 - 2	1 - 2	1 - 2	2 - 5	1 - 2	5 - 10	2 - 5

Data were analyzed to show cumulative WY precipitation depths during survey years (i.e. WY 2016 and 2017) relative to all 76 years of recorded data. Of the 76 years of retrievable precipitation data, with cumulative precipitation ranked from largest to smallest, the 2017 WY was the 1st ranked rain year (i.e. largest cumulative precipitation depth on record) and 2016 was the 10th ranked (Figure 55). Higher precipitation was recorded during the 1889 – 1890 WY (1889.5 mm) (NOAA 1998), but the record occurred when precipitation data were collected by the U.S. Weather Bureau (currently the National Weather Service) prior to its reassignment to the Department of Commerce and was not easily retrievable within the NOAA archive database. Cumulative precipitation during the 2017 WY was over 20% higher than the second largest recorded year. So while rainfall depths on shorter temporal scales were not abnormal, the complete WY for the project time period was larger than 83 and 100 percent of the other recorded years during the 2016 and 2017 WY, respectively.

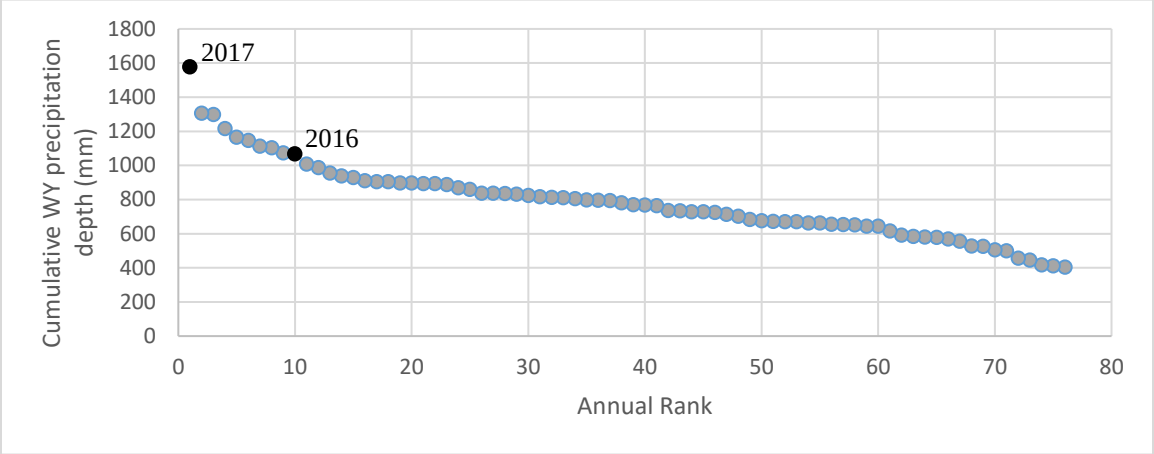

Figure 55. Water years ranked by cumulative precipitation depths from 1941 – 2017 at the Woodley Island Weather Forecast Station.

Other Main Channel Surveys

Channel Bank Pins

The mean change in the length of exposed pins was compared across channel units and survey years (Figure 56). No change was recorded along the main channel banks within Unit 3 for either survey year and this observation is likely attributed to the increased bank stabilization caused by the rapid propagation of dense vegetation onto the channel banks. As a result, data for Unit 3 are not presented in figures. Additionally, several transects experienced large bank slumps (i.e. Units 1 and 2 expansion sections) resulting in the complete removal of the bank pins. In these instances, a conservative maximum value of 200 mm scour was recorded for analysis purposes. As a result, the mean scour values can be considered a minimum value. Two-way analysis of variance (ANOVA) was conducted in RStudio v1.0.143 at the $\alpha = 0.5$ confidence level using the year and channel unit as factor variables. Results indicated the larger scour recorded during the 2017 summer surveys was significantly larger ($F_{1, 101} = 17.963$, $p = 4.99 \times 10^{-5}$) than scour depths

observed during summer 2016 surveys; however, no significant difference was identified between channel units ($F_{1, 101} = 1.696$, $p = 0.196$). The increase in scour between survey years was not surprising as the 2016 – 2017 WY experienced larger precipitation depths and, consequently, larger volumes of water flowed through the main channel.

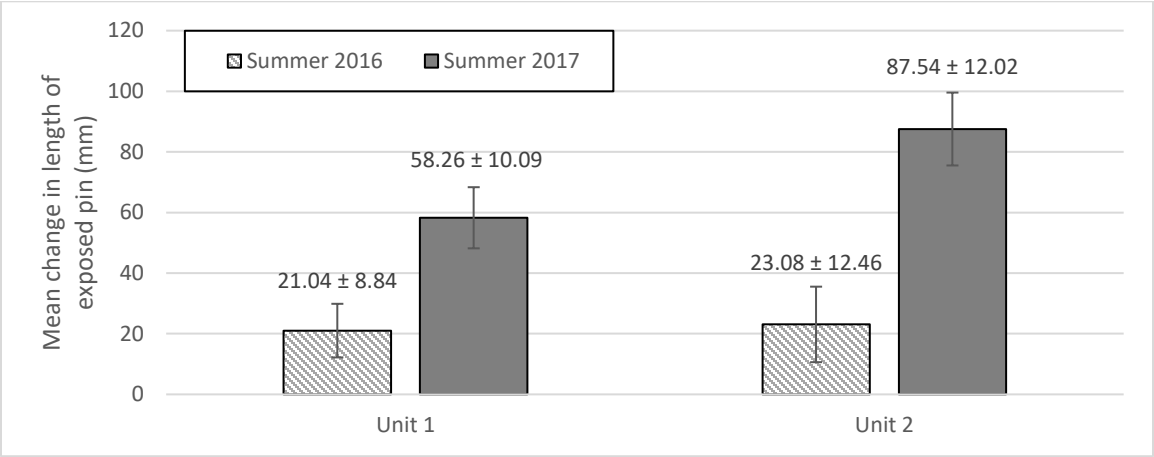

Figure 56. Change in mean length of exposed pins installed within the main channel by survey year and channel unit.

To further assess the vertical distribution of scour within the main channel, mean exposure lengths of pins were plotted by survey year and the relative vertical location of pins within the main channel (i.e. all pin arrays had pins installed both high and low on the channel banks, see 'Data Collection Methods' for additional details) (Figure 57). Negative values indicate deposition was recorded and less of the pin was exposed than the previous survey. An additional two-way ANOVA at the $\alpha = 0.5$ confidence level was performed using the relative pin elevation and survey year as factor variables. Channel units were pooled as no significant difference was found between them. As is clearly indicated in Figure 57, a significant difference was identified ($F_{1,101} = 12.07$, $p = 0.000756$) between the relative channel elevations.

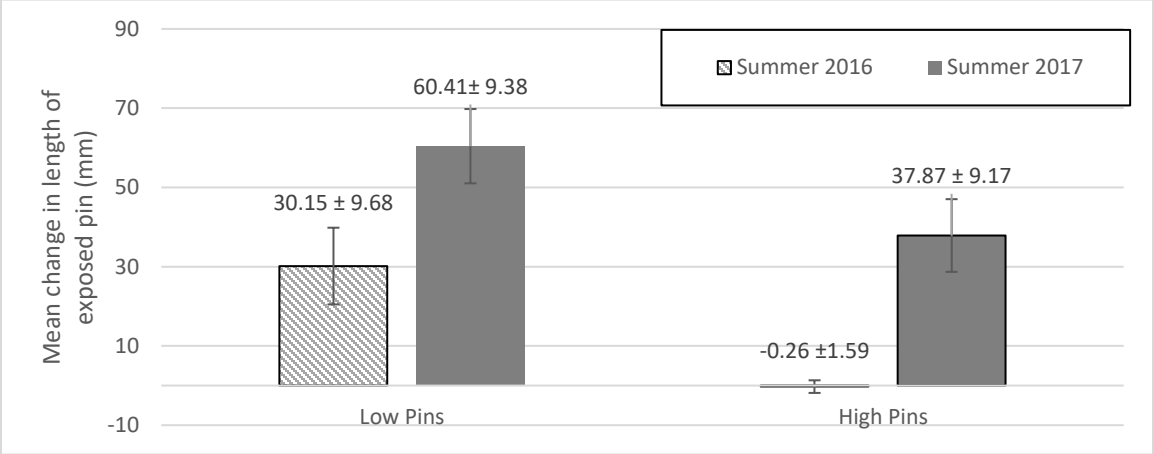

Figure 57. Mean length of exposed pins installed within the main channel by survey year and relative channel elevation.

Failure Inventory

The failure inventory is displayed as a map identifying point locations of bank failures recorded during the summer of 2016 and 2017 (Figure 58) and summary information for each ID (Table 12). Bank slumps increasing in area are further compared and percent increase was calculated (Figure 59). The identification of failures originating from groundwater seeps was straightforward, as water flowing from the base of the failure scarp was typically visible. However, definitive environmental factors influencing hydraulically induced failures are more difficult to determine, as it's likely a combination of hydrologic processes and bank materials. Additional research on each bank slump would be required to pinpoint the specific cause, but likely sources have been hypothesized by integrating other known survey data and general channel morphology at each location. When referring to a specific bank failure, locations are identified with corresponding ID from Figure 58 and Table 12 (e.g. ID 1).

The series of bank slumps within the most downstream reach were associated with large groundwater seeps on the southern bank (i.e. IDs 1 and 3). The failure on the opposite bank (i.e. ID 2) is likely connected to perturbations caused by the original groundwater induced slumps during high flows and is currently the largest single slump in area within the project area (58.97 m^2). The original slump remained stable between 2016 and 2017, but the associated failure exhibited the largest relative increase in erosion area (618%). This included the development of a deep pool whose base is the lowest elevation point within the entire project reach (Figure 14) and likely undercut the banks of ID 2.

The highest concentration of fluvial dominated bank failures occurred within the project area's large central meander (i.e. IDs 9 – 22). However, there was no preferential channel bank for failures along the meander providing support that failures are due to local substrate and fluvial conditions and not an insufficiently sinuous channel. Additionally, with the exception of IDs 2 and 4, all newly formed bank slumps recorded between the summer 2016 and summer 2017 surveys occurred within the reach. The sinuosity index for the reach of approximately 1.06 is sufficiently low to be classified as straight (Leopold and Wolman 1957), indicating the reach may potentially contain lenses of sand sediments. This would occur as soils with intermixed sands cannot be as heavily compacted and possess lower cohesion values lowering the total stability of the channel banks. Channel bank material combined with a dynamic mixed intertidal flow regime has created conditions of high instability within the reach. This finding is supported by the

relatively large increases in cross-sectional area and highly variable elevation changes of the main channel bottom determined by the longitudinal profile.

Nearly every bank failure which increased in area was associated with an adjacent scour pool within the main channel (Table 12) suggesting increased scour may be propagated by bank undercutting. Further evidence is provided by the presence of intact blocks within the main channel, suggesting low cohesion sediment at the base of the bank was eroded during high flows and the upper bank collapsed due to gravitational forcing and a lack of base support.

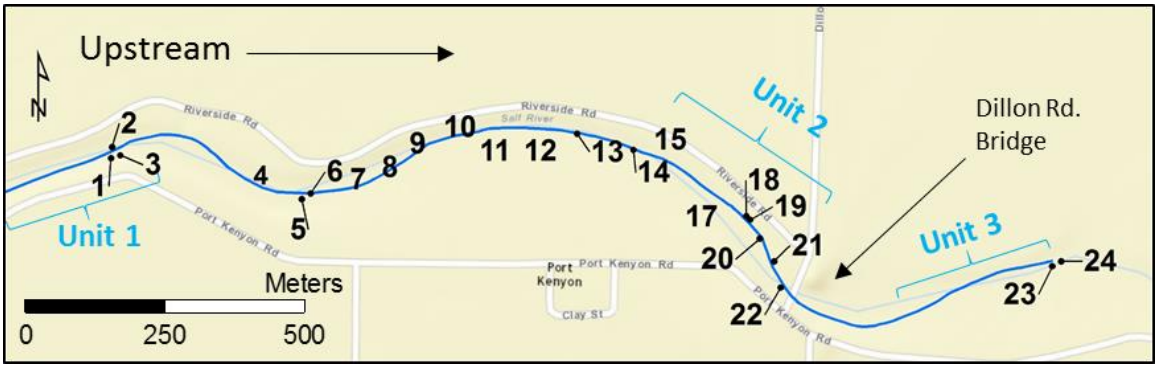

Figure 58. Locations of identified bank failures.

Table 12. Summary of bank failures.

ID	Channel Bank	2016 Area (m^2)	2017 Area (m^2)	2017 length (m)	Pool Depth (m)	Comparison	Potential Source
1	South	---	9.09	3.08	0.7	New	Groundwater spring
2	North	3.12	22.47	10.71	0.7	Larger	Disrupted flow dynamics from IDs 1 and 3
3	South	58.97	58.97	9.62	0.7	Unchanged	Groundwater spring
4	South	---	2.78	4.90	---	New	Fluvial processes; meander bend
5	South	10.21	12.06	10.88	---	Larger	Fluvial processes; meander bend
6	South	---	4.42	6.58	---	New	Fluvial processes; meander bend
7	South	---	19.97	23.29	---	New	Disrupted flow dynamics from ID 8

ID	Channel Bank	2016 Area (m^2)	2017 Area (m^2)	2017 length (m)	Pool Depth (m)	Comparison	Potential Source
8	South	14.70	14.70	7.78	---	Unchanged	Groundwater spring
9	North	---	26.90	19.72	0.5	New	Fluvial processes; meander bend
10	South	---	10.64	13.75	0.4	New	Fluvial processes; meander bend
11	North	7.28	18.89	16.15	0.4	Larger	Fluvial processes; meander bend
12	South	18.32	18.32	17.50	---	Unchanged	Fluvial processes
13	North	5.29	5.29	5.20	---	Unchanged	Scour around large woody debris
14	North	---	15.15	12.90	---	New	Fluvial processes
15	North	9.13	17.45	14.54	0.7	Larger	Fluvial processes; undercut bank
16	North	---	3.91	7.13	1.0	New	Fluvial processes; undercut bank
17	South	9.07	9.07	9.33	1.0	Unchanged	Fluvial processes; undercut bank
18	North	---	6.22	13.74	0.8	New	Fluvial processes; undercut bank
19	South	4.20	4.20	5.22	0.8	Unchanged	Fluvial processes
20	North	16.80	16.80	16.30	0.4	Unchanged	Fluvial processes; undercut bank (unit 2 entrance)
21	North	20.66	28.67	19.45	0.8	Larger	Fluvial processes; undercut bank
22	South	8.37	9.56	10.30	0.8	Larger	Fluvial processes; undercut bank
23	South	54.21	54.21	18.76	0.8	Unchanged	Fluvial processes; undercut bank (unit 3 entrance)
24	North	13.59	28.53	27.35	0.8	Larger	Fluvial processes; undercut bank
	TOTAL	***253.91***	***418.26***				

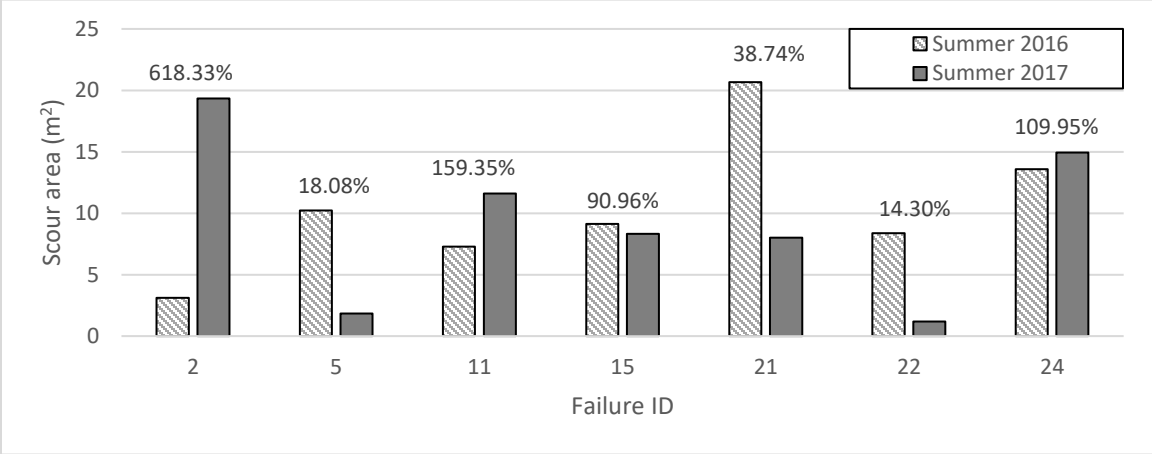

Figure 59. Comparison of scour areas for failures which increased in area between survey years including the year-to-year percent increase. Summer 2016 bars indicate original surveyed scour area and summer 2017 indicates increased scour area.

DISCUSSION

Due to the large overlap of physical processes between research objectives, the discussion is structured to directly address the project objectives outlined in the 'Introduction.' The objectives are addressed within the context of a macro-scale conceptual model where quantitative data are used to highlight the distribution of dominant processes to prioritize and inform future research on the SRERP and anabranching channel restoration designs. This strategy is intended to provide a more accessible framework to extract useful information for practical application purposes.

This project was developed as an initial assessment of an uncommonly utilized anabranching restoration design. The goal was to characterize a large array of physical, hydrologic, and hydraulic functionality. As a result of the broad scope, some research objectives were not completely achieved due to limitations of time, resources, and relevant literature. In particular, the sediment transport volume estimates and robust statistical modeling objectives would have required specific micro-scale measurements deserving of an entire Master's project. Where objectives were not met, suggestions for future research and a description of project limitations are discussed.

Objective 1: Characterize the distribution and rate of deposition and erosion within the main channel and active bench.

Overall, the data showed consistently strong trends within fluvial dominated reaches identifying dominant depositional environments within the active bench secondary channels and scour within the main channel. The observed erosion within the main

channel has resulted in the development of a narrow, well-defined thalweg throughout nearly the entire project reach with some sections experiencing significantly higher rates of channel bottom scour. Within the larger scour areas, incipient pools have developed and subsequently deepened during wet seasons. Additionally, cross-section and channel bank pin data demonstrate a tendency for lower reach channels to experience some minor bank erosion resulting in an overall trend of channel widening and deepening. Conversely, the fluvial dominated secondary channels on the active bench exhibited variable longitudinal deposition environments and the sediment grain sizes are likely linked to the channel unit entrance flow rates, channel orientation, and longitudinal position. However, secondary channel characteristics within the intertidal channel unit (Unit 1) demonstrated a tendency for variable longitudinal scour during the larger cumulative precipitation rain season (i.e. WY 2017). The contrast between sedimentation characteristics within the intertidal and supratidal secondary channels is likely attributed to the varied hydrological processes, the interaction of upstream fluvial flows colliding with lower reach tidal waters during flood events, and potentially higher proportions of coarse grains within Unit 1.

Main Channel

The average elevation decrease of the main channel bottom and change in cross-sectional area increased in the downstream direction from summer 2016 to summer 2017 (Table 4). In effect, the main channel is, on average, experiencing higher vertical and lateral erosion rates as a function of its distance downstream. However, the widest and deepest portions

of natural stream systems are typically found in the downstream reaches as they have the largest watershed areas and are responsible for transporting the largest volumes of water and sediment (Leopold and Maddock 1953, Ward and Trimble 2004, Dedkov 2004). Channel bank pin data show lateral erosion is significantly higher along lower areas of the channel banks leading to more rectangular channel geometries. This is unsurprising as the depth of water above these points and the duration of exposure to flows is always larger, resulting in larger shear stresses for extended periods of time. The increased fluvial exposure may be compounded by a lack of root stabilization as lower bank vegetation is limited in these areas.

The largest cross-sectional areas during the baseline winter 2005 cross-section surveys were recorded within the highest upstream channel unit (Unit 3) (Table 6). This may partially explain the stable Unit 3 main channel banks, relative to the downstream channel units as downstream geometries are comparatively undersized for their longitudinal position and are expanding to reach an equilibrium. However, given the 2017 WY was the wettest on record, the increase in cross-sectional areas may be an anomalous response to an abnormally wet year, as similar expansion rates were not identified in the summer of 2016, with the exception of the Unit 2 expansion cross-section which experienced a bank slump.

Another factor potentially contributing to the variability in main channel erosion rates is controlled by the dominant hydrologies within each channel unit. Vegetation data were not recorded as a portion of this project, but vegetation, particularly grasses, was

anecdotally observed as having propagated more rapidly down the main channel banks, after construction, within the freshwater dominated upstream reach. Nanson and Knighton (1996) identify bank stabilization as a key factor to the development of sand-dominated island forming anabranching rivers, and vegetation growth rates are commonly higher within riparian wetlands than brackish or salt marsh areas (Mitch and Gosselink 1993, Merritt et al. 2009). The rapid expansion of vegetation within Unit 3 stabilized the channel banks resulting in reduced erosion rates. Conversely, the intertidal and brackish conditions experienced within Units 1 and 2, respectively, may have reduced vegetation propagation rates leaving the channel banks exposed to large flood events. Soil salinity measurements between vegetated and unvegetated channel bank areas would be an inexpensive initial step to assess this concept.

Future repeat cross-section surveys across a larger variety of water years may provide additional insights on the magnitude of channel response to determine whether the channels continue to expand or have reached an equilibrium. However, the data firmly support the concept that the inclusion of a narrow, deep primary channel within an anabranching system can effectively transport large sediment volumes through low gradient reaches.

Secondary Channels

Deposited sediments were highly variable in their spatial distribution, magnitude, and texture between all surveyed secondary channel units. The fluvial dominated secondary channels function as depositional environments, while the intertidal secondary channel

unit appears to act as both a storage and source of sediment depending on the magnitude and duration of annual flood events. The variability between channel units is likely attributed to the orientation and dominant hydrology of the secondary channel entrance.

At Unit 1, WSE data were not recorded during the 2017 WY due to an equipment failure and channel entrance flow rates were not recorded due to access issues, but interesting findings can be gleaned by assessing the secondary channel topographical response based on the sedimentation and longitudinal profile surveys. The Unit 1 secondary channel functions as a depositional environment when tidal flow dynamics are the dominant hydrological process but may produce variable scour during periods of strong fluvial inputs. Deposition was observed within the Unit 1 secondary channel following the 2016 dry season (Figure 27) indicating the tide is slowly depositing sediments onto the secondary channel with the largest deposition depths occurring at the entrance and at 240 m from the entrance. As such, the adverse slope of the Unit 1 secondary channel may be related to its elevational relationship with high tide lines. Christiansen et al. (2000) found that within intertidal systems, sediments are typically deposited on rising tides at the highest extent of the tide providing evidence for the presence of increased deposition within areas distant from the entrance. While the entrance deposition is likely attributed to a rapid reduction in water depths as tidal flows spill onto the active bench, distant deposition occurs at an elevation of approximately 1.7 m – 1.8 m NAVD 88 (Figure 19), roughly the WSE of lower high water for both neap and spring tides (Figure 36). This would result in a feedback cycle where tidally transported sediments would continue to

be deposited further from the secondary channel entrance due to its higher elevation and continue to increase from the increased deposition. The contraction of secondary channels when limited to tidally dominant hydrologies suggests anabranching channels designs may not be sustainable within strictly intertidal environments. The designs require sizable seasonal freshwater inputs to flush fine-grained sediments deposited during the dry season for maximum sustainability.

Relatively high sand content was identified within the Unit 1 secondary channel (Figure 31) which may influence scour dynamics observed within the middle section following the 2017 wet season (Figure 19). While coarse-grained sediments require larger flow velocities to transport in suspension, they lack the cohesion of finer grained sediments and require lower shear stresses to initiate motion (Ritter et al. 2006). While the sediment texture may be conducive to scouring, grain size distributions were relatively uniform throughout the entire secondary channel and the specific fluid dynamics initiating sediment movement during large flows is likely related to the channel geometry. Dominant scour patterns begin approximately where the floodplain widens (Figure 23). The specific mechanism for this correlation is unknown and the relationship is opposite of the patterns observed within the fluvial dominated channel units. In general, the intertidal secondary channel was highly dynamic and performed much differently than upstream units, so additional research is warranted on the specific interactions of tidal waters and freshwater flows if anabranching channel restoration designs are planned within intertidal habitats.

Relatively uniform deposition of fine-grained sediments was observed within the Unit 2 secondary channel (Figures 21 and 27), suggesting effective discharge rates are producing mean water velocities approximately equal to the settling velocity of silts and clays. Relatively low channel entrance flow rates (Figures 44 and 46) and the general lack of observed sand deposits indicates the majority of entrained sediment entering the floodplain are within finer grain size classes. Observationally, water flows at the channel entrance appear to simply spill onto the floodplain, similar to a backwater environment, due to WSE exceeding the channel opening elevation and are not pushed by the water's momentum. Additionally, the relatively shallow slope (Table 7) ensures the majority of flows are relatively tranquil and may promote the settling of fine-grained sediment. However, the spike in deposited sand content within the middle section of Unit 2 (Table 8) indicates some flow velocities are sufficient to transport coarser particles, either as bed or suspended load. Additional research should be conducted on the local sedimentology to confirm, but it's likely the reach contains a surficial sand lens functioning as a source for coarser sediments within the channel itself and these were transported a short distance before depositing on the tile. This is supported by the high density of main channel bank slumps adjacent to this reach (Figure 58), the low channel entrance flow velocities, and the absence of deposited sand particles at tiles closer to the secondary channel entrance.

Deposited sediment displayed variable spatial distribution within the Unit 3 secondary channel and followed a strong gradient of grain sizes, with coarser grains constituting larger proportions closer to the channel entrance and successively decreasing downstream

towards the reconnection with the main channel. Kleinhans et al. (2012) describe how flow divisions at channel bifurcations within lowland river systems are largely controlled by backwater effects and gradient advantages may result in a larger proportion of the flow division. So in addition to the observed differences between the Units 2 and 3 channel entrances listed in the 'floodplain entrance flow rate' results, the relatively high slope within the Unit 3 secondary channel (Table 7) may also be connected to the higher channel entrance flow rates. In any event, the higher flow rates transport coarser grain sizes in suspension onto the active bench and appear to settle as the floodplain reaches its maximum width (Figure 25). Observationally, water shoots onto the floodplain mainly from a secondary flow induced by a downstream drainage inflow from an adjacent field (Figure 48). The path of the higher velocity water produced the scour path observed on the Total Station surveys (Figure 35).

Large deposition peaks were noted immediately at channel entrances in both the Total Station and longitudinal profile surveys within Units 2 and 3. This has been a long recognized phenomenon for asymmetrical bifurcations. Early researchers noted that deposition is maximized at offshoot angles of 30 – 45° (Garde and Raju 1978) which is roughly within the range of the 50° and 40° angles observed at Units 2 and 3, respectively. Novak et al. (2007) noted this could be minimized by designing off-shoots on the outer bends downstream of meanders; however, this is the exact positioning of the Unit 2 entrance that displayed a large elevation change between summer 2016 and summer 2017. However, the study was looking primarily at the deposition of bedload

sediments which are unable to access the secondary channels due to the elevation increase at the floodplain entrance. The placement of the entrance does appear to be at least partially responsible for the high deposition rates because lower flow velocities are decreased as high velocity flows within the main channel have already been diverted downstream of the meander towards to opposite bank resulting in backwater-type spill flows. This has contributed to the observed deposition rates of fine-grained sediments as the low entrance velocities create flow conditions below the sediment's settling thresholds. A large amount of additional research should be undertaken to more fully understand the relationship between the observed differences, magnitude of effect, and result on sediment transport capacity on anabranching channel bifurcations.

Objective 2: Quantify the volume and efficiency of water and sediment discharge within the main channel along a continuum of storm return intervals.

An attempt was not made to estimate volumetric sediment transport capacities within the main channel, due to limitations in the availability of equipment, and the large variability and uncertainty involved with making such measurements. The main limitation pertained to the estimation of bedload transport which can be highly variable across both space and time (Gomez 1991). High channel depths and velocities restrict wading surveys and the area exhibits a lack of sampling bridges so data collection would have required multiple bedload samplers, requiring installation within a channel shown to be predominantly lowering in elevation (Table 4). Numerous transport equations have been developed to estimate bedload transport given a set of site-specific variables (Einstein 1950, Parker 1976, Bagnold 1980, Parker 1990). However, the empirical relationships were typically

derived within flumes and noncomparable stream environments and have been shown to typically overestimate transport volumes by several orders of magnitude (Barry et al. 2008). While the application of these equations can be appropriate during the design phase, their usefulness decreases following implementation as direct measurements are possible to monitor the restoration's function.

The calculation of water discharge volumes was also complicated and not completed due to the unexpected overtopping of the permanently vegetated island creating a single large channel across the entire width of the project instead of two well-defined independent channel systems (i.e. main and secondary channels). Flood events flowing in an overtopping regime occurred 3.85% and 3.12% of the wet season at channel Units 2 and 3, respectively (Table 9). This duration was sufficient to render the calculation of flow volumes impossible without a modified survey procedure. It would likely be impossible to measure flow rates across the entire channel during this flow regime without the use of a boat or velocity sampler suspended on a pulley system spanning the entire channel width.

While volumetric estimations were not made, relative efficiency of sediment transport can be derived by qualitatively assessing the response of elevation markers based on longitudinal profile surveys. As the main channel is not aggrading and experiencing dominant scour characteristics, the efficiency of sediment transport can be estimated at with reasonable confidence to be 100%. The main channel is functioning as intended with regards to the efficient transportation of sediment. In fact, the downcutting of the main

channel, discussed in greater detail in Objectives 5 and 6, may become an issue in the future.

The initial hypothesis during the development phase for the grain size distribution protocol involved coarse-grained sediments decreasing across a longitudinal gradient from the entrance to the secondary channel. The reasoning followed the principle that flows entering secondary channels would be loaded with coarse sediments and would fall out of suspension around the expansion section of the active bench. The gradient of sand sized particles follows this pattern very closely at Unit 3, but the deposition of coarse-grained particles at Units 1 and 2 increase from the expansion to a maximum in the longitudinal middle before decreasing at the downstream backwater section (Figure 33). Anomalous results were anticipated within Unit 1 due to the dominant tidal hydrology, adverse slope, and highly variable fluvial-tidal dynamics during flood events. The secondary channel at Unit 2 is fluvial dominated and results similar to Unit 3 were expected. These results may be attributed to a) the width of the active bench at the expansion section had not reached a critical width to reduce flood depths and velocities below the settling velocity for sand and/or b) the active bench is composed of a larger proportion of sand particles mobilizing during flood events, travelling a short distance and depositing on the tiles. As the middle section of Unit 2 is roughly adjacent to some of the larger scour pools within the main channel, it may support the hypothesis that local area contains sand lenses being partially mobilized during flood events. This concept would also explain, at least in part, why the middle section of the Unit 1 secondary

channel experienced higher scour rates than the expansion or backwater areas, as identified on the longitudinal profile (Figure 22).

Prior to restoration efforts, KHE (2005) determined that the D_{50} and D_{90} of aggraded sediments were composed of fine (0.1 mm – 0.25 mm) and very fine sand (0.05 mm – 0.1 mm) at almost every survey location and was believed to compose the dominant grain size entering the system from upstream watersheds. However, they also found fine sands constituted only 10% of the suspended sediment load, indicating a large proportion of these grain sizes were being slowly transported as bed load. The low width to depth ratio of the current main channel appears to have increased the hydraulic efficiency to transport these dominant grain sizes in suspension. The presence of observed sand bed forms and bed aggradation would be expected if a large proportion of sands were transported as bed load. Neither of these responses were identified; however, fine sands were the dominant deposited grain size within the Unit 3 secondary channel (Table 8). As the entrance is situated at least one meter above the main channel bed, all sediments conveyed onto the active bench would have been transported as suspended load within the main channel. As a result, it can be concluded that the main channel has effectively increased the mean grain size carried as suspended load, resulting in higher sediment loads being transported through the system compared to pre-restoration conditions.

Nanson and Knighton (1996) categorize the types of naturally occurring anabranching rivers and would describe the SRERP as a Type 2 river consisting of sand-dominated, island forming environments. As a part of each classification, ranges of values for

prominent geomorphic characteristics are provided listing Type 2 areas as experiencing 'moderate' aggradation. The lack of observed aggradation within the main channel based on longitudinal profile surveys indicates the SRERP is operating with greater hydraulic efficiency than would be expected under natural conditions. The main channel is transporting material delivered from upstream areas yet maintains excess shear sufficient to cause channel degradation. This occurs because the low width to depth of the main channel concentrates base and flood flows, creating shear velocities sufficient to support the entrainment and suspension of the dominant grain sizes. Even within the low gradient reaches of the intertidal section, it appears sediments are not being deposited within the main channel bed. Given both surveyed years did not experience any high intensity, large recurrence interval storms over short time periods (i.e. 1 – 2 days; Table 11) the main channel, under current conditions, efficiently conveyed all sediment through the system for effective discharge of one to two year recurrence interval storms.

Phase 2A (Upper) of the SRERP is currently under construction which will incorporate flows from Francis Creek, a tributary that transports 'very high' sediment levels during flood events (KHE 2011). While a dearth of bed load transport surveys have been conducted, Fenton (2011) found mean suspended sediment yields within Francis Creek were approximately 20455.1 tons/ year between 2008 and 2011. Benda and Berg (2007) calculated the total annual sediment yield for the entire Salt River Watershed as 29,300 tons/ year. Downie and Lucey (2005) adapted sediment yields from USDA (1993) and estimated Francis Creek accounted for approximately 18% of the total Salt River

Watershed yields. While there is large disagreement between the estimated yields due to differing methodologies, it can be stated the incorporation of Francis Creek into the project reach will substantially increase sediment volumes reaching the SRERP main channel. Given the scope of collected data, it would be imprudent to hypothesize the response of the main channel to such a large influx of future sediment, but the current lack of deposition is a positive indicator that the main channel has the potential for additional carrying capacity. Per the adaptive management plan, project managers are required to conduct future longitudinal profile surveys to provide needed information regarding the response of the main channel given the large anticipated increases in sediment volumes (HTHA 2010).

Objective 3: Identify locations not meeting performance standards and provide data to inform the implementation of adaptive management protocols.

Several areas currently do not meet performance standards specified by HTHA (2011) which warrant varied management actions. Main channel cross-section areas that change by 10% between any survey period or from as-built designs are subject to management action. This criterion is met by two-thirds of the channel cross-section survey locations within Units 1 and 2 (Table 6). Cross-section area increases within Unit 1 were primarily attributed to adjustments and deepening of the thalweg, while the banks remained relatively stable. Channel geometries were highly stable under lower flow conditions experienced during the 2016 WY (Table 6) and can be assumed to remain stable in the presence of future moderate water years. The downcutting of the thalweg should be monitored, but is not an immediate concern as adjustments to post-restoration channel

bottoms are expected (Shea 2011, Dey 2014). However, the large bank slump located at the upstream portion of the unit was identified as the most rapidly expanding erosion area within the entire project reach between the summer 2016 and 2017 (i.e. Figure 58 and Table 12; failure ID 2). The slump has propagated rapidly from altered flood flow dynamics in the presence of a groundwater seep induced slump on the opposite bank and should be given immediate attention. This occurs as flows within the main channel are diverted into the primary groundwater slump, creating a secondary eddy blocking the main flow and pushing it into the opposite bank. Adaptive management within the area is further complicated by its exposure to the full tidal regime. Additional investigation is required to develop a long-term solution for the area, as groundwater seepage will likely influence any attempts to reinforce the original slump.

The middle reach, downstream from the Dillon Rd. Bridge through the central meander, encompassing channel Unit 2, is collectively the most unstable within the project reach, based on longitudinal profile, channel cross-section, and failure inventory survey data. While several bank failures remained stable through the 2017 WY, additional failures developed between survey years and channel cross-section areas continue to increase due to bank steepening and channel bottom downcutting. Channel adjustments do not currently affect sediment transport within the main channel based on the lack of observed deposition. However, if these trends continue, sediment transport capacity will likely decrease in upcoming years as the channels widen and deepen which threatens the primary objective of the SRERP. Additional targeted research should be implemented to

identify the source of bank failures within this reach. Sediment grain size analyses should be conducted on both the channel banks and within scour pools to determine if localized sand lenses are undermining the integrity of channel geometries. Additionally, a more thorough investigation of flood stage flow dynamics should be undertaken to identify locations and sources of more turbulent flows. At a minimum, large scour pools and bank failures within the reach should be closely monitored, both within the dry season and observed during flood stages, to determine if erosional processes continue or stabilize as the project ages. Targeted planting of bank failures may be a low cost adaptive management measure to limit further erosion by encouraging bank stabilization through root growth.

Fluvial dominated upstream reaches exhibited high stability along both channel banks and the main channel bottom. The exception within the reach is failure IDs 23 and 24 (Figure 58; Table 12), which have formed directly adjacent to the Unit 3 secondary channel entrance. ID 23 occurred immediately following the completion of the channel's contouring and remained stable throughout the 2017 WY. The design team determined the bank contained high proportions of non-resistant sandy material and failed due to flows being directed from the opposite bank (C. Shea, pers. Comm., 2017) However, the scour pool is relatively deep and threatens to undermine channel banks as occurred for ID# 24. The large bank slumps are already scheduled for adaptive management actions, including recontouring of the main channel (D. Hansen, pers comm., 2016) which should restore flow dynamics and, hopefully, reduce flow rates entering the floodplain. To assist

and inform future adaptive actions to problem areas, all elevation survey data have been shared with project managers. A copy of this paper will also be provided to project managers.

Objective 4: Develop a model to determine the long-term trajectory of hydraulic conveyance capacities and evolution of channel morphologies incorporating projected changes in storm frequency and intensity.

As collected information spans a range of data types from different survey methodologies, a quantitative comparison of collected data is not possible to develop a robust statistical model describing the trajectory of the project. A quantitative model would have required additional resources to be invested in the collection of higher resolution data pertaining to a single parameter. As an example, more tiles could have been deployed with a larger spatial distribution and monitored on finer temporal scales to provide a more detailed response of sedimentation to storm events. However, this would have reduced efforts to another survey and reduced the scope of the project to the explanation of a single variable instead of a broader description of the function of the project reach.

However, the data sets do provide sufficient information to develop a qualitative conceptual model based on quantitative data to describe the broad physical and hydraulic trends, allowing extrapolation for application of future scenarios. Currently, the main channel efficiently transports sediment downstream to the point that boundary shear stresses and settling velocities are sufficiently high to induce dominant scour regimes. Vertical and lateral main channel scour may be a concern for the long term hydraulic

conveyance if the channels continue to increase in cross-sectional area, as depths will decrease resulting in reduced stream competence. However, mean vertical erosion where present (Units 1 and 2), currently exceeds lateral erosion, which should maintain the low width-to-depth ratios necessary to concentrate base flows.

A concern for the long-term trajectory of hydraulic conveyance is the main stream vertical erosion combined with the aggradation of active bench entrances. Kleinhans et al. (2012) describes the positive feedback loop that develops on bifurcations with asymmetric elevations leading to hydrologic abandonment of the floodplain. As the elevations become increasingly distant, less water flows onto the floodplain and decreases entrance flow depths, resulting in increased aggradation further decreasing entrance flow depths. The total change in elevation between the mean main channel thalweg depth and the secondary channel leveeing at Units 2 and 3 was 0.32 and 0.26 m, respectively. Cumulative precipitation depths for the 2017 WY were abnormally high (Figure 55) and channel deposition and scour were proportionally high. As the SRERP has only experienced 3 wet seasons, the difference in elevation between the secondary channel entrances and main channel bed may simply be short-term adjustments to local conditions. The entrances may currently be too wide to maintain flow velocities sufficient to transport coarse material to more distant floodplain areas and will adjust by scouring deeper, narrower channels through the recently deposited sediments. Channel entrances should be closely monitored following future wet seasons to determine the absolute trajectory of these areas.

Hypothetically, assuming the trend in increasing elevation differences proceeds unchecked, using a conservative estimate of half the observed elevation difference (i.e. the net elevation difference calculated by adding the increased elevations on secondary channel entrances and the decreasing elevation on the main channel bottom) using the WY 2017 continuous WSE data the active benches within fluvial dominated channel units would be almost entirely abandoned within 8 years (Figure 60). If a hydrological disconnection occurred, main channel shear stresses would increase as all flows would be conveyed through the channel likely resulting in increased erosion rates.

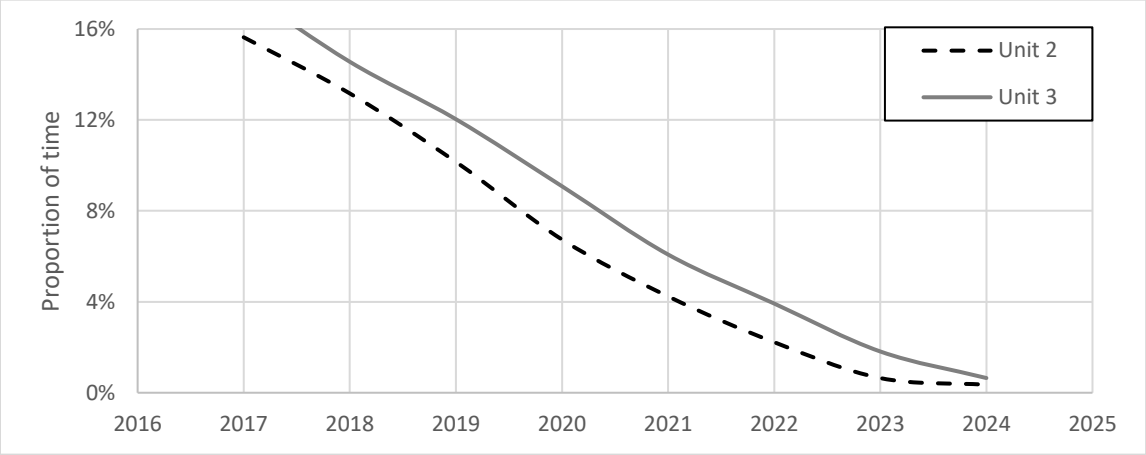

Figure 60. Proportion of time flows would occur within the channel flow and island overtopping flow regimes extrapolating 2017 WY WSE data and half the observed change in elevation between main channel thalweg and secondary channel entrances.

Multiple channel evolution models have been created (Schumm and Parker 1973, Simon and Hupp 1987, Rosgen 1996) but each agrees that the observed main channel widening and deepening will eventually lead to channel aggradation without mitigation. However, as previously mentioned, channel depth is increasing faster than bank erosion which maintains the depth-to-width ratio and preserves sediment transport capacities. Lateral

erosion rates calculated from erosion pins were nearly imperceptible compared to vertical erosion rates observed during channel cross-section surveys. Additionally, as vegetation continues to propagate down channel banks, increased bank stability should be added to decrease lateral erosion rates.

Future channel-cross section and longitudinal profile surveys should be replicated to monitor future changes during a broader range of cumulative precipitation water years, but the observed changes should not be of particular concern as the channels are still undergoing adjustments from the initial construction. However, areas with defined bank slumps causing rapid channel widening should be closely monitored to determine if the erosion rates are increasing or banks are stabilizing to the new channel geometry.

Objective 5: Extrapolate the long-term ability of the project to accomplish project goals.

Extrapolating the project's long-term effectiveness to efficiently transport water and sediment is complicated by the summer 2017 implementation of Phase 2 Upper of the SRERP which directs sediment laden flows of Francis Creek to the study area. The dominant thalweg scour patterns exhibited within the main channel indicates an excess of carrying capacity. However, without more detailed data on flow dynamics (e.g. measures of shear velocity and turbulence) for each flow regime within localized reaches, it's difficult to quantify the capacity of the channel to transport increased sediment volumes. No specific project life duration is discussed within any of SRERP planning documents however "10 years of mitigation site monitoring is required for regulatory compliance" (HTHA 2011).

A description of the hypothetical trajectory of time durations the SRERP would experience hydrologic connectivity to floodplains is discussed for the previous objective (Figure 60). However, as cumulative precipitation records for the monitoring period were the highest in 70 years (Figure 55), the response patterns of sediment are likely equally anomalous. Generally, the project reach has remained relatively stable and performed as designed regarding the efficient transport of water and sediment. On a qualitative level, accounting for the abnormal rainfall records during the 2017 WY, the project should perform adequately for at least the 10 year monitoring period but there are several 'red flags' which should be closely monitored within the upcoming years so problem areas may be addressed to prolong the project life.

With the incorporation of Francis Creek, the continued monitoring of the channel cross-section, main channel thalweg, and secondary channel entrances will be crucial to informing adaptive management decisions. Cross-sectional area and adjustments to the width to depth ratios for channel cross-section profiles should be watched closely to determine the rate of continued vertical and lateral erosion. If width to depth ratios and cross-sectional area continue to increase, water velocities will correspondingly decrease as the same volume of water is conveyed through a larger, wider area resulting in increased deposition. Particular attention should be given to reaches experiencing tidal inundation. If erosion continues to be observed, targeted plantings on channel banks should be considered to increase stabilization. Additionally, the areal extent of current bank slumps should be monitored to ensure slumps are not propagating up or downstream

along failure scarps. Fortunately, many slumps remained stable through the 2017 WY, indicating they may have just resulted from sand lenses incorporated into construction materials or fluvial adjustments in highly turbulent reaches.

Longitudinal profile surveys will provide the most useful information assessing the hydraulic transport capacities with the addition of Francis Creek. If down cutting of the main channel thalweg continues at similar rates, the main channel can be regarded as possessing a carrying capacity sufficient for Francis Creek sediment. However, at current downcut rates, channel banks are at risk of being undercut within the lower reaches. Particular attention should be paid to changes in longitudinal length and elevation at the bases of identified scour pools which have the highest potential to undercut banks where sloughing has not yet occurred. In the event deposition is observed, additional research should be undertaken to identify locations where sediment may be stored upstream or diverted to floodplains, as this may lead to the self-perpetuating aggradation conditions initially responsible for the necessity for the SRERP. The ideal response of the main channel would involve no elevation change with the introduction of flows from Francis Creek.

While not incorporated into the Adaptive Management Plan (HTHA 2011), sedimentation rates at secondary channel entrances, particularly within fluvial dominated reaches, should be monitored to prevent reductions in the proportion of time flows enter floodplain areas. A natural leveeing process has been documented within the Unit 2 and 3 secondary channel entrances which could result in hydrologic disconnections reducing

the ability of floodplain areas to function as sediment sinks and storages. Additionally, a disconnection from floodplains would disturb the current flow dynamics and require the main channel to convey larger volumes of water and sediment. If deposition continues at current rates, it may be necessary to selectively excavate entrance sediment to maintain the desired channel geometry and elevation relative to the main channel.

Objective 6: Provide recommendations to inform the implementation of similar future projects.

A primary component in the design of an anabranching channel system is the relative function and hydraulic conveyance of the main and secondary channels in regards to project objectives. Extensive thought must be given to the desired outcomes for hydraulic transport and sedimentation to inform adequate channel geometry and secondary channel bifurcation and confluence designs. Data collected for this project have demonstrated the capacity for efficient sediment transport of narrow deep channels with low elevation gradients in the presence of high sediment loads. However, undersized channels have the potential to concentrate flows and increase velocities to speeds sufficient to initiate channel bed and bank scour. Increased scour rates may eventually result in sediment aggradation by increasing channel cross-sectional areas. To avoid these issues, main channels should be designed so shear velocities during effective bankfull discharge rates roughly approximate the settling velocity of the dominant grain size. Utilizing this design element, mean sediment transport should effectively transport loose sediment through the system in suspension while not applying excess shear stress to stable channel sediments.

The design of channel connections should be related to dominant sediment grain size distribution and magnitude of desired floodplain storage. Extensive thought and analysis should be given to the orientation and location of confluences, as they function as controls on the volume and size of sediments entering the secondary channels. If designed properly, active benches can be used to selectively deposit a specific magnitude and range of sediment size classes for storage within the system. Additionally, the location of desired sediment deposition should be carefully analyzed to construct a system which accounts for the expected relative elevational changes between the main channel and secondary channel entrance to prevent hydrological discontinuities from the original design.

A general dearth of information exists to completely partition the magnitude of effect each difference exhibits on the sediment grain sizes allowed to enter the Unit 2 and 3 floodplains. However, it stands to reason that shooting water entering anabranching channels will carry a larger proportion of coarser grained suspended load, as larger shear velocities are capable of buoying these heavier grains. Therefore, areas functioning under these flow regimes may be designed to capture and store coarser grained sediments within smaller spatial areas as the large grains will inevitably fall out of suspension as the floodplain widens and depths decrease. This may be useful for secondary channel sediment retention areas where it is desirable to plan the periodic removal of coarser grained particles. While secondary channel entrances designed at more obtuse angles and within reaches where the main channel thalweg is actively directed away from the

entrance (e.g. downstream of outer meander bends) will function under backwater conditions where lower velocity water simply spills onto the floodplain. These areas will transport smaller grained particles and deposit them more uniformly across a larger spatial range.

If a static channel anabranching design is desired where water paths are not permitted to naturally shift courses within the floodplain, it may be prudent to reinforce the lip of active bench entrances with hardscape structures such as concrete or large wood pylons. Reinforcing the channel entrances would provide multiple monitoring and maintenance benefits. The installation of hardscape structures will reinforce entrance geometries, eliminating the risk of scour points propagating down the secondary channel. This study showed rapid deposition occurs immediately at channel entrances due to decreased flow depths. The addition of hard structures would enable a quick determination of the inter-annual deposition magnitudes as structures serve as permanent benchmarks to measure deposition depths without requiring time consuming elevation surveys. Additionally, deposited sediment could be quickly excavated to the original design elevation and would serve as a permanent geometry preventing natural leveeing and hydrologic disconnections. Structures would inhibit the growth of vegetation immediately at channel entrances, thereby decreasing roughness and the associated high deposition rates caused by decreased water velocities. Additionally, care should be taken to reinforce bifurcations with well-consolidated cohesive sediment to limit the potential for channel scour.

LITERATURE CITED

Ackers P and WR White. 1973. "Sediment transport: New approach and analysis." *Journal of the Hydraulics Division,* ASCE, 99(11):2041-2060.

Adams PN, RL Slingerland, and ND Smith. 2004. "Variations in natural levee morphology in anastomosed channel flood plain complexes." *Geomorphology,* 61(1–2): 127–42.

Al-Hamdan OZ, FB Pierson, MA Nearing, CJ Williams, JJ Stone, PR Kormos, J Boll, and MA Weltz. 2013. "Risk assessment of erosion from concentrated flow on rangelands using overland flow distribution and shear stress partitioning." *American Society of Agricultural and Biological Engineers,* 56 (2): 539–48.

Allen PA. 1997. *Earth Surface Processes*. Blackwell Science. Oxford, England.

Bagnold RA. 1980. "An empirical correlation of bedload transport rates in flumes and natural rivers." Proc. R. Soc. London, Ser. A, 372, 453–473.

Barry JJ, Buffington JM, Goodwin P, King JG, and WW Emmett. 2008. "Performance of bed-load transport equations relative to geomorphic significance: Predicting effective discharge and its transport rate. *Journal of Hydraulic Engineering* 134(5): 601 – 615.

Benda L and A Berg. 2007. Sources, magnitude, and mitigation of erosion and sedimentation in the Salt River basin, with emphasis on Francis and Williams Creek basins. Prepared for: Humboldt County Resource Conservation District, California Coastal Conservancy, and California Department of Fish and Game.

Berry W, N Rubinstein, B Melzian, and B Hill. 2003. "The biological effects of suspended and bedded sediment (sabs) in aquatic systems: a review." United States Environmental Protection Agency, Duluth MN.

Brooks KN, PF Folliot, and JA Magner. 2013. *Hydrology and the management of watersheds, Fourth Ed*. John Wiley and Sons, Hoboken, NJ.

Brown AG. 2002. "Learning from the past: palaeohydrology and palaeoecology." *Freshwater Biology*, 47: 817‐829.

Benke AC. 1990. "A perspective on America's vanishing streams*." Journal of the North American Benthological Society*, 9(1): 77-88

Cheetham, MD, AF Keene, RT Bush, LA Sullivan, and WD Erskine. 2008. "A comparison of grain-size analysis methods for sand-dominated fluvial sediments." *Sedimentology* 55:1905-1913.

Christiansen T, PL Wilberg, and TG Milligan. 2000. "Flow and sediment transport on a tidal salt marsh surface". *Estuarine, Coastal, and Shelf Science* 50: 315 – 331.

Dedkov A. 2004. "The relationship between sediment yield and drainage basin area." *IAHS Publication,* 288: 197–204.

DeFries R, and KN Eshleman. 2004. "Land-use change and hydrologic processes: a major focus for the future." *Hydrological Processes,* 18(11): 2183–86.

Dey H. 2014. *Fluvial Hydrodynamics: Hydrodynamic transport and sediment transport phenomenon*. Springer Berlin Heidelberg, Heidelberg, Germany. 687 pp.

Downie ST and KP Lucey. 2005. Salt River Watershed Assessment. Coastal Watershed Planning and Assessment Program. Department of Fish and Game.

Eaton BC, RG Millar, and S Davidson. 2010. "Channel patterns: Braided, Anabranching, and single-thread." *Geomorphology,* 120:353-364.

Einstein HA. 1950. "The bedload function for sediment transportation in open channel flows." United States Department of Agriculture Technical Bulletin No. 1026.

Einstein HA and RB Banks. 1950. Fluid resistance of composite roughness. *American Geophysical Union,* 31(4): 603-610.

Engelund FR and E Hansen. 1967. A monograph on sediment transport in alluvial streams. Tekniskforlag. Copenhagen, Denmark.

Fenton C. 2011. "Francis Creek annual suspended sediment yield, Turbidity threshold sampling summary report: Hydrologic year 2011." Report prepared for the Salt River Ecosystem Restoration Project.

Fitzpatrick FA, JC Knox, and HE Whitman. 1999. Effects of historical land-cover changes on flooding and sedimentation, North Fish Creek, Wisconsin. US Department of the Interior, US Geological Survey.

Foster GR. 1982. "Modeling the erosion process". In *Hydrologic Modeling of Small Watersheds*, 295-382 CT Haan, HP Johnson, and DL Brakensiek (eds). ASAE Monograph No. 5: St. Joseph, Mich.

Garde RJ and KG Ranga Raju. 1978. *Mechanics of Sediment Transport and Alluvial Stream Problems*. Wily: New Delhi; 483.

Gomez B. 1991. “Bedload transport.” *Earth Science Reviews* 31(2): 89 – 132.

Graf WL. 2001. “Damage control: restoring the physical integrity of America’s rivers.” *Annals of the Association of American Geographers*, 91(1): 1–27.

Graf WL. 2006. “Downstream Hydrologic and Geomorphic Effects of Large Dams on American Rivers.” *Geomorphology* (79): 336 – 360.

GEC (Grassetti Environmental Consulting). 2011. Final environmental impact report: Salt River Ecosystem Restoration Project, February 2011, SCH# SD2007-05-6. Prepared for: Humboldt County Resource Conservation District, Eureka, CA. In association with California State Coastal Conservancy and Kamman Hydrology & Engineering, Inc.

Gregory KJ. 1985. “Types of rivers/ stream channels”. In *Encyclopaedic Dictionary of Physical Geography*, Goudie, A (ed). Blackwell Science. Oxford, England.

HCRCD (Humboldt County Resource Conservation District). 2014. “Salt River Ecosystem Restoration Project: A short history.”

Hjulstrøm F. 1939. “Transportation of debris by moving water.” In *Recent Marine Sediments; A Symposium: American Association of Petroleum Geologists*, Trask, PD (ed). 5-31.

HTHA (H.T. Harvey & Associates) 2011. Salt River Ecosystem Restoration Project, Habitat Mitigation and Monitoring Plan (HMMP). Prepared for Humboldt County Resource Conservation District, Eureka, CA.

Huang HQ, and GC Nanson. 2007. “Why some alluvial rivers develop an anabranching pattern.” *Water Resources Research*, 43(7).

Jansen JD, and GC Nanson. 2010. “Functional relationships between vegetation, channel morphology, and flow efficiency in an alluvial (anabranching) river.” *Journal of Geophysical Research* 115(4).

KHE (Kamman Hydrology and Engineering, Inc.). 2011. “Salt River Ecosystem Restoration Project: Preliminary Channel Design.”

Kleinhans MG, RI Ferguson, SN Lane, and RJ Hardy. 2012. Splitting rivers at their seams: bifurcations and avulsion. *Earth Surface Processes and Landforms* 38(4): 47 – 61.

Kondolf GM. 1995. “Geomorphological stream channel classification in aquatic habitat restoration: uses and limitations.” *Aquatic Conservation: Marine and Freshwater Ecosystems* 5: 127–41.

Kondolf GM, and ER Micheli. 1995. “Evaluating stream restoration projects.” *Environmental Management,* 19(1): 1–15.

Latrubesse EM. 2008. “Patterns of Anabranching channels: The ultimate end-member adjustment of mega rivers.” *Geomorphology* 101: 130 – 145.

Laursen EM. 1958. “The total sediment load of streams.” *Journal of the Hydraulics Division,* ASCE, 84(1):1-36.

Leopold LB and T Maddock Jr. 1953 “The hydraulic geometry of stream channels and some physiographic implications.” Geological Survey Professional Paper 252.

Leopold LB and MG Wolman. 1957. “River channel patterns: braided, meandering and straight”. Professional paper 282-B, United States Geological Survey, Washington, DC

Makaske B. 2001. “Anastomosing rivers: a review of their classification, origin and sedimentary products.” *Earth-Science Reviews,* 53(3): 149–96.

Makaske B, DG Smith, HJA Berendsen, AG de Boer, MF van Nielen-Kiezebrink and T Locking. 2009. “Hydraulic and sedimentary processes causing anastomosing morphology of the Upper Columbia River, British Columbia, Canada.” *Geomorphology* 111(3–4): 194–205.

Merritt DM, ML Scott, N LeRoy Poff, GT Auble, and DA Lytle. 2009. “Theory, methods and tools for determining environmental flows for riparian vegetation: riparian vegetation-flow response guilds.” *Freshwater Biology* 55(1)

Mitch WJ and JG Gosselink. *Wetlands 2nd ed*. Nostrand Reinhold, New York, New York, USA.

Mount JF. 1995. *California Rivers and Streams: The Conflict Between Fluvial Processes and Land Use*. University of California Press, Berkeley, CA.

Naiman R, H Decamps and M Pollock. 1993. “The role of riparian corridors in maintaining regional biodiversity.” *Ecological Application* 3(2): 209–12.

Nanson GC, and MR Gibling. 1978. “Anabranching rivers.” In *Encyclopedia of Earth Science*, 17–20. Springer, Berlin Heidelberg.

Nanson GC and AD Knighton. 1996. “Anabranching rivers: their cause, character and classification.” *Earth Surface Processes and Landforms* 21: 217–39.

NOAA (National Oceanic and Atmospheric Administration’s National Weather Service). 1998. “Climate of Eureka, CA”. NOAA Technical Memorandum NWS WR-252.

NOAA (National Oceanic and Atmospheric Administration's National Weather Service). 2017. Precipitation Frequency Data Server. "NOAA Atlas point precipitation frequency estimates". https://hdsc.nws.noaa.gov/hdsc/pfds/pfds_map_cont.html?bkmrk=ca. Accessed July 2017.

Novak P, AIB Moffat, C Nalluri, and R Narayan. 2007. *Hydraulic Structures Fourth ed.* Abingdon Spon.

Palmer M, JD Allan, J Meyer, and ES Bernhardt. 2007. "River restoration in the twenty-first century: data and experiential knowledge to inform future efforts." *Restoration Ecology* 15(3): 472–81.

Parker G. 1990. "Surface-based bedload transport relation for gravel rivers." *Journal of Hydraulic Research* 28: 417–436.

Pasternack, GB and GS Brush. 1998. Sedimentation Cycles in a River-Mouth Tidal Freshwater Marsh. *Estuaries* 21: 407-415.

Price MF, AC Byers, DA Friend, T Kohler, and LW Price. 2013. *Mountain Geography: Physical and Human Dimensions*. University of California press.

Ritter DF, Kochel CR, and JR Miller. 2006. *Process Geomorphology, Fourth Ed.* Waveland Press, Inc. Long Grove, Illinois, USA.

Rosgen DL. 1996. *Applied River morphology*. Wildland Hydrology, Pagosa Springs, CO.

Schumm A. and RS Parker. 1973. "Implications of complex response of drainage systems for quaternary alluvial stratigraphy". *Nature (Physical Science)* 243: 99-100.

Shea, C. 2011. "The Salt River Ecosystem Restoration Project: Salt River Channel Design Assessment."

Simon A and CR Hupp. 1986. "Channel Evolution in Modified Tennessee Channels. In: *Proc. 4th Federal interagency Sedimentation Conference*, Las Vegas. US Government Printing Office 5.71 – 5.82.

SWQCB (State Water Quality Control Board). 2001. "Guidelines for citizen monitors." Products of the 2000-2001 Technical Advisory Council on Citizen Monitoring.

USACE (United States Army Corps of Engineers). 2010. *HEC-RAS River Analysis System: User's Manual V4.1*." United States Army Corps of Engineers, Hydraulic Engineering Center, Davis, CA.

USDA (United Stated Dept. of Agriculture, Soil Conservation Service). 1993. “Salt River Watershed, Local Implementation Plan, USDA Soil Conservation Service, Water Resources Planning: 82.”

USDA (United Stated Department of Agriculture). 2014. “Kellogg Soil Survey Laboratory Methods Manual, Version 5.0.” USDA Soil Survey Investigations Report No. 42. Washington D.C., USA.

USEPA (US Environmental protection Agency). 2009. “National water quality inventory: report to Congress 2004 reporting cycle.” United States Environmental Protection Agency: Office of Water Washington D.C.

Wallingford HR. 1990. Sediment Transport, the Ackers and White Theory Revised. Report SR237, England.

Ward J and JA Stanford. 1995. “Ecological connectivity in alluvial river ecosystems and its disruption by flow regulation.” *Regulated Rivers: Research & Management* 11(1): 105–19.

Ward AD and SW Trimble. 2004. *Environmental Hydrology 2nd Ed*. CRC Press, Boca Raton, Fl.

Wohl E. 2005. “Compromised rivers: understanding historical human impacts on rivers in the context of restoration.” *Ecology and Society* 10(2): 2.